

RESEARCH PROJECT, EASA.2022.C11

D-4.3 FINAL REPORT

Helicopter Vortex Ring State Experimental Research

Disclaimer



Funded by the European Union. Views and opinions expressed are however those of the author(s) only and do not necessarily reflect those of the European Union or the European Union Aviation Safety Agency (EASA). Neither the European Union nor EASA can be held responsible for them.

This deliverable has been carried out for EASA by an external organisation and expresses the opinion of the organisation undertaking this deliverable. It is provided for information purposes. Consequently it should not be relied upon as a statement, as any form of warranty, representation, undertaking, contractual, or other commitment binding in law upon the EASA.

Ownership of all copyright and other intellectual property rights in this material including any documentation, data and technical information, remains vested to the European Union Aviation Safety Agency. All logo, copyrights, trademarks, and registered trademarks that may be contained within are the property of their respective owners. For any use or reproduction of photos or other material that is not under the copyright of EASA, permission must be sought directly from the copyright holders.

Reproduction of this deliverable, in whole or in part, is permitted under the condition that the full body of this Disclaimer remains clearly and visibly affixed at all times with such reproduced part.

DELIVERABLE NUMBER AND TITLE:	VRS, D-4.3 Final report
CONTRACT NUMBER:	EASA.2022.C11
CONTRACTOR / AUTHOR:	ONERA / Laurent Binet – Pierre-Marie Basset
IPR OWNER:	European Union Aviation Safety Agency
DISTRIBUTION:	Public

APPROVED BY:	AUTHORS	REVIEWER	MANAGING DEPARTMENT
	Laurent Binet Philippe Gasquez	Raffaele Di Caprio	Helder Mendes

DATE: 26 March 2025

CONTENTS

CONTENTS	3
ABBREVIATIONS	6
1. Introduction	8
1.1 Scope of the document	8
1.2 Limits	8
2. Flight test campaigns	9
2.1 Summary	9
2.2 Test objectives	10
2.3 Description of helicopters and Flight Test Instrumentation	10
2.3.1 Fennec AS550-U2	10
2.3.2 Dauphin SA365N	11
2.3.3 Flight Test Instrumentation	11
2.4 Test method and means	14
2.5 Repeatability of the VRS entries	15
2.6 VRS confirmation in flight	16
2.7 General description of the recovery manoeuvres	18
2.8 Repeatability of recovery manoeuvres	19
2.9 Test runs procedure	19
2.10 Test runs distribution	20
3. Vortex-Ring-State phenomenon	21
3.1 VRS domains	21
3.1.1 Fennec	21
3.1.2 Dauphin	24
3.2 Influencing parameters	27
3.2.1 Collective pitch versus Vertical speed	27
3.3 Vibration analyses	28
3.3.1 Vibration measurements	28
3.3.2 Vibration analysis	28
3.3.3 VRS Domains based on vibration analysis	32
3.4 Pilot feedbacks	41
3.5 Conclusions on Vortex-Ring-State phenomenon	42
4. Recovery techniques evaluation	43

4.1	Recovery performance	43
4.1.1	Performance criteria	43
4.1.2	Fennec helicopter	43
4.1.1	Dauphin helicopter	45
4.1.2	Performance summary	47
4.2	Influencing parameters	47
4.2.1	Effect of vertical speed	47
4.2.2	Effect of torque	50
4.2.3	Effect of the pitch angle on the performance	54
4.2.4	Effect of the variation of roll angle on the performance (Vuichard recoveries)	59
4.2.5	Effect of the forward speed variation during Vuichard recoveries on both helicopters	61
4.2.6	Effect of the helicopter mass	62
4.2.7	Summary of the influencing parameters	62
4.3	Entry conditions	63
4.3.1	Exits at VRS onsets / established VRS	63
4.3.2	Influence of the horizontal speed	64
4.3.1	Influence of the lateral speed	68
4.3.2	Effect of delayed increase of collective	70
4.4	Pilot feedback	72
	Pilot feedback regarding c	73
4.4.1	lassical recoveries	73
4.4.2	Pilot feedback regarding Vuichard recoveries	74
4.4.3	Analytic comparison	81
4.5	Summary	83
4.5.1	Fennec	83
4.5.2	Dauphin	84
4.6	Lessons learnt	86
5.	Numerical approach	87
5.1	Summary	87
5.2	VRS models	87
5.2.1	ONERA VRS model description	87
5.2.2	ATR VRS model description	89
5.3	Differences between current and previous flight test campaigns	90
5.4	Strategy to follow flight test data	91
5.5	RESULTS	92
5.5.1	Forward recovery in fully VRS with and without collective increase	92
5.5.2	Forward recovery at VRS onsets	93

5.5.3	Forward recovery in decelerated flight	94
5.5.4	Vuichard recovery in fully VRS	95
5.5.5	Vuichard recovery at VRS onsets	96
5.5.6	Inversed Vuichard recovery in fully VRS	97
5.6	Summary of comparisons between simulation results and flight data	98
5.7	Off-line parametric studies	100
5.7.1	Collective efficiency in fully developed VRS	100
5.7.2	Collective efficiency at VRS onsets	101
5.7.3	Collective versus vertical speed	103
5.7.4	Delayed collective application during recoveries	104
5.7.5	Pitch attitude in forward recovery	105
5.7.6	Roll attitude in Vuichard recovery	105
5.8	Simulator trials	107
5.8.1	Simulator trial results	108
5.8.2	Pilot feedback on simulator trials	109
5.9	Conclusions of the numerical investigation	110
6.	General conclusions.....	112
	Bibliography	113
	Appendix	114

ABBREVIATIONS

ACRONYM	DESCRIPTION
DDL0	Lateral cyclic input (%)
DDM0	Longitudinal cyclic input (%)
DDN0	Pedal input (%)
DDT0	Collective input (in % if pilot control, in deg for collective blade pitch angle)
FTI	Flight Test Instrumentation
ft	Feet
ft/min	Feet per minute
g	Gravitational constant
HOST	Helicopter Overall Simulation Tool – Airbus Helicopters flight mechanics code
IAS / KIAS	Indicated AirSpeed / IAS in kts
kt(s)	Knot(s)
M	Helicopter mass
MGB	Main Gear Box
n	Normal acceleration
P2P	Peak to peak
P _{TQ50%}	Power corresponding to 50% of torque
R	Rotor Radius
Rho (ρ)	Air density (Kg/m ³)
ρ ₀	Air density at Standard Sea-Level conditions (1.225 Kg/m ³)
RoD	Rate of Descent
RPM	Rotation speed (Rev. Per Minute)
Sigma (σ)	Relative air density ρ/ρ ₀
T	Rotor thrust
T _{manoeuvre}	Time at which the recovery manoeuvre is initiated
TOP	Take-Off Power
TQ	Rotor Torque
t _{vortex}	Time at which the pilot considered being in VRS
T _{vz0}	Time at which the recovery manoeuvre is ended (vertical speed equal to 0)
V _H	Helicopter horizontal speed (airspeed): $V_H = \sqrt{V_X^2 + V_Y^2}$
V _i	Induced velocity
V _{i0}	Induced velocity in hover
V _{Ground}	Helicopter ground speed: $V_{Ground} = V_{air} + V_{wind}$
V _{up} / V _{up_GPS}	Helicopter vertical speed from GPS
V _x	Helicopter longitudinal speed (airspeed)
V _y	Helicopter lateral speed (airspeed)
V _{wind}	Wind velocity

V_z	Helicopter vertical speed
VRS	Vortex Ring State
W	Helicopter Weight
ZP	Pressure Altitude
θ / TETA	Helicopter pitch angle
ϕ / PHI	Helicopter roll angle
ψ / PSI	Helicopter heading

1. Introduction

1.1 Scope of the document

This report represents the final deliverable (D-4.3) of the Helicopter Vortex-Ring-State Experimental Research project (EASA.2022.C11). The research was conducted by ONERA and supervised by EASA. The flight test campaign was performed by the Direction Générale de l'Armement - Essais en Vol (DGA-EV). This document adds to the VRS knowledge Report already issued in the frame of the same research project (reference [1]).

The objective of this document is to describe the flight test campaign realized in the framework of this project, to detail the analyses performed on the flight test data (flight parameters and vibration measurements when available) and the investigations done on numerical VRS models.

This final report is issued at completion of the entire research programme, in which all the available results of the study as well as conclusions and recommendations are made. In particular, for the test helicopters, this final report addresses the following:

- VRS flight domain determination and study of the VRS characteristics and associated influencing parameters;
- comparison of the results with available predictions obtained with analytical and simulation methods; and
- evaluation of the effectiveness of the Vuichard VRS recovery manoeuvre compared to the forward recovery for the used helicopter types (precise definitions of both manoeuvres will be given).

It is important to highlight that, despite not foreseen in the initial research tender specification, a comparison between the Vuichard recovery technique and the recovery technique defined by the helicopter manufacturer was performed in order to provide a baseline for future similar evaluations on other aircraft/rotor designs.

1.2 Limits

Flight tests remain essential to better understand all the mechanisms involved in VRS generation and the evaluation of recovery techniques, but VRS flight tests are very demanding in terms of instrumentation, competences, and costs.

Unfortunately, the scope of the work cannot be infinite in the framework of a project, as well as the number of flights and helicopter types. ONERA, DGA-EV and EASA were fully aware that the analyses performed in the framework of this current research project would be based on a relatively low number of flights and on only two helicopter types with similar rotor systems.

Besides the limited vibration measurements (three 3-axis accelerometers integrated during five of the eight flights), the test helicopters were not provided with any instrumentation to measure loads and strains on structural elements. Therefore, the effect of the VRS on the helicopter structure and parts has not been investigated.

Finally, although a quite large number of test runs were nevertheless performed, a limited number of scenarios and flight test cases were investigated.

Therefore the results of this project have to be considered with regards to these limits.

2. Flight test campaigns

2.1 Summary

The purposes of this study were to validate the prediction of the VRS domain by using the ONERA criteria detailed in reference [5] and to compare the forward recovery method (forward motion) with the recovery method suggested by M. Claude Vuichard (lateral motion).

The test campaign included 4 tests flights on a Airbus Helicopters Fennec AS550-U2 (hereafter only named "Fennec"), and 4 tests flights on a Airbus Helicopters Dauphin SA365N (hereafter only named "Dauphin") with a total of 229 test points performed.

Out of the 105 Fennec test points, a total of 80 valid runs were exploited, including 40 forward recoveries, 33 Vuichard recoveries, and 7 "inversed" Vuichard recoveries (toward the right instead of the left).

Out of the 124 Dauphin runs, a total of 97 valid runs were exploited, including 32 forward recoveries, 58 Vuichard recoveries, and 7 "inversed" Vuichard recoveries.

The Fennec flights were performed between 21/11/2023 and 15/12/2023 with a crew of 4, with a helicopter weight between 1970 kg and 2150 kg.

The Dauphin flights were performed between 20/12/2023 and 03/04/2024 with a crew of 3 to 4, with a helicopter weight between 3000 kg and 3465 kg.

Hover and translation at low airspeed were achieved using the aircraft flight test instrumentation (VIMI system).

The observed VRS domain matches the predicted ONERA domain.

In the test conditions, and even when trying to standardize the VRS entries and recoveries, an important dispersion was observed on the height loss and recovery time for the Fennec and the Dauphin.

For both recovery methods, a number of influencing parameters affect the performance, notably the initial vertical speed, the average torque applied during the recovery, and the initial horizontal speed, although their effects tend to be less clear on Dauphin than on Fennec due to a higher point dispersion.

When considering these effects, performance in term of height loss and recovery time are similar between Vuichard and forward recoveries on both helicopters, with the exception of recoveries at the onset on Fennec where Vuichard recoveries show slightly better performance.

On Fennec, the torque applied has a clear positive effect on the height loss for forward recoveries, and can be directly controlled by the pilot. Therefore, on Fennec helicopters it is recommended to apply all the available power during a forward recovery when a VRS occurs close to the ground.

On both helicopters, the pilot workload was judged low to medium in forward recoveries, with pilot inputs mostly observed on the longitudinal cyclic after an initial action on the collective. The workload was judged high in Vuichard recoveries.

On Fennec, during Vuichard recoveries, inputs were observed on both cyclic axes, on the collective while monitoring the power, and on the foot pedals to try to maintain heading, with a nose down parasitic effect in the second part of the recovery. The variations observed from one Vuichard recovery to another, even for similar sets of entry conditions, did not allow the pilots to usefully anticipate the required actions.

On Dauphin, during Vuichard recoveries, after an initial and voluntary action on the lateral cyclic, on the collective and on the foot pedal to start the translation while maintaining the heading, the pilot had to act quickly on all the controls to compensate a succession of parasitic effects, while carefully monitoring the power

to avoid limitations exceedances. Since delaying the power increase at the end of the translation significantly reduces both the workload and the risk of exceeding limitations without significantly degrading the recovery performance, it is recommended to apply the Vuichard recovery method on a Dauphin only if a forward recovery is inadvisable (due to the presence of obstacles in the forward sector for example), and to delay the power increase after the end of the lateral translation, once the rotor is back to an horizontal position.

On both helicopters, the Vuichard recoveries were also overall judged less intuitive than forward recoveries by the test pilots, who are trained to regain speed by moving forward in case of failure occurring in hover – and less comfortable due to the sudden attitude changes often experienced especially on the Dauphin. These assessments did not change with the increased familiarity with the method over the course of the test campaign. Additionally, in operational conditions and with normal piloting skills, there would be a risk to exceed the aircraft power limitations during a Vuichard recovery on both helicopters.

Additional test runs would be recommended to perform a complete parametric study to confirm the list of influencing parameters and quantify their effect on the recoveries performance.

2.2 Test objectives

The two objectives of the flight test campaign were the following:

- to experimentally determine as precisely as possible the flight conditions at which the VRS starts to develop on the defined test points;
- to experimentally evaluate the effectiveness of the Vuichard recovery technique in comparison to the forward one. The evaluation criteria selected were the recovery performance defined in terms of height loss and time to recovery. While not properly considered as performance criteria, the ease of the manoeuvre along with the pilot workload were evaluated.

These objectives were fulfilled on the 2 helicopter types used during the flight test campaign: AS550-U2 Fennec and SA365N Dauphin.

The role of DGA-EV was to issue a consolidated judgement regarding the effectiveness of the Vuichard recovery method, taking into account basic metrics for the recovery performance and the “pilotability” of this method by an “average skilled pilot” for each helicopter. ONERA then analysed the test results (including this flight test reports, the raw data from the flight test installations, and the raw data from the additional vibration measurements) in order to clearly identify VRS entries and exits, and to evaluate more accurately the performance of each recovery manoeuvre thanks to an objective analysis of the flight parameters and all available data.

Based on the Fennec and Dauphin flight test reports written by DGA-EV and the analysis of the flight test data by ONERA, this final report is concatenating all the flight test results.

2.3 Description of helicopters and Flight Test Instrumentation

2.3.1 Fennec AS550-U2

The helicopter under test during the first part of the test campaign was a Fennec AS550-U2 (n°2803).

The Fennec helicopter is the French military version of the civilian Ecureuil (Squirrel).

The AS550U2 is a light-weight single engine helicopter with a Maximum Take Off Weight of 2250kg. It is fitted with a single ARIEL 1D1 engine.

The helicopter is equipped with a 3-blades STARFLEX® main rotor (Main rotor diameter=10.69m) and a conventional twin-blades teetering tail rotor (Tail rotor diameter=1.86m).

2.3.2 Dauphin SA365N

The helicopter type under test during the second part of the test campaign was a Dauphin SA365N (two helicopters were used: Dauphin SA365N n°6116 and Dauphin SA365N n°6111).

The Dauphin SA365N is a medium-weight twin-engine helicopter with a Maximum Take-Off Weight of 4000kg. It is fitted with two ARIEL 1C engines.

The helicopter is equipped with a 4 blades STARFLEX® main rotor (Main rotor diameter=11.93m) and a Fenestron® tail rotor.

Due to the availability of the aircraft fleet, the harmonization flights and the first test flight were performed on Dauphin n°6116, and the three other test flights were performed on Dauphin n°6111.

Both helicopters used were in a similar configuration, with a small difference of the empty weight (2620 kg for n°6116, 2495 kg for n°6111).

2.3.3 Flight Test Instrumentation

The prototype aircraft were equipped with a Flight Test Instrumentation (FTI) installed by DGA-EV. In addition, an optional vibrations measurement instrumentation was used for Fennec flights 2, 3 and 4 and for Dauphin flights 1 and 4).

The Flight Test Instrumentations (FTI) provides a real-time display of the flight parameters, along with a continuous recording of the data in order to perform post-flight analyses.

The FTI contains three major parts: the sensors, the acquisition unit (used as a concentrator), and the end-user interface (either the recorder and/or the real time display system).

The following parameters are acquired either through the aircraft own instruments, or through additional FTI sensors:

- flight controls position before and after autopilot actuators;
- engine parameters: torque, power throttle and anticipator, combustion chamber input pressure, fuel flow;
- rotor speed and engine output shaft speed, gas generator speed, combustion chamber temperature, attitudes and heading, radar height;
- specific flight test sensors or units: outside air temperature, sideslip angle, anemometric data and inertial data.

A specific inertial GPS navigation system (SAGEM I5000) was also installed for the Fennec test flights. This equipment uses an embedded GPS receiver and internal accelerometers in order to provide hybridized and more accurate position, altitude and vertical speed.

On the Dauphin, a differential GPS installation (MiraNG) was used during the flights to provide a more accurate position, altitude, and vertical speed.

In addition to the sensors data, all the elaborated or derived parameters computed are also recorded.

The detailed list of the recorded parameters is provided in Appendix.

Based on the sensors of the Flight Test Instrumentation, the embedded PC can compute elaborated or derived parameters to enrich the real time display system supplying test pilot and/or flight test engineer screens.

Among these parameters, two sets were particularly useful for this test campaign: VIMI NUM and VIMI GPS.

The VIMI system (“Vitesse Indiquée par Moyen Interne” or internal mean indicated airspeed), also referred to as VIMI NUM (for “VIMI Numérique”), provides an estimation of the longitudinal and lateral airspeed based on the aircraft attitudes and on the cyclic stick position.

The VIMI concept is described in French patent n° 74 287 086 issued on 22nd of August 1974. The objective of this system is to provide the pilot with a reliable airspeed estimation when the airspeed is too low for the anemometric sensors (below 30 kt).

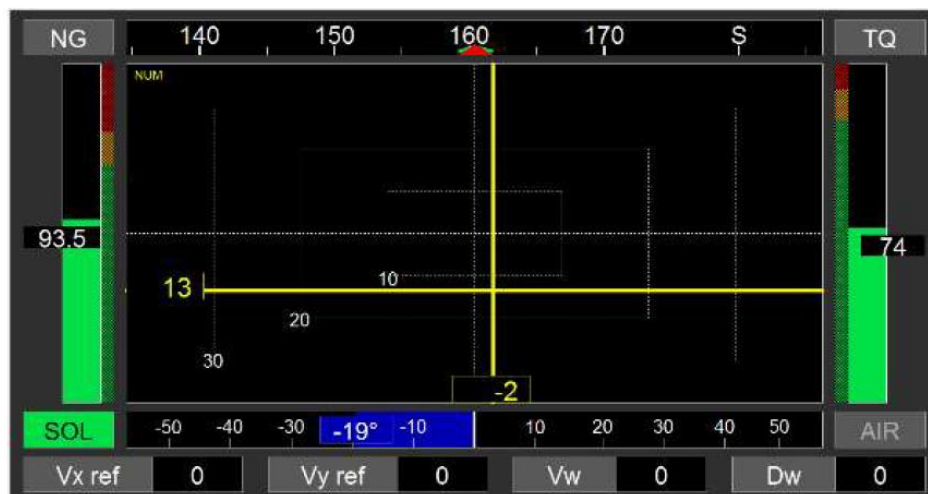
The elaboration of VIMI NUM speeds involves the following steps:

- On the ground: with the helicopter adjusted on jacks to get the rotor mast vertical, the relative longitudinal and lateral attitudes laws of the cyclic plate are established based on the flight controls positions after autopilot actuators. The attitudes of the helicopter are also measured in this position to get the offsets in helicopter reference frame.
- In flight:
 - the attitudes of the helicopter are computed from the acceleration in the 3 axes to get rid of any latency or bias;
 - the absolute attitudes of the cyclic plate are computed thanks to the computed helicopter attitudes and the laws established on ground to convert flight controls position into relative cyclic plate attitudes;
 - then, the absolute cyclic plate attitudes are converted into V_x and V_y based on empiric laws previously established by matching the cyclic plate attitudes with the airspeed (often obtained through GPS speed information in an area with a known or null wind).

The VIMI NUM therefore provides an accurate estimation of low airspeeds, and help the pilot to reach hover even without external reference points.

The interface displayed to the pilot is shown in Figure 2-1. The pilot must align the yellow cross with the center of the screen to achieve hover out of ground effect (HOGE). VIMI is however not validated at EASA level for hovering performance definition, but is for this study deemed sufficient to insure reproducible entry conditions for VRS analysis.

► Figure 2-1 VIMI NUM screen



The VIMI GPS is another system that can be used to help the pilot at low speed, but with a different working principle.

It relies on the GPS data to accurately obtain the ground speed of the aircraft. The airspeed can then be calculated by taking into account the local wind.

The display is similar to the one shown in Figure 2-1, except that the speeds displayed can be either ground speeds or air speeds. An offset can also be entered by the Flight Test Engineer (V_x ref and V_y ref) so that the pilot actually achieves an horizontal translation at the required airspeed when centering the yellow cross.

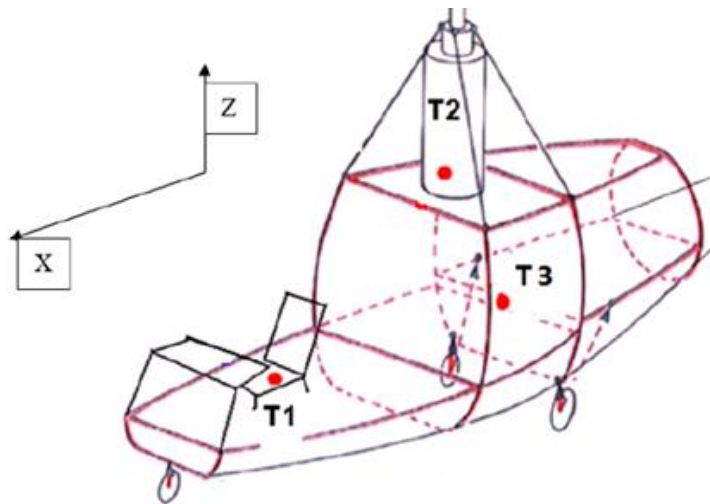
This system obviously requires a steady wind condition at the test altitude. Its advantage over the VIMI NUM is that the GPS remains reliable even when the aircraft attitudes are unusual, which is often the case once in VRS. Therefore, in this test campaign VIMI GPS was the preferred method to measure horizontal speeds during VRS.

The process during the test flights was therefore:

- To estimate the wind (force and direction) by performing a level flight facing the wind. This was done by aligning the route and heading of the helicopter (therefore obtaining the wind direction), and comparing the GPS speed and the aircraft true airspeed (therefore obtaining the wind strength). These parameters could then be entered in the FTI to offset the local wind and display an airspeed on the pilot screen;
- To confirm the wind estimation by performing a hover using the VIMI GPS screen. If the wind is correct, both VIMI GPS and VIMI NUM should be consistent (yellow cross centered, no horizontal air speed), and the pilot could also check that a constant position of the foot pedals resulted in a constant rotation speed. Otherwise, the previous step was repeated to obtain a new wind estimation.
- And then to use VIMI GPS for speed measurements during the VRS test points, while periodically checking the wind and updating the FTI parameters if required.

In addition to the Flight Test Instrumentation, specific vibration sensors were placed in the aircraft during Fennec flights n°2, 3 and 4 and Dauphin flights n°1 and 4 to gather vibration measurements. Instead of an OROS system, as originally planned, three less intrusive vibration sensors Slamstick S4-E100D40 (made by enDAQ) were placed at the three locations described in Figure 2-2.

► Figure 2-2 Slamstick accelerometers location (same on both helicopters)



These 3 positions (called T1, T2 and T3) were:

- T1: under the pilot seat;
- T2: on the lower rear left MGB attachment rod;
- T3: on the mechanical floor next to the Center of Gravity.

The Slamstick sensors were screwed on specially designed fixation supports, as shown on the Fennec in Figure 2-3.

► *Figure 2-3 Slamstick sensor (T2) on its fixation support in the Fenec*



Each Slamstick S4-E100D40 sensor holds three piezoelectric accelerometers (+/- 100 g), and was configured with a sampling frequency of 8192 Hz.

After the flight, the Slamsticks could simply be removed and the data collected through a USB cable.

After each flight, the data collected by the FTI was converted into csv files, with the list of parameters previously agreed upon with ONERA, and at an extraction frequency of 10 Hz.

These csv files were provided to ONERA and were also used by DGA-EV in order to provide the results analysis for the test reports.

The flight test engineer notes were used to obtain a first estimation of the VRS times, along with the pilots feedback for each test run.

The vibration data measured by the Slamstick sensors was converted to Matlab file format (.mat), and transmitted to ONERA.

2.4 Test method and means

The two objectives described previously in §2.2 focus on two different phases of the VRS.

The first objective involves the entries, i.e. the conditions in which the helicopter can enter into a VRS and the observations made during such a state.

The second objective is dealing with the exit, and the efficiency of the pilot technique used to recover from a VRS.

Regarding the first objective, the focus was to refine the predicted VRS domain computed by ONERA as given in Figure 2-4, mainly based on DGA-EV test flights performed between 2000 and 2015 on Dauphin and Fenec

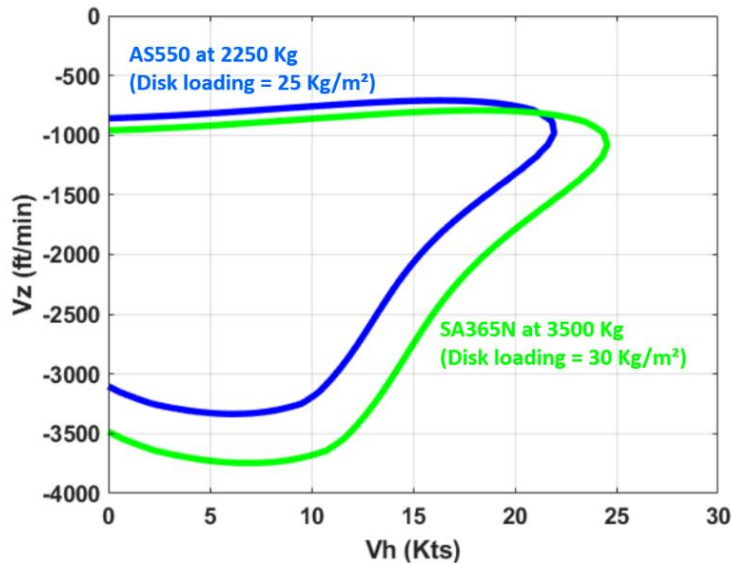
helicopters, and where V_h is the horizontal airspeed in the helicopter reference frame ($V_h = \sqrt{V_x^2 + V_y^2}$). The blue curve shows the Fenec AS550-U2 domain, the green curve shows the Dauphin SA365N domain.

The VRS domain is divided into three main zones, as illustrated on Figure 2-5:

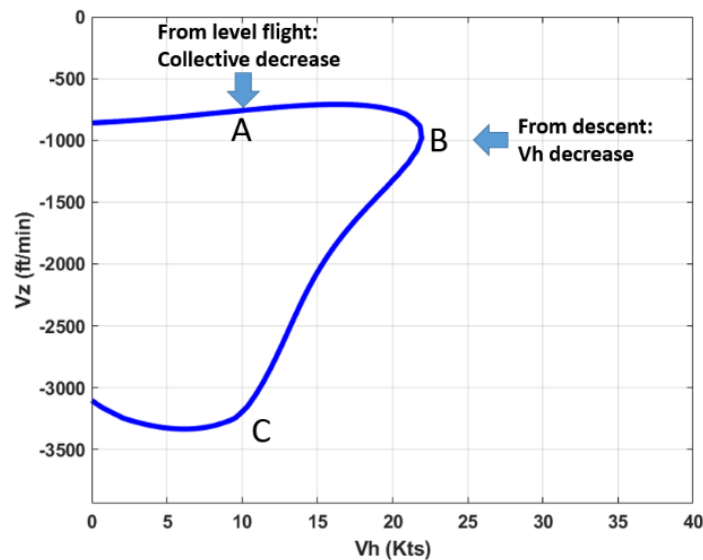
- The “upper boundary” → zone A;
- The “knee” → zone B;
- The “lower boundary” → zone C.

This study included entries through the A and B boundaries. The C boundary (lower part) of the VRS domain does not match any operational conditions, and was therefore not investigated as an “entry” boundary. Nevertheless, it corresponds in flight to the stabilisation of the vertical speed after VRS entries from the upper boundary or the knee.

► Figure 2-4 Vortex-Ring-State prediction domain the two helicopters



► Figure 2-5 Generic Vortex-Ring-State domain with main zones



2.5 Repeatability of the VRS entries

During the harmonization flights, several parameters were noticed to have an influence on the time to enter VRS for similar flight conditions, such as the dynamic of the power reduction. In order to avoid the influence of unwanted parameters on the results, the following actions were taken to improve the repeatability of entry manoeuvres, and to ensure the validity of the comparisons between both recovery methods for similar entry conditions.

First, two test pilots were trained to ensure they were adequately performing the Vuichard recovery manoeuvre. They also flew harmonization flights together to calibrate their movements and avoid any discrepancy. They were the only evaluators involved in this test campaign. When only one of them was available for a flight, he was the single evaluator during the flight, and another DGA-EV pilot was present as a safety pilot.

Secondly, the action on the collective stick was “standardized” by decreasing the power rapidly to a torque of about 50%, and then wait a few seconds. If the aircraft did not enter VRS, the power would then be decreased slowly towards 20% torque. The 50% torque was chosen based on observation made during preliminary flights, as it was found to be slightly above the power level at which VRS was entered in the test conditions.

To verify the “upper boundary” (zone A) as defined in Figure 2-5, the action sequence was therefore:

- the initial conditions were captured : hover, or horizontal translation (in level flight). The sampling to verify the VRS prediction domain was done with increment of 5kt on the horizontal airspeed V_h from 0kt to +15kt;
- the collective grip was reduced rapidly to the preset power ($P_{TQ50\%}$). Then, if needed, the power was reduced further until VRS started to develop (the required power level was typically lower when starting in translation, as opposed to starting from hover).
- once in VRS (identified by the crew as described in §2.6), the chosen recovery technique was applied.

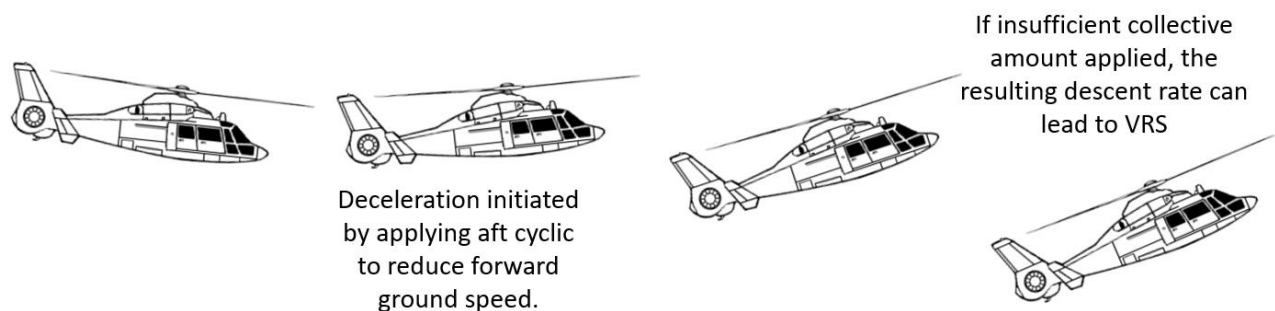
To verify the “knee” (zone B) of the domain, the sequence was:

- to establish a rate of descent V_z of around -1000ft/min and an airspeed of about 30kt ;
- to reduce the power (rapidly toward $P_{TQ50\%}$, then more slowly) and adjust the airspeed to maintain the rate of descent, up to the point where the VRS starts to develop;
- once in VRS (identified by the crew as described in §2.6, the chosen recovery technique was applied.

The “lower boundary” (zone C) was considered to correspond to the stabilisation of the vertical speed after VRS entries from the “upper boundary” or the “knee”.

Some test runs were performed starting from a quick-stop to evaluate dynamic entries. A quick-stop is a manoeuvre used to quickly reduce speed from a forward flight or a descent to a hover, starting with a flare (nose up) and then a deceleration(as illustrated in Figure 2-6). If the pilot allows the helicopter to descend, the helicopter can enter VRS. Pilots were instructed to perform quick-stops as they were trained, and if necessary to enter VRS by accepting a higher than usual descent rate.

► Figure 2-6 Quick-stop manoeuvre



2.6 VRS confirmation in flight

Tests runs were performed with either a recovery initiated at the first signs of VRS (recovery at vortex onsets, as recommended by Mr Vuichard), or once the VRS was established.

Recoveries at vortex early stages (onsets):

For the test runs with recoveries at vortex onsets, the real-time decision was based on the pilot and crew perceptions: change or increase of the vibration levels or noise, increase of the descent speed (and fleeting feeling of “lightness”), or change of the controls’ efficiency for example. For the entries performed in descent, the entry in VRS was not as noticeable, but could be identified when the pilot could not maintain the targeted vertical speed anymore. Although necessarily subjective, this judgment was deemed reproducible.

It should be noted that attempting a recovery at the vortex onsets does not guarantee that the recovery begins as soon as the aircraft enters the VRS domain: it only ensures that the recovery is initiated as soon as the vortex is detected by the crew. Depending on the early signs and on the pilot's reaction time, a recovery "at the onsets" - such as defined in the context of this report - may occur once the aircraft is well inside the VRS domain, in what is physically an established VRS.

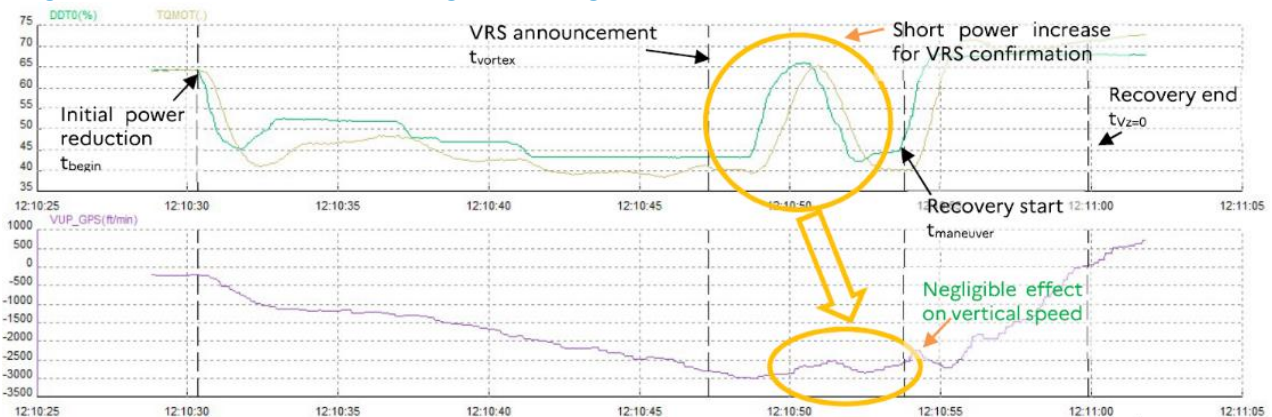
Data analysis after the flight could not be used to confirm the VRS, except to simply check that the vertical rate of descent was inside the predicted VRS domain.

As this will be explained later in §3.1, ONERA re-evaluated the test cases performed at VRS onsets and considered flight test parameters instead of pilot judgement to proceed to the analyses.

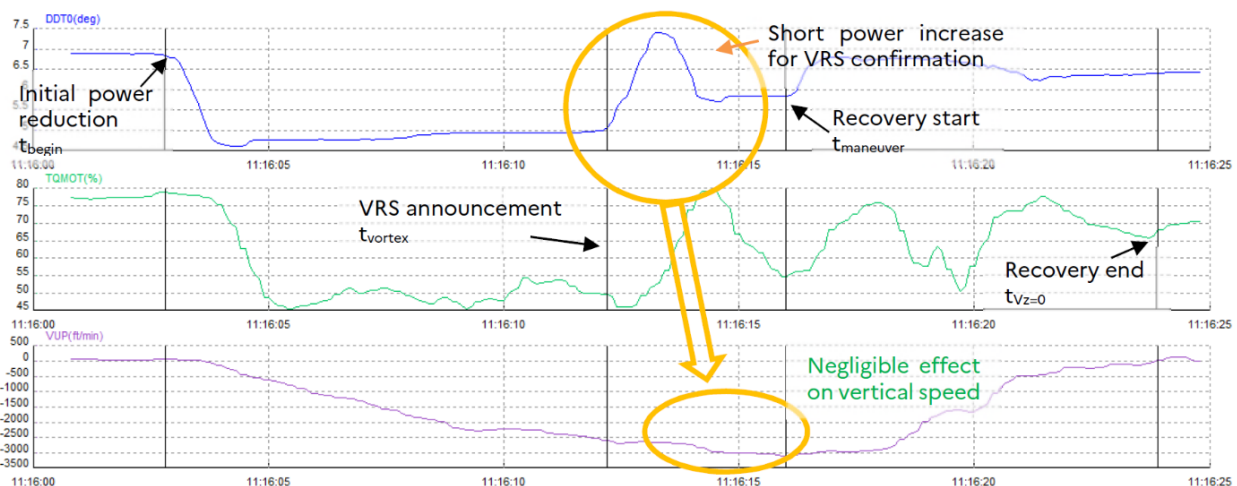
Recoveries from an established vortex:

For the test runs with recoveries from an established vortex, the real-time analysis from the crew could be confirmed with an evaluation of the effect of short power increase. Indeed, in VRS an increase of power has a limited effect on the vertical speed, whereas in normal conditions the same increase of power will significantly reduce the vertical speed. This effect was studied during the Dauphin harmonisation flight. Based on this result and on both helicopters, the VRS was confirmed post-flight if the effect of the collective increase on the vertical speed was negligible (in practice, lower than about 500 ft/min), as shown on both Figure 2-7 and Figure 2-8 for example.

► Figure 2-7 VRS confirmation during Fennec flight

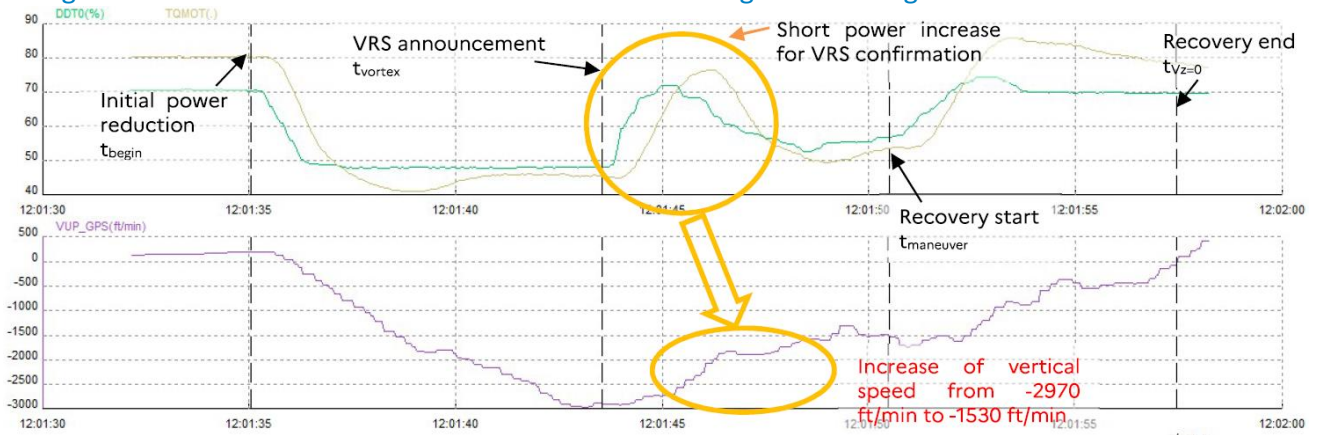


► Figure 2-8 VRS confirmation during Dauphin flight



Otherwise, when the effect was significant, as shown in Figure 2.9 for example, the test point was invalidated.

► Figure 2-9 Invalid run due to the unconfirmed VRS during a Fenec flight



2.7 General description of the recovery manoeuvres

Based on reference [2], the two main recovery techniques can be described as follow:

“Forward” recovery technique:

- Reduce collective
- Ease cyclic forward to adopt a nose down attitude
- Maintain heading by using the pedals
- When the airspeed is above translational lift, increase collective to maximum continuous power to climb

“Vuichard” recovery technique:

- Raise collective to use all the available power;
- Simultaneously, apply lateral cyclic in the direction of the tail rotor thrust (for CCW rotor-system escape to the right and for CW rotor-system escape to the left);
- Simultaneously, maintain heading by using the pedals, i.e. apply crossed pedal input corresponding to anti-torque rotor thrust;
- Once the descend is stopped, ease cyclic forward to regain airspeed.

But, as a useful element of context regarding the forward recovery, Airbus Helicopters currently recommends a recovery by checking power, and if residual power is available, **increase** the collective and apply forward cyclic pitch to accelerate. Once the airspeed is above 20-30kt and the RoD is managed, adjust the cyclic and collective pitches to establish the desired attitude, airspeed and altitude (as described in SIN-3123-S-00, reference [3]).

In addition, during the first harmonization and test flights, it was noticed that height loss during a VRS recovery appeared to be correlated with the torque applied during the manoeuvre (as confirmed by the results in §4.2.2). The higher the torque applied, the smaller the height loss. It was thus agreed to perform the forward recovery by **increasing** the collective toward an optimal power level (about 70% of torque on both aircraft) to reduce the height loss without exceeding the engines limitations. This level of 70% of torque was applied at the initiation of the recovery manoeuvre.

Thus, the “forward” recovery technique that was applied during the flights can be described as follow:

- Ease cyclic forward to adopt a nose down attitude and simultaneously **increase the collective** to 70% of torque
- Maintain heading by using the pedals
- When the airspeed is above translational lift, increase collective to maximum continuous power to climb

The “Vuichard” recovery technique that was applied during the flights was similar to the previous description and based on reference [2].

2.8 Repeatability of recovery manoeuvres

As a mean of standardisation, the following parameters were defined for both recovery techniques:

- The Vuichard recoveries were performed – as recommended by Mr Vuichard – by using the available power, that is to say the higher power that could be applied without exceeding the aircraft limitations, while simultaneously using the cyclic stick to reach a roll angle of $\varphi=-20^\circ$ (toward the left) maintained for one second and the foot pedals to maintain the heading. After about one second, the roll angle was brought back to zero. Since a parasitic nose-down motion resulted in a tendency to increase the forward speed during the last part of the recovery, some test points were performed trying to fight this parasitic effect and to come back to hover as soon as possible, and others by accepting this forward speed and focusing on recovering a positive vertical speed;
- The inversed Vuichard recoveries were performed similarly to the Vuichard recoveries, but with an exit on the “wrong side” at a roll angle $\varphi=+20^\circ$, i.e. toward the right for the Fennec and Dauphin. This idea was to assess the consequences of either a mistake by the pilot, or of the impossibility to perform a Vuichard recovery toward the left, due to an obstacle for example;
- The forward recoveries were performed using an optimal power setting, balancing between the positive effect of power on recovery performance, and the workload typically associated to watching the aircraft limitations at higher power settings. For both helicopters, this optimum was found at a target of about 70% of torque. In addition, in order to gain forward speed, an optimum of -15° of pitch down angle was found.

2.9 Test runs procedure

Due to the limited number of flight hours allotted to this campaign, and to avoid losing too much time outside the VRS domain, the following procedure was followed to optimise the completion of both objectives and to ensure a good repeatability of the pilot actions in both entries and exits of VRS:

- the approach conditions were stabilised with the low airspeed indications at predefined value in stabilised flight path (either in level flight or in descent depending on the test points);
- the pilot then reduced the power to $P_{TQ50\%}$. If VRS was not entered during the next few seconds, the pilot could then reduce the power further. This ensured a good repeatability of the collective stick actions leading to VRS entries. The test runs from a dynamic entry such as a quick-stop were the exception to this rule: the pilot was free to manage the power level to reproduce as realistically as possible the expected trajectory.
- then, once in VRS:
 - for the runs with an exit at **the VRS onsets**, the pilot immediately started the recovery procedure (forward or Vuichard);

- for the runs with an **exit from an established VRS**, the pilot first applied an increase of power to check the effect on the vertical speed (which should be negligible if in VRS), reduced the power back to its initial level, and then started the recovery procedure.
- finally, two criteria were used to evaluate the exit from the VRS:
 - the announcement from the pilot that he had regained control of the aircraft and was out of VRS;
 - the time at which the vertical speed came back to a positive value.

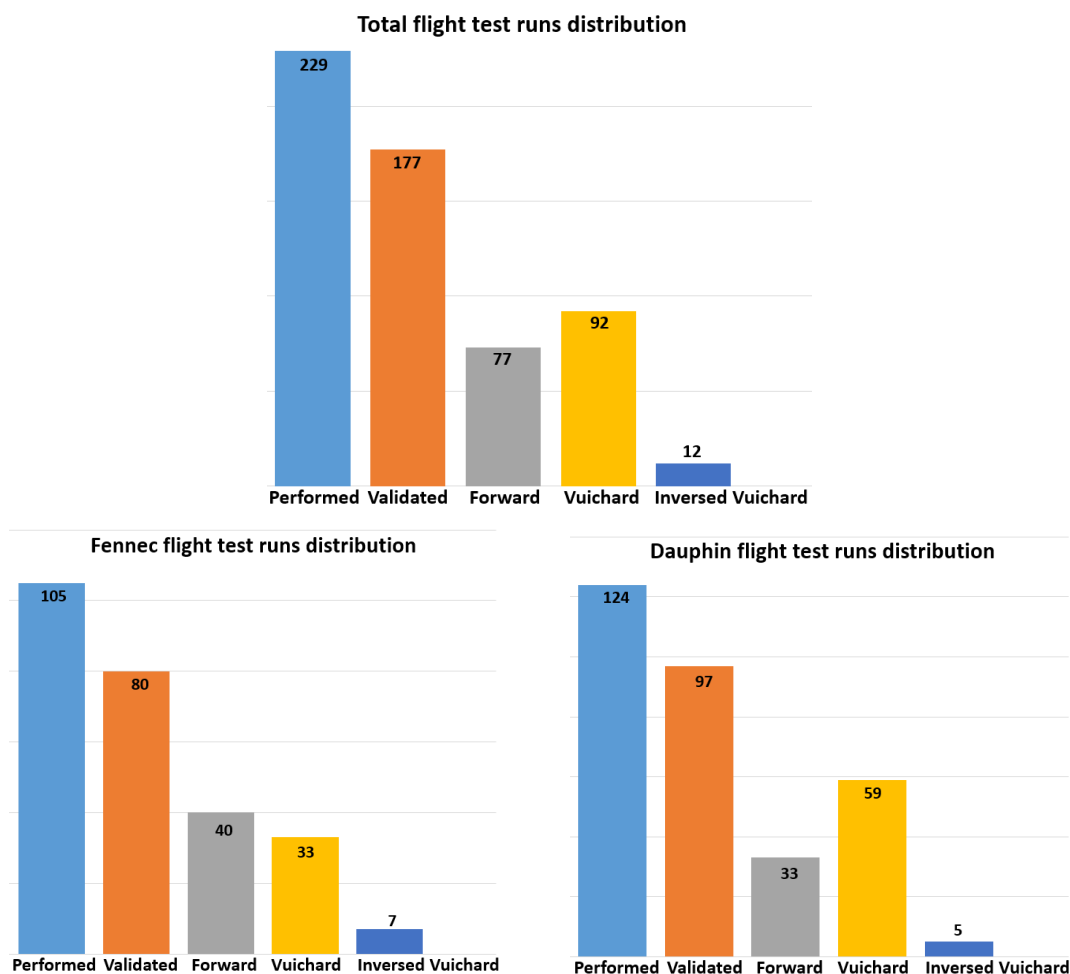
All tests were performed above a safety altitude of 3000 ft, below which a forward recovery procedure would be initiated if still in VRS.

The take-off weight and centre of gravity were similar for each flight, which were performed with the same configuration, fuel on board, and crew size. The reduced weight (Mass/σ where σ is the relative air density ρ/ρ_0) was maintained as constant as possible for the entries into VRS.

2.10 Test runs distribution

On a total of 229 runs performed during the eight flights, 177 runs were finally validated. 146 recoveries were performed in a fully developed VRS and 31 at VRS onsets. Following figures provide the flight test runs distribution.

► Figure 2-10 Flight test runs distribution



3. Vortex-Ring-State phenomenon

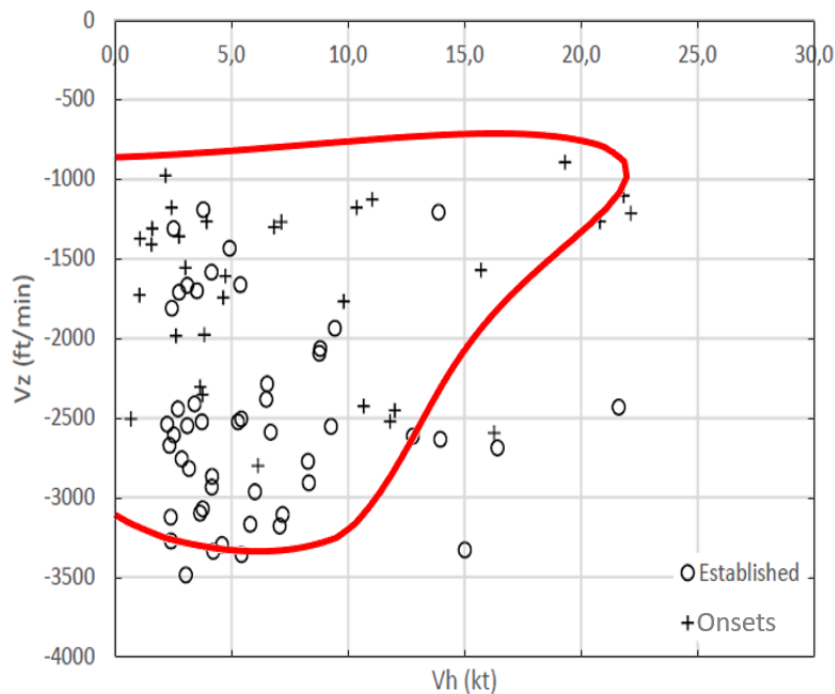
3.1 VRS domains

3.1.1 Fennec

The VRS Domain observed after the Fennec test campaign is shown in Figure 3-1.

For each validated test run, the vertical speed and the horizontal speed (all obtained from the GPS-inertial hybridisation) were extracted at the time the pilot announced he was in VRS (t_{vortex}).

► Figure 3-1 Fennec VRS domain based on pilot perception



When overlaid with ONERA predicted VRS domain (red curve), a good consistency is observed between the predicted VRS domain and the actual test points.

It should be noted that for the runs realised at the VRS onsets, no verification could be done to confirm the VRS (neither in real-time or post-flight), therefore there is a lower confidence of actually being in VRS during these runs and prudence is recommended in their exploitation.

The points observed at speed higher than 15 kt were obtained either in descent, or during a quick-stop manoeuvre, with rapidly changing speeds, and are therefore very sensitive to the timing of the pilot announcement.

A first look at the figure shows that the vertical speeds at the time VRS were detected are higher on average for the runs with a planned exit at the VRS onsets, compared to the runs with a planned exit in established VRS. In theory the choice onsets/established should only affect the time " t_{maneuver} " at which the recovery is initiated (and indirectly the corresponding rate of descent, expected to be higher when a longer time is spent in VRS). It should not however affect the time at which the VRS is detected, nor the rate of descent at this time.

Two reasons can explain this observation:

- After the first flight, runs in established VRS were systematically performed before the runs at VRS onsets, for a given set of entry conditions, precisely to help the crew identify the VRS signs. Therefore, the VRS signs were better recognised or easier to notice during the latter runs;
- Also, as runs in established VRS were less time sensitive, the pilot could take more time to make sure he was in VRS before announcing it.

Two facts can be observed when comparing with VRS estimated domain in Figure 3-1:

- The VRS were detected – or more precisely announced – often once well inside the VRS domain. This can be explained by the strong changes on the vertical speed when entering VRS: a few seconds taken by the pilot to make sure he recognises the signs of VRS quickly result in an additional -1000 ft/min in vertical speed (on a related note, the vertical speed plotted can change significantly based on the timing of the pilot announcement. Another test method would be required to better estimate the vertical speed of the VRS domain upper boundary, see below);
- To avoid any confusion, points “at the VRS onsets” are to be understood (in the context of this report) as recoveries performed as soon as the VRS is detected, but not necessarily as soon as the VRS domain is entered. This means that a recovery “at the onsets” can actually be performed from a well-established VRS when considering the airflow around the helicopter.

The analysis of the data collected has been performed by ONERA and is presented hereafter.

As indicated previously, the DGA-EV determined the VRS boundaries through pilots feedback and their ability to recognise the phenomenon. In the following figures, upper boundary (blue plots) were determined thanks to the analysis of several flight parameters such as the vertical acceleration, pilot controls, a specific data processing of the altitude or more specifically for the Fennec, the analysis of the sideslip measurement device positioned just above the windscreen. These analyses were based on an empirical approach, in which each flight test run was processed separately. The numerical gradient of the pressure altitude ZP was computed. Thus, gradient (ZP) returns the one-dimensional numerical gradient of the pressure altitude recorded vector. The output corresponds to $\partial ZP/\partial x$, which are the differences in the x (“horizontal”) direction. The spacing between points is assumed to be 1. As an example, considering the n-th sample of ZP, then :

$$\text{gradient ZP}(n) = \frac{ZP(n+1) - ZP(n-1)}{2}$$

In addition, the standard deviations of the accelerations and the sideslip angle were calculated over a sliding window of 0.5s. The estimation of the VRS entry was then based on an overall analysis of these parameters and different criteria were considered:

- Increase of the standard deviation of the acceleration or/and;
- Increase of the standard deviation of the sideslip angle or/and;
- A pressure altitude gradient lower than -3 ft;

The value of -3ft for the pressure altitude gradient criterion was empirically determined.

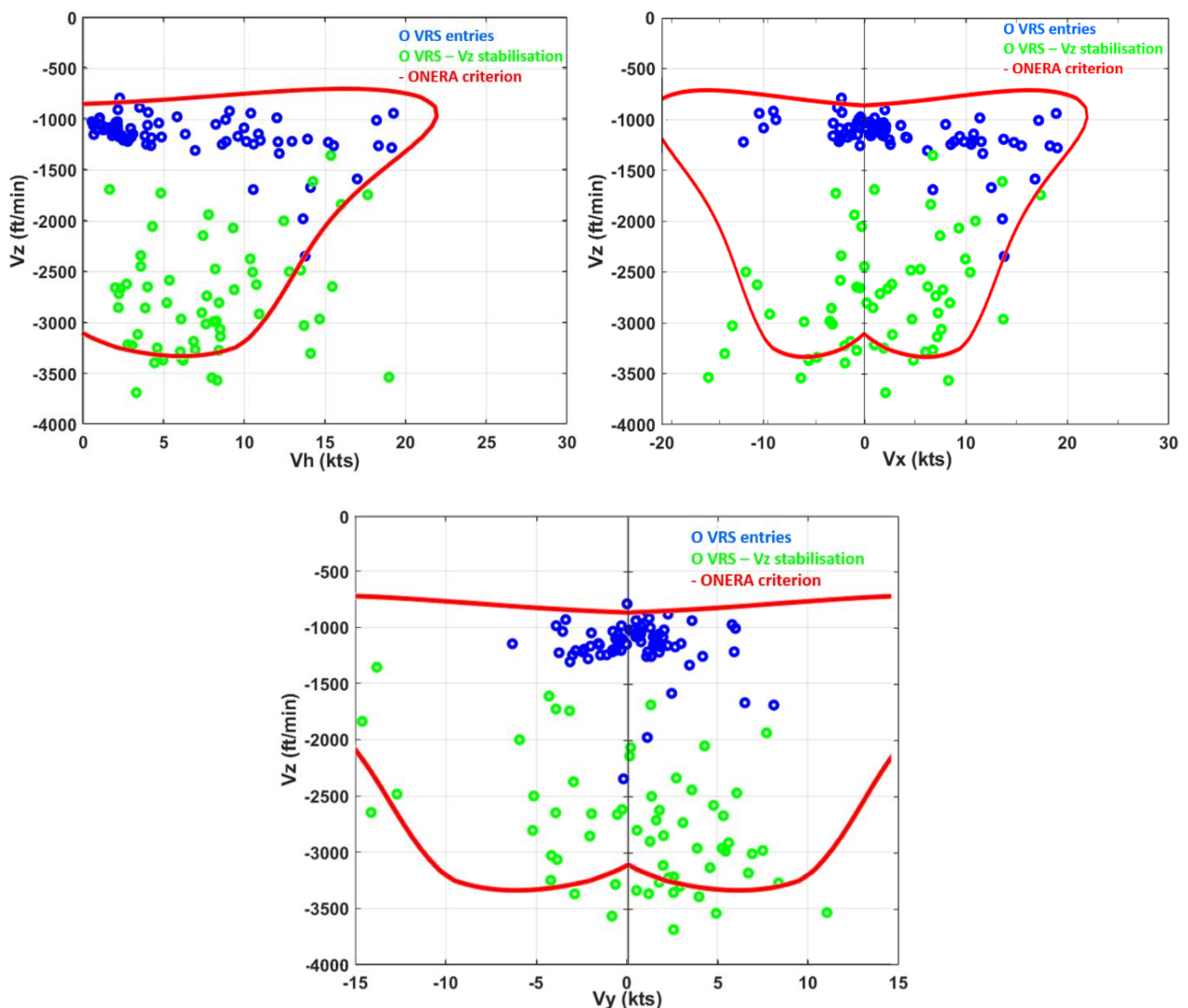
Regarding the level of the standard deviations on all parameters, no specific thresholds or absolute values were considered but a large and rapid increase compared to the beginning of the run. Not all of these criteria had to be met to establish a VRS entry. In some cases, it was impossible to determine the VRS entry thanks to these analyses and the pilot announcement in flight was thus retained.

Regarding the lower boundary (green plots), it was determined through the analysis of the vertical speed and the green plots in the figures correspond to a stabilisation of the descent rate. In many cases, the recovery manoeuvres were initiated before this stabilisation, leading to the impossibility to determine the lower VRS domain boundary in these conditions. Figure 3-2 shows the Fennec VRS domain. The first upper-left graph

represents the domain in terms of horizontal speed V_h and vertical speed V_z . The upper-right graph shows this domain in terms of longitudinal speed (V_x) with respect to the vertical speed V_z . The lower graph finally shows the VRS domain in terms of lateral speed V_y and the vertical speed V_z . Blue points are corresponding to estimated VRS entries, the green points the lower boundary (as previously shown in Figure 2-5) corresponding to the stabilisation of the vertical speed.

While a large dispersion of the points can be observed, especially for the lower VRS boundary, the domain is comparable to the one determined by the DGA-EV. The observed VRS domains match the predicted ONERA domain presented in red, even if the maximum descent rates reached in flight seem a bit higher than the predicted ones. As shown on the second graph, while some points corresponding to the lower boundary were reached at higher descent rates and negative longitudinal speeds, the VRS domain seems symmetrical with respect to the longitudinal speed. This is also the case regarding the VRS boundaries with respect to the lateral speed as shown in the lower graph. Additional flights should be performed with lateral speeds to investigate the VRS domain at lateral speeds between 10 kts to 20 kts and see if the boundaries are comparable to those observed with longitudinal speeds. In this analysis, the fact that the points could be performed at VRS onsets or established VRS is not considered.

► Figure 3-2 Fennec VRS domain based on post-flight processing and analysis



3.1.2 Dauphin

The first Dauphin flight was performed on Dauphin D6116, all the next ones on Dauphin D6111.

As described in §2.3.3, two type of low speeds measurements were available :

- VIMI NUM : which is based on the cyclic position (through a complex calibration process) and gives the speed of the H/C in the air mass (which is what we want) BUT is not reliable in a VRS or with unusual H/C attitudes;
- VIMI GPS : which calculates the airspeed by subtracting the local wind to the GPS speed. It is reliable even during VRS, although it relies on the wind being laminar and stable. It was the preferred method for speed measurements in VRS.

During the first flight, and during the calibration of the VIMI GPS, discrepancies between the VIMI GPS calculated horizontal speed and the VIMI NUM (and the external red string) were observed : basically the VIMI GPS was giving a non negligible airspeed while the helicopter was clearly in hover. After several attempts, it was decided to use the VIMI NUM, which is reliable to set the initial entry conditions, but not once descending to enter VRS.

This problem was not observed in the following flights on the Dauphin D6111, where VIMI NUM and GPS were consistent.

This is why flight n°1 was excluded when trying to assess the effect of the horizontal speed on the recovery performance. This is also why the the VRS Domain observed after the Dauphin test flights and shown in Figure 3-3 doesn't integrate flight n°1 data.

For each validated test run, the vertical speed and the horizontal speed were extracted at the time the pilot announced he was in VRS (“ t_{vortex} ”).

It should be noted that for the runs performed at the VRS onsets, no verification could be done to confirm the VRS (neither in real-time or post-flight), therefore there is a lower confidence of actually being in VRS during these runs and prudence is recommended in their exploitation.

The points observed at speed higher than 15 kt were obtained either in descent, or during a quick-stop manoeuvre, with rapidly changing speeds, and are therefore very sensitive to the timing of the pilot announcement.

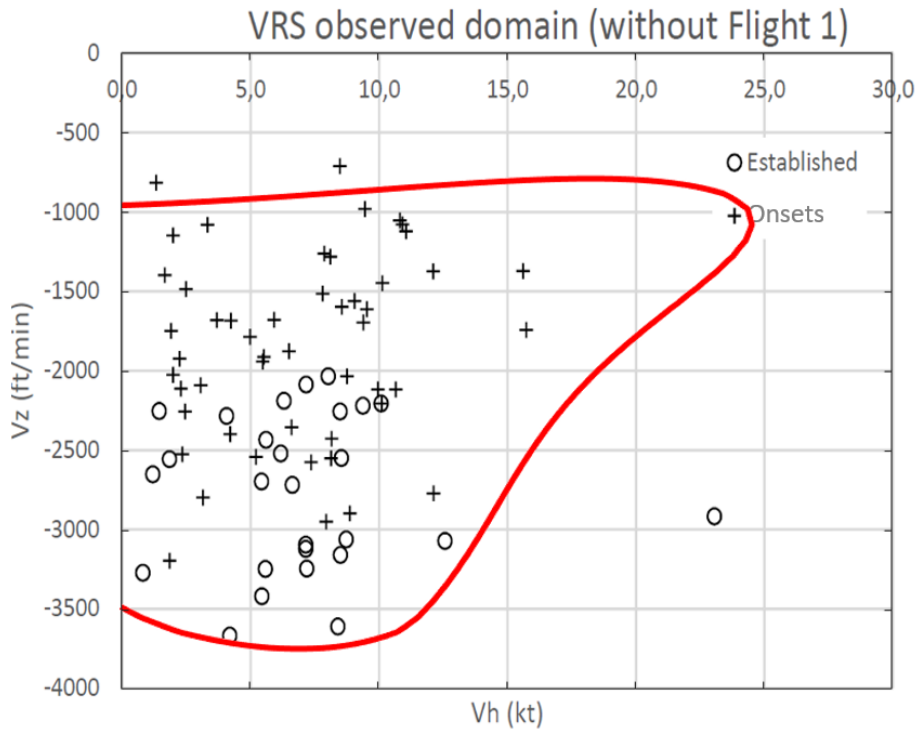
A first look at the figure shows that the rates of descent at the time VRS were detected are generally lower on average for the runs with a planned exit at the VRS onsets, compared to the runs with a planned exit in established VRS.

In theory the choice onsets/established should only affect the time “ t_{maneuver} ” at which the recovery is initiated (and indirectly the corresponding rate of descent, expected to be higher when a longer time is spent in VRS). It should not however affect the time at which the VRS is detected, nor the rate of descent at this time. A similar observation was made following the Fennec flights.

Two reasons can explain this observation:

- After the first flight, runs in established VRS were systematically performed before the runs at VRS onsets, for a given set of entry conditions, precisely to help the crew identify the VRS signs. Therefore, the VRS signs were better recognised or easier to notice during the latter runs;
- Also, as runs in established VRS were less time sensitive, the pilot could take more time to make sure he was in VRS before announcing it.

► Figure 3-3 Dauphin VRS domain based on pilot perception



When overlaid with ONERA predicted VRS domain (red curve), a good consistency is observed between the ONERA predicted VRS domain and the actual test points. The only outlier is Run 9.2 of flight n°3, which was achieved from a descent and with an unusual combination of a rearward speed (-14kt) and lateral speed (18 kt) at the time of the announcement.

Two facts can be observed from this figure:

- The VRS were detected – or more precisely announced – often once well inside the VRS domain. This can be explained by the strong changes on the vertical speed when entering VRS: a few seconds taken by the pilot to make sure he recognizes the signs of VRS quickly result in an additional -1000 ft/min in vertical speed (on a related note, the vertical speed plotted can change significantly based on the timing of the pilot announcement. Another test method would be required to better estimate the vertical speed of the VRS domain upper boundary, see below);
- To avoid any confusion, points “at the VRS onsets” are to be understood (in the context of this report) as recoveries performed as soon as the VRS is detected, but not necessarily as soon as the VRS domain is entered.

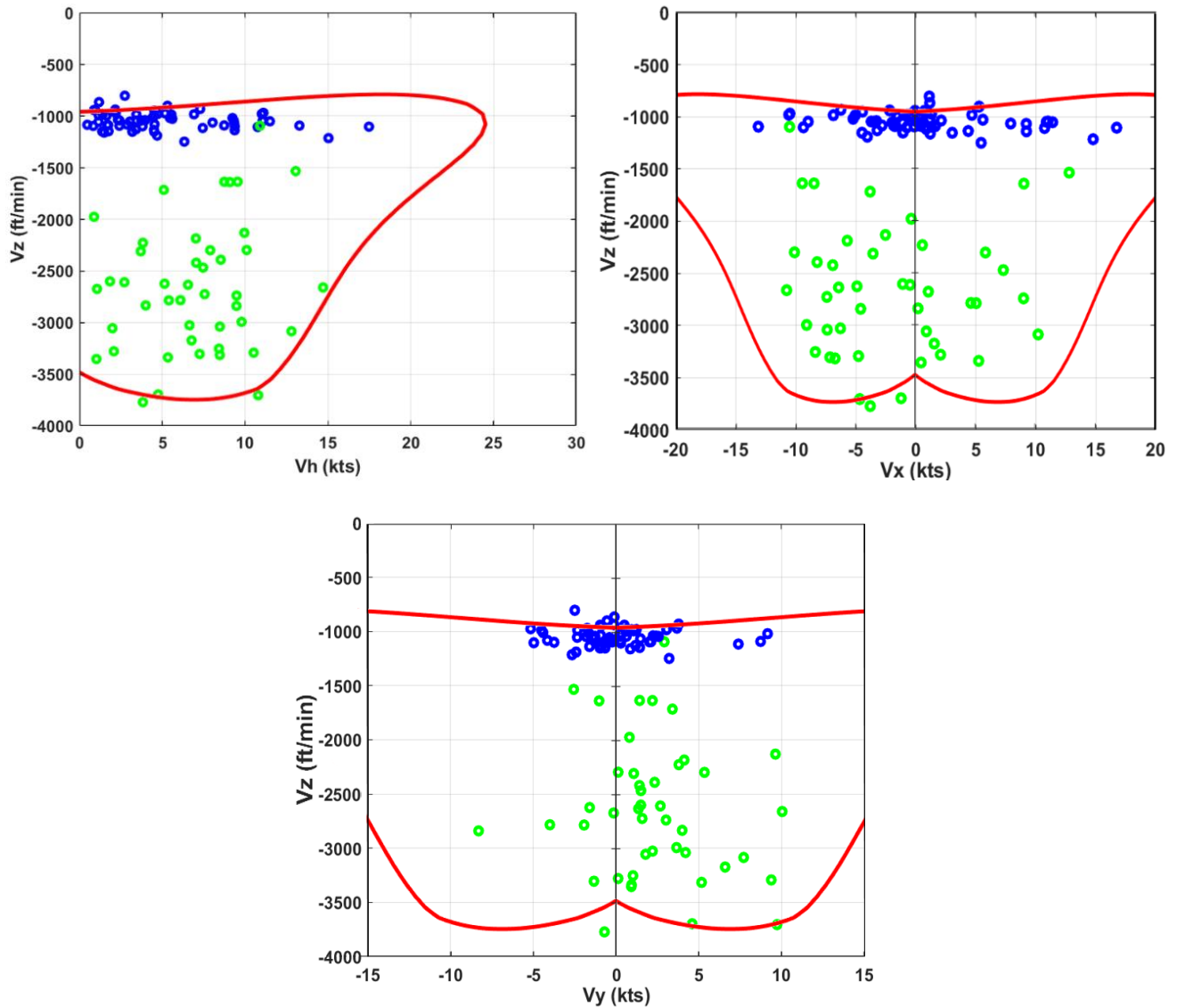
This means that a recovery “at the onsets” can actually be performed from a well-established VRS when considering the airflow around the helicopter.

As explained previously, ONERA analysed the flight data and the Dauphin VRS domain is shown in Figure 3-4. The first upper-left graph represents the domain in terms of horizontal speed V_h and vertical speed V_z . The upper-right graph shows this domain in terms of longitudinal speed (V_x) with respect to the vertical speed V_z . The lower graph finally shows the VRS domain in terms of lateral speed V_y and the vertical speed V_z .

As observed on the Fennec, the VRS domain seems relatively symmetrical with respect to the longitudinal or lateral speeds. Here again, additional test cases could be done to gather more data with higher lateral speeds. Compared to the ONERA predicted domain, the maximum horizontal speeds are lower in flight. This can be explained by the limited number of such test cases performed in flight on this helicopter and the difficulties to determine the VRS domain in these conditions. Generally, the “knee” is determined through decelerated flights,

but no case of this type has ever been flown during this campaign. Some runs were performed at -10 kts and 10 kts, and as for lateral speeds, additional flights could be done to investigate forward speeds between 10 kts and 25 kts.

► Figure 3-4 Dauphin VRS domain based on post-flight processing and analysis



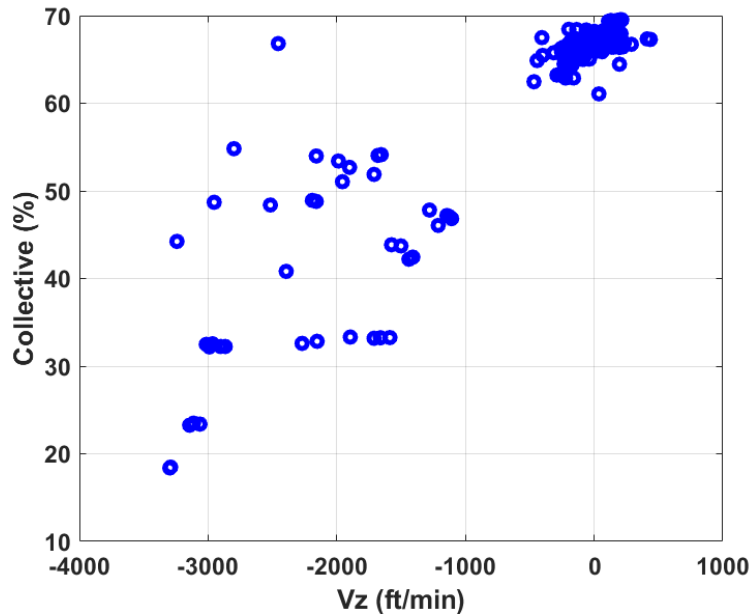
Based on different criteria, VRS domains are a bit different between DGA-EV and ONERA. This does not mean that one is better than the other, but it simply shows the influence of the selected criteria to define a VRS domain. This will be further seen when taking into account the increase of vibrations to determine VRS entries and exists.

3.2 Influencing parameters

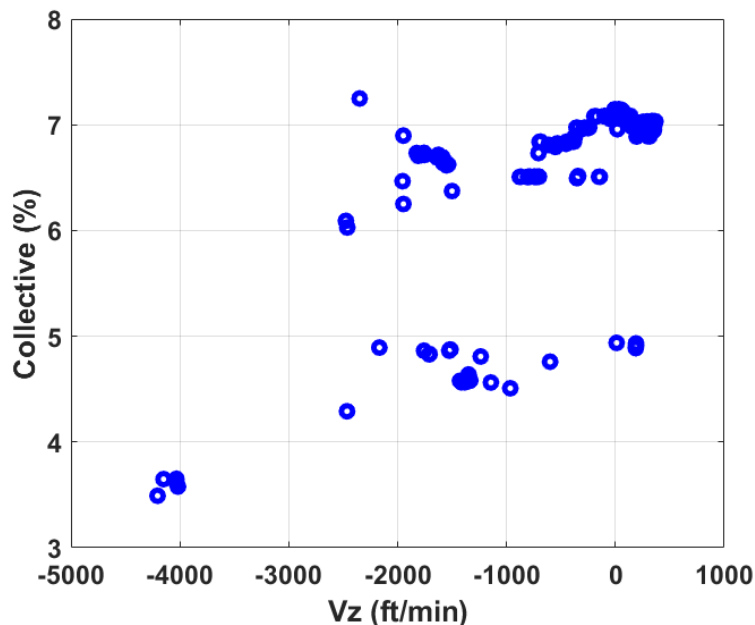
3.2.1 Collective pitch versus Vertical speed

As already observed in previous flight test campaigns and discussed in reference [1], the relation between level of collective and vertical speed is modified in VRS.

► Figure 3-5 Collective pitch versus vertical speed on Fennec – Forward recovery, established VRS



► Figure 3-6 Collective pitch versus vertical speed on Dauphin – Forward recovery, established VRS



In Figure 3-5, the blue points are taken from the first Fennec flight performed in the framework of this project and corresponds to the level of collective plotted with respect to the vertical speed in “stabilised” conditions. Actually, these points are plotted when during a run, and function of time, the variation of the vertical speed is

lower than 75 ft/min, the collective variation is lower than 1%, and for forward speeds between -5kts and +5kts. Figure 3-6 is showing the level of collective pitch plotted with respect to the vertical speed in “stabilised” conditions during forward recoveries in established VRS on the Dauphin.

On both helicopters, and more specifically on the Fennec, it can be seen that below -1000 ft /min down to -3000 ft/min, the collective/Vz curve is no more monotonous and several very different descent rates can be reached with the same level of collective.

On the Fennec, in climb and vertical descent down to -500 ft/min, a dispersion exists but the average collective/Vz curve is relatively monotonous. This is also the case for descent rates higher than -3000 ft/min.

On the Dauphin, a larger dispersion is observed.

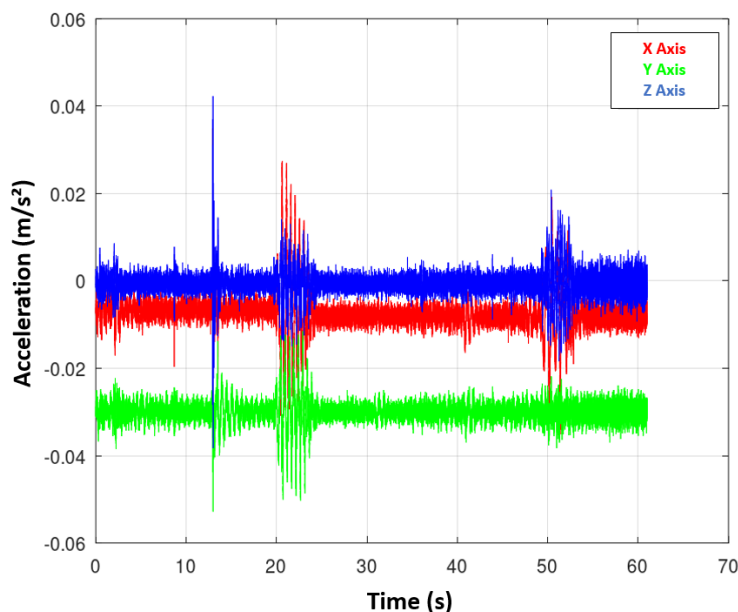
Nevertheless, considered as a criterion, this characteristic could be also used as the Vz drop, to define the VRS domain of a helicopter.

3.3 Vibration analyses

3.3.1 Vibration measurements

In order to synchronise the three different Slamstick sensors with the FTI time base, an action of the ground technician on the helicopter tail was done before the engine(s) start. As seen on Figure 3-7, This action resulted on a noticeable acceleration peak (here at 20 s), which was used during post-processing to synchronise the recordings.

► Figure 3-7 Synchronization of the slamstick sensors



3.3.2 Vibration analysis

Figure 3-8 represents the spectrogram established on the data taken from all axes of the three accelerometers during flight 3 (run 1) of the Fennec and corresponding to an established VRS. A spectrogram is a visual representation of the spectrum of frequencies as it varies with time. As shown on the graphs, a common format is a graph with two geometric dimensions: one axis represents time, and the other axis represents frequency; a third dimension indicating the amplitude (i.e. energy) of a particular frequency at a particular time is represented by the intensity or colour of each point in the image. In these cases, spectrograms are calculated from the time signal using the Fast Fourier transform.

As the acquisition frequency of the accelerometers was 8192Hz, the graph shows the frequencies contained in the signal up to 4096 Hz.

During this run, the pilot detected the VRS at 30 s. Based on post-flight analysis, ONERA considered the VRS entry at 22.9 s. The recovery manoeuvre started at 34 s and a null vertical speed was reached at 41.5 s.

From Figure 3-8, it can be seen that the vibration spectra is changed for low, but also for high frequencies. Rotor harmonics and energy are dissipated into a larger bandwidth signal.

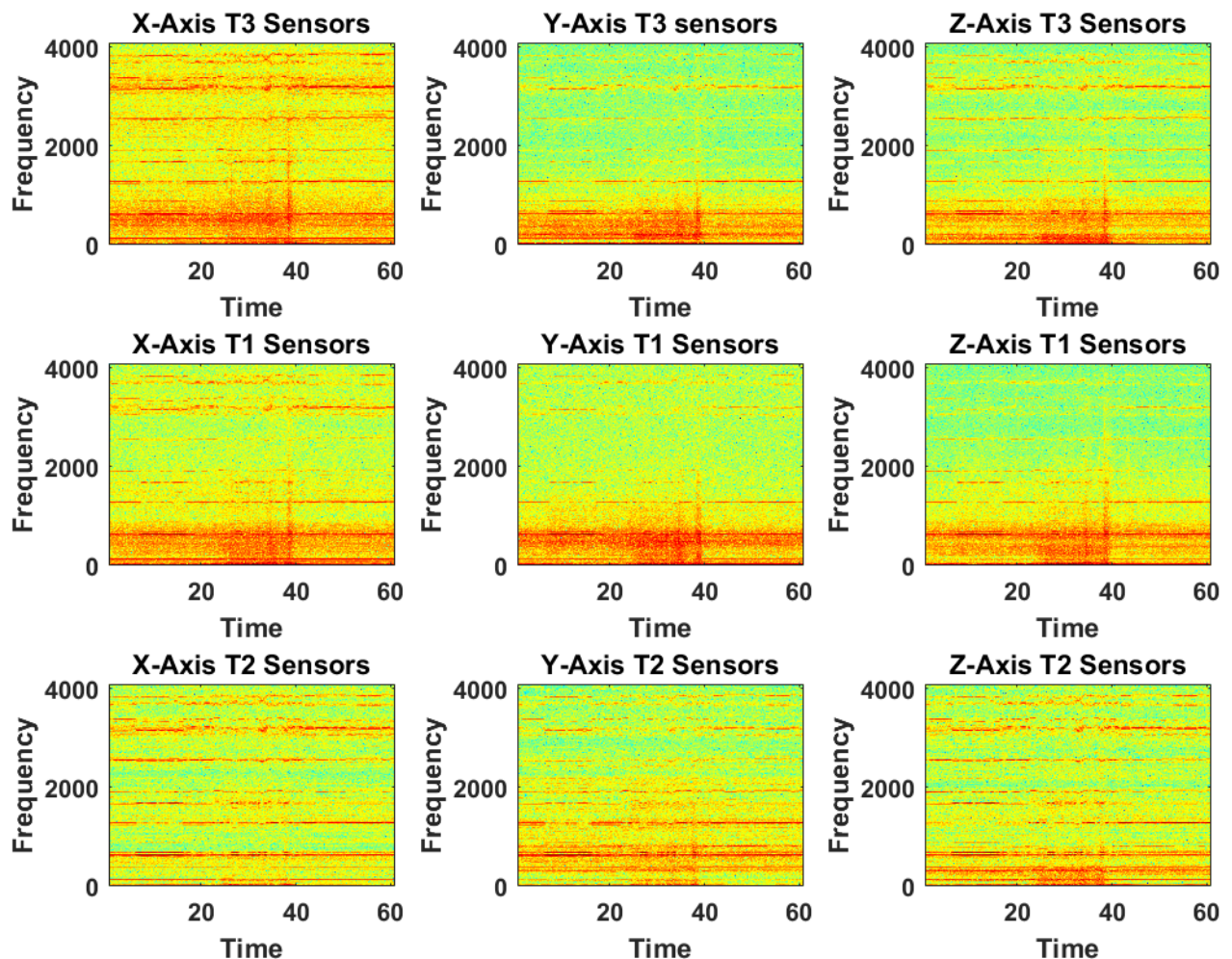
The graphs shown in Figure 3-9 are focussing on the Fenec main rotor blade passing frequency equal to:

$$\text{Main rotor blade passing frequency: } \frac{\text{Rotor RPM} \times \text{Nb of blade}}{60}$$

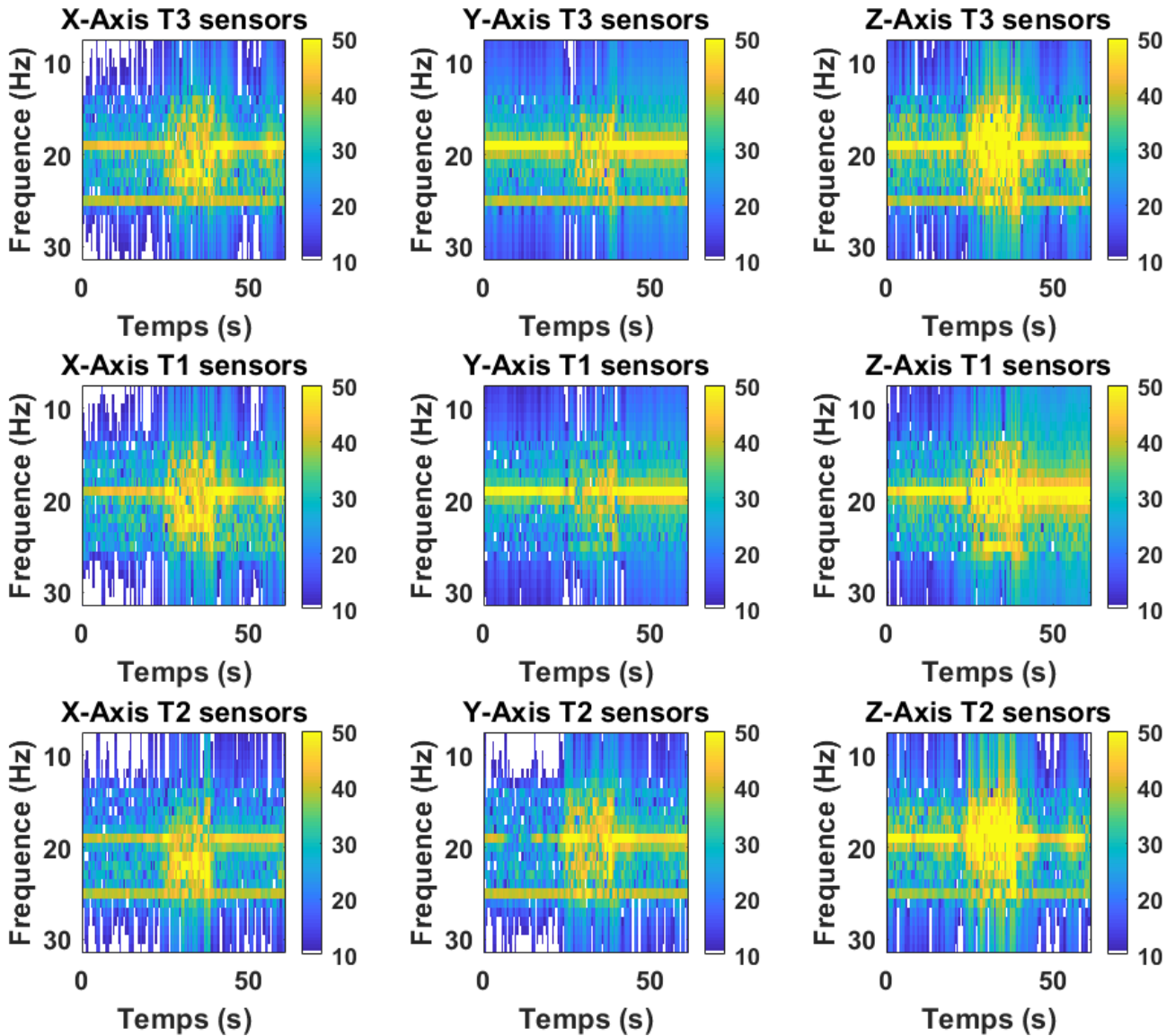
$$\text{Here: } \frac{390 \times 3}{60} = 19.5 \text{ Hz}$$

Considering the changes in the frequency spectra, and the energy dissipation around the main rotor blade passing frequency, vibrations due to VRS set-up are visible at around 25 s. It can be seen that the vibration spectra returned to normal at 42, corresponding to the VRS exit.

► Figure 3-8 Time-frequency plots



► Figure 3-9 Example of time-frequency plots – focus on main rotor frequency

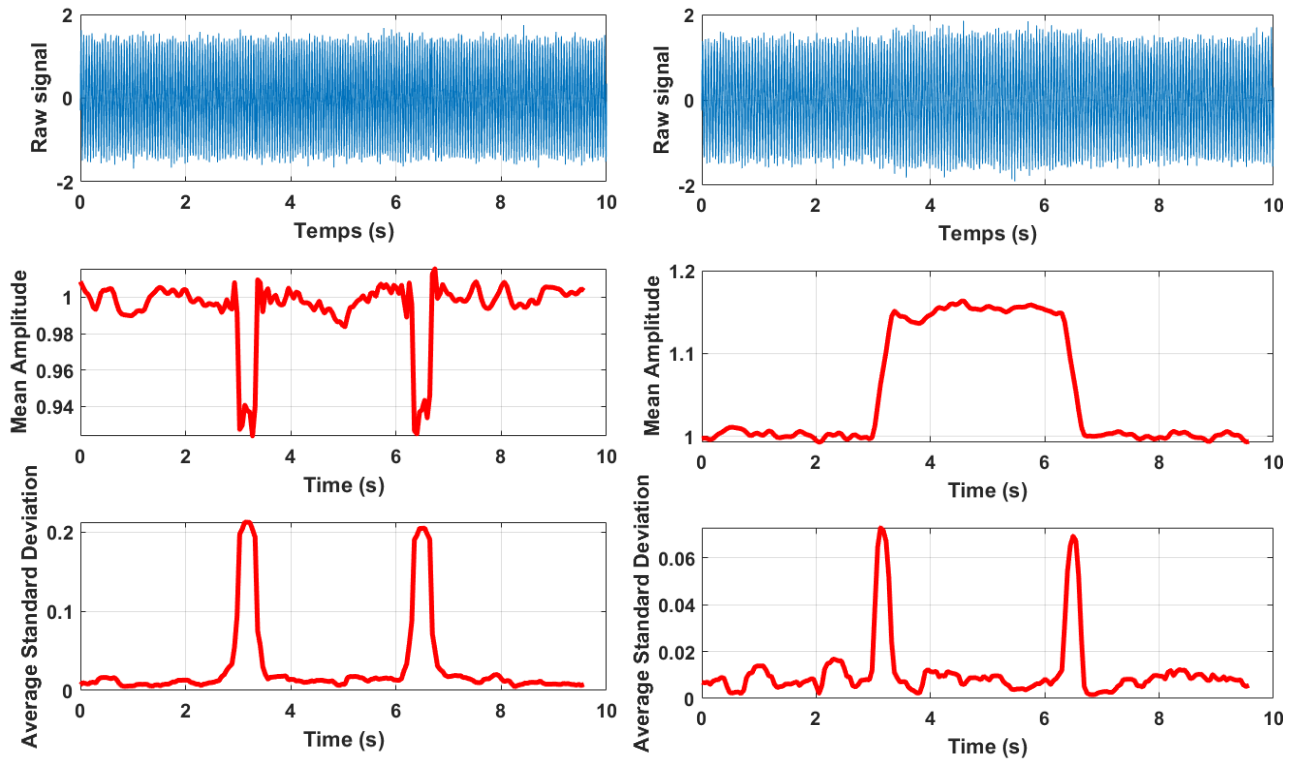


A vibration analysis has been carried out, by applying a Hilbert transform to the accelerometer data to extend the real signal into the complex domain. A Fast Fourier Transform (FFT) is then applied to the signal obtained by Hilbert transform. Then, the signal obtained by FFT is filtered from minus 5Hz to plus 5Hz around the fundamental frequency of the main rotor. The filtered signal is reconstituted by applying an inverse Fourier transform and producing a spectrogram on the reconstructed signal and removing the negative frequency part of the spectrum. The standard deviation of the amplitude of the spectrogram is calculated over a sliding window of predefined duration. If the calculated standard deviation is greater/lower than predefined thresholds, a detection signal is generated enabling the determination of VRS entry/exit.

Hereafter, examples are given to show the capability of the data processing to detect variation in a signal. A sinusoidal signal is generated for 10 s, on which a normally distributed white noise is added. On the left graphs of Figure 3-10, the frequency of the signal is set to 19.5 Hz from 0 s to 3.3 s, set to 20.5 Hz from 3.3 s to 6.6 s, and finally set again to 19.5 Hz from 6.6 s to 10s. While being impossible to see on the raw signal, the signal processing used is able to detect the time at which the changes in the frequency occur (see the average

Standard Deviation). On the right graphs of the Figure 3-10, the amplitude of the signal is changed from 1 to 1.15 between 3.3 s and 6.6 s. Here again, the change is almost impossible to perceive on the raw signal but the change of the amplitude is well capture on the second plot.

► Figure 3-10 Examples of signal processing



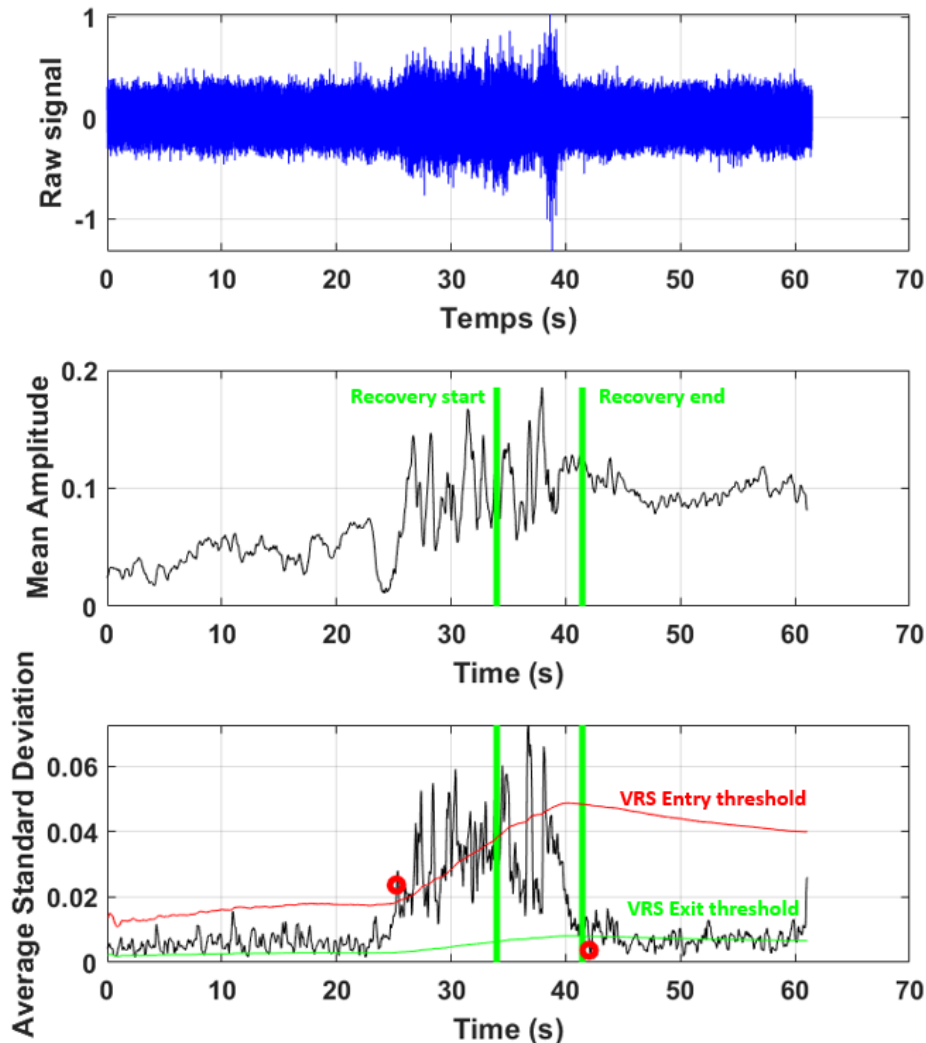
In the following Figure 3-11 the signal corresponding to the vertical axis of the Slamstick sensor placed under the pilot seat is analysed. A vertical descent was performed the collective pitch being decreased at 20 s. The pilot considered he was in VRS at 30 s.

The upper graph is the raw signal, the second one represents the mean amplitude and the third the averaged standard deviation. Green lines are corresponding to recovery manoeuvre start and end ($V_z=0$).

On the third graph, the red and green lines are corresponding to the VRS entry and exit thresholds during the manoeuvre.

The red circles represent the determined VRS entry and exit based on the data processing (i.e. when the calculated standard deviation is greater (entry)/lower(exit) than these thresholds).

► Figure 3-11 Example of a vibration analysis during a VRS on Fenec (Flight 3 run 1 – Established VRS, Forward recovery performed)



3.3.3 VRS Domains based on vibration analysis

As detailed previously, vibration measurements were analysed and can provide an estimation of the VRS entry and exit (red circles plotted in previous Figure 3-11).

Figure 3-12 and Figure 3-13 represent the VRS domains obtained thanks to this vibration analysis on both Fenec and Dauphin helicopters.

In addition to the VRS entries (blue circles) and VRS exit (green circles), which are here characterised by the start and end of the vibrations, the maximum level of vibration is also plotted. The red circles correspond to the maximum average standard deviation computed, and the black circles correspond to the maximum peak to peak (i.e. the difference between the highest and the lowest values in raw signal) measured during the run. The VRS domains based on the vibration increase are different from the ones shown previously. It can be seen that the vibration increase corresponds to the “normal” VRS domain, while the end of vibrations generally occurs later during the manoeuvre, when the helicopter is already out of the VRS (for higher forward speeds and positive vertical speeds). The maximum level of vibration seems to occur outside the VRS domain and during the recovery manoeuvre. This clearly shows that depending on the criteria taken into account to define the VRS domain, it can be different from one to another.

Figure 3-12 Fennec VRS domain based on vibration increase

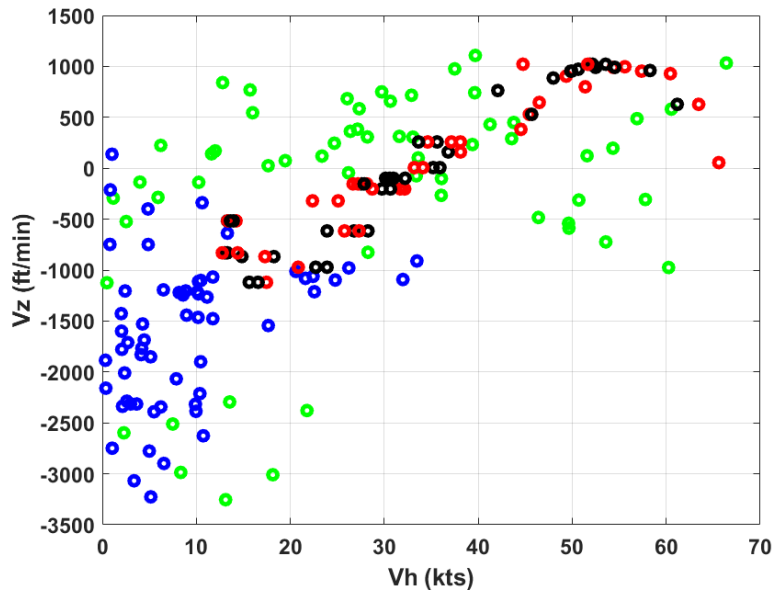
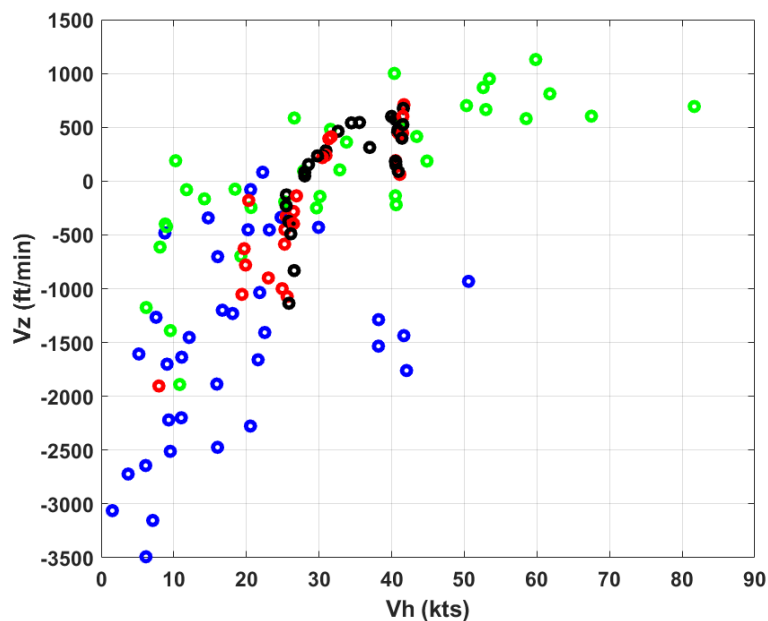


Figure 3-13 Dauphin VRS domain based on vibration increase



In addition, the maximum level of vibration may be experienced differently depending on the procedure followed during the runs. As indicated before, the recovery manoeuvres were performed as soon as the pilots considered they were in VRS. This is why it is difficult to estimate if the level of vibration is due to the VRS by itself, or the recovery manoeuvre.

A specific analysis has been done on the accelerometer data placed under the pilot seat. As shown in Figure 3-14, three stages of the runs have been considered. The first one (in green and noted as (1)) corresponding to the initiation of the run, in stabilised or at least “normal” flight conditions and used as the reference. The second one (in orange and noted (2)), being the initiation of the VRS, between the VRS detection performed by the previously detailed algorithm and the start of the recovery manoeuvre. The third stage (in red, noted (3)) only

considering the vibrations during the recovery manoeuvre (from the start of the manoeuvre to a null vertical speed).

As before, two parameters were analysed during these three stages: the average maximum peak to peak (noted P2P in the tables) measured in the raw signal, and the average maximum standard deviation (noted STD in the tables) processed (three coloured circles in Figure 3-14). The three axes of the accelerometer were analysed. In addition, two ratios provide the increase of level of vibration on the vertical axis (Z) during the VRS start (2) and recovery manoeuvre (3) compared to the initial flight conditions (1). Results are given in table 3-1 for the Fennec, table 3-2 for the Dauphin.

► Figure 3-14 Vibration analysis at different stages of the run

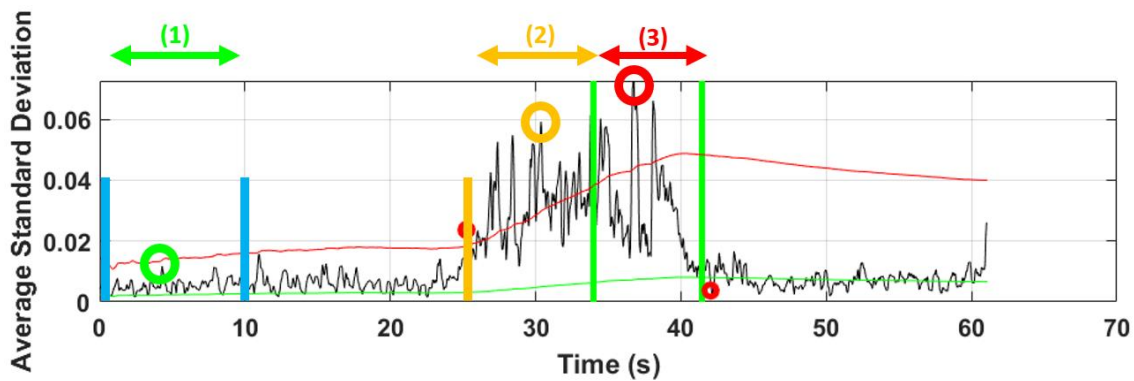


Table 3-1 Vibration VRS – Fennec

Recovery method - Conditions	P2P X (1)	P2P Y (1)	P2P Z (1)	P2P X (2)	P2P Y (2)	P2P Z (2)	P2P X (3)	P2P Y (3)	P2P Z (3)	Ratio Z 3/1	Ratio Z 2/1
Forward - Established	1.377	0.697	1.142	1.355	1.591	2.115	1.692	1.511	2.124	1.859	1.851
Vuichard - Established	0.972	0.664	1.109	1.368	1.65	1.903	2.054	1.687	2.77	2.496	1.715
Forward - Onsets	1.434	0.851	1.373	1.406	0.938	1.343	1.483	1.644	2.285	1.663	0.977
Vuichard - Onsets	1.283	0.71	1.121	1.338	0.781	1.361	1.361	1.376	2.158	1.925	1.213
Inversed Vuichard	0.791	0.466	0.772	0.889	0.75	1.256	1.247	0.955	1.771	2.29	1.625

Recovery method - Conditions	STD X (1)	STD Y (1)	STD Z (1)	STD X (2)	STD Y (2)	STD Z (2)	STD X (3)	STD Y (3)	STD Z (3)	Ratio Z 3/1	Ratio Z 2/1
Forward - Established	0.013	0.009	0.016	0.041	0.023	0.065	0.058	0.034	0.082	4.935	3.927
Vuichard - Established	0.013	0.009	0.016	0.037	0.02	0.061	0.06	0.03	0.103	6.269	3.705
Forward - Onsets	0.015	0.01	0.025	0.02	0.009	0.025	0.056	0.034	0.099	3.874	0.998
Vuichard - Onsets	0.012	0.008	0.013	0.012	0.007	0.019	0.046	0.023	0.074	5.326	1.390
Inversed Vuichard	0.011	0.007	0.01	0.03	0.019	0.057	0.067	0.035	0.079	4.749	3.466

Table 3-2 Vibration VRS – Dauphin

Recovery method - Conditions	P2P X (1)	P2P Y (1)	P2P Z (1)	P2P X (2)	P2P Y (2)	P2P Z (2)	P2P X (3)	P2P Y (3)	P2P Z (3)	Ratio Z 3/1	Ratio Z 2/1
Forward - Established	0.584	0.596	0.896	0.725	0.765	1.3	1.184	1.225	2.185	2.436	1.450
Vuichard - Established	0.732	0.756	1.147	0.759	0.759	1.307	1.32	1.108	2.187	1.905	1.139
Forward - Onsets	0.714	0.62	1.249	0.781	0.701	1.446	1.3	1.18	2.858	2.288	1.157
Vuichard - Onsets	0.59	0.598	0.991	0.556	0.556	0.912	1.247	1.15	2.493	2.514	0.92

Recovery method - Conditions	STD X (1)	STD Y (1)	STD Z (1)	STD X (2)	STD Y (2)	STD Z (2)	STD X (3)	STD Y (3)	STD Z (3)	Ratio Z 3/1	Ratio Z 2/1
Forward - Established	0.008	0.004	0.013	0.019	0.011	0.037	0.032	0.021	0.064	4.62	2.687
Vuichard - Established	0.01	0.006	0.01	0.016	0.01	0.029	0.029	0.02	0.062	3.62	1.71
Forward - Onsets	0.007	0.004	0.02	0.015	0.007	0.027	0.029	0.023	0.044	2.073	1.27
Vuichard - Onsets	0.007	0.004	0.01	0.005	0.003	0.01	0.026	0.015	0.063	3.898	0.625

On both helicopters, the vertical axis (Z) is the most subject to vibrations in any conditions. For all recovery manoeuvres and conditions (onsets or established), the higher ratio is the one corresponding to the recovery manoeuvre. The ratio corresponding to the early stage of the VRS phenomenon is always lower. Comparing recovery conditions, ratios are always higher during established VRS than at VRS onsets.

Two conclusions can thus be drawn: The increase of vibration takes time to reach its maximum value, and the recovery manoeuvre is also contributing to the increase of vibrations.

On Fenec, ratios are slightly higher during Vuichard recoveries while this trend is not so clear on the Dauphin.

Table 3-3 Vibration VRS – Dauphin

Recovery method - Conditions	Average vibration duration (s)	Average vibration duration (s)
	Dauphin	Fenec
Forward - Established	10.7	20.3
Vuichard - Established	17.4	17.0
Forward - Onsets	11.5	15.0
Vuichard - Onsets	5.4	5.7
Inversed Vuichard		13.9

Table 3-3 shows the duration of the vibrations depending on the recovery manoeuvre and conditions. Considering Vuichard manoeuvres, these durations are comparable between Dauphin and Fennec, while they are quite different when considering forward manoeuvres. For instance, the average vibration duration during forward procedure is 10.76 s on the Dauphin, 20.39 s on the Fennec. The average vibration duration is also very limited during Vuichard recovery at VRS onsets, while comparable to the others during inversed Vuichard manoeuvre (only measured on the Fennec).

In addition to the previous vibration study, a power spectral density analysis has been done. This Power Spectral Density (PSD) analysis has been performed on the signal recorded from the vertical axis accelerometer placed under the pilot seat, providing the measure of signal's power content versus frequency.

Power Spectral Density refers to the magnitude square of the Discrete-Time Fourier Transform (DTFT) of an autocorrelation function, which provides information about the distribution of power with respect to frequency in a signal.

As a reminder, the blade pass frequency is the rotor speed (Ω) multiplied by the number of blades (b):

$$\text{BPF} = b\Omega$$

Harmonics are integer multiples of the blade pass frequency: $kb\Omega$

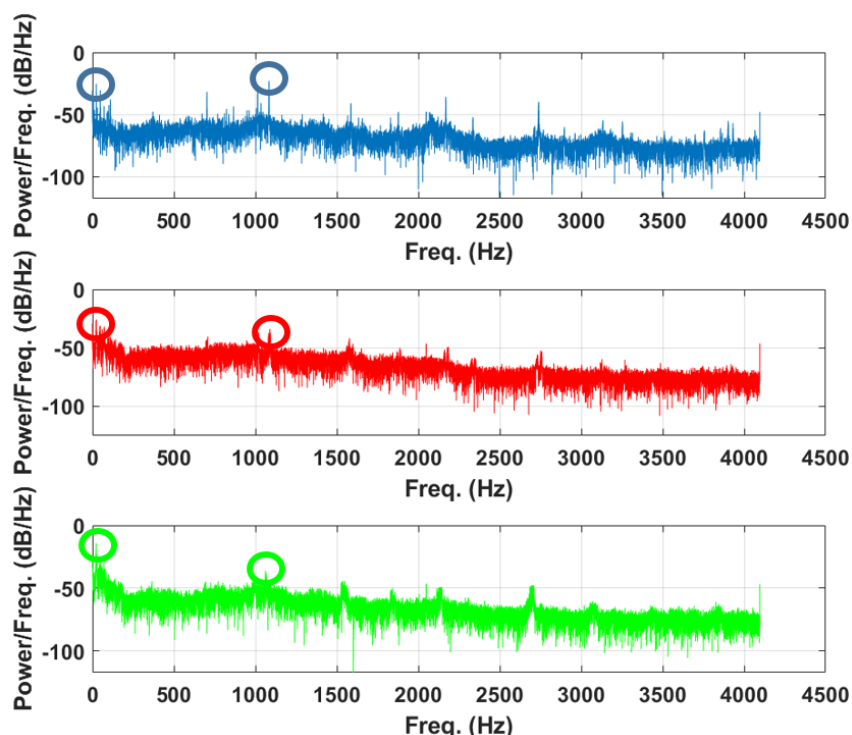
BPF = 1st harmonic; 2nd harmonic = $kb\Omega$ with $k=2$; etc.

For the Fennec helicopter, with a nominal main rotor speed of 390 RPM, the BPF is equal to 19.5Hz.

For the Dauphin helicopter, with a nominal main rotor speed of 350 RPM, the BPF is equal to 23.33Hz. For the Fenestron rotor, equipped with 13 blades and turning at 4706 RPM, the BPF is equal to 1019.63 Hz.

Figure 3-15 shows the PSD performed at three different moments of the run. The blue curve corresponds to a PSD done on the first 4 s of the run (reference), the red curve to the moment at which the VRS is detected by the previous algorithm, and the green curve corresponds to the moment at which the maximum peak to peak value is determined on the raw signal.

► Figure 3-15 Example of power spectral density analysis – Dauphin flight 4 – run 1

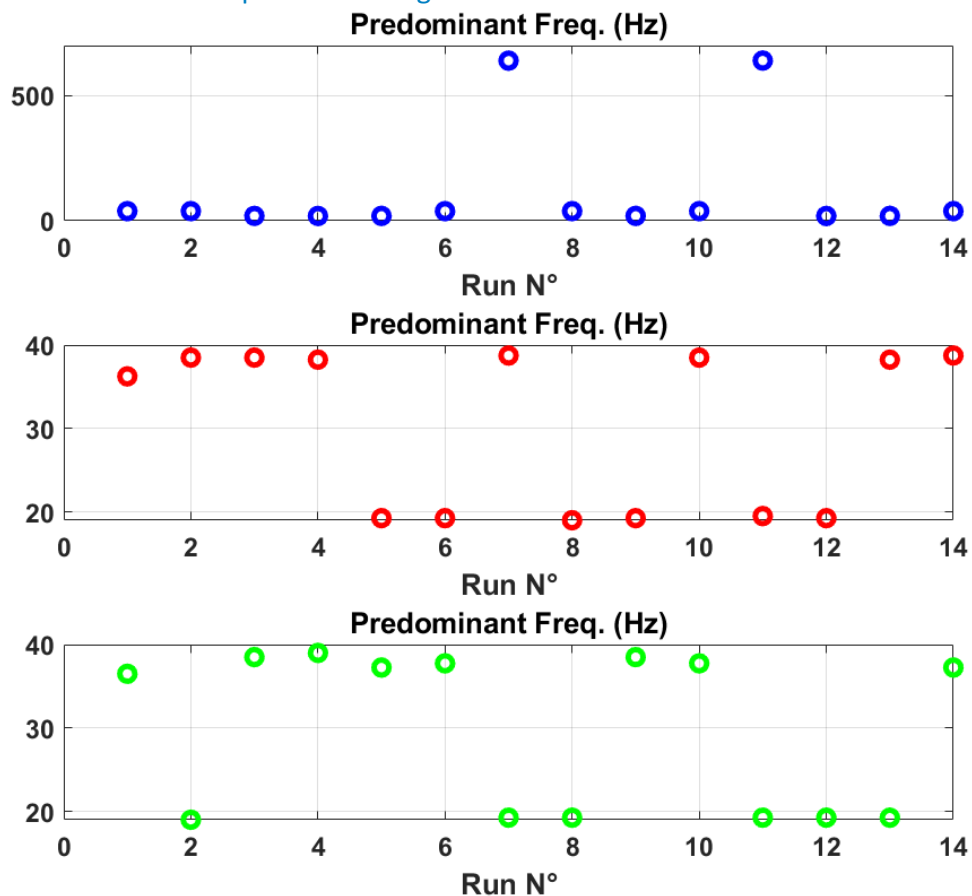


In this example, the maximum of power occurs at the frequency of 1083 Hz in the first graph, corresponding to the Fenestron rotor. At VRS detection and later during the VRS (red and green curves), the maximum power is observed on the main rotor BPF and 2nd harmonic.

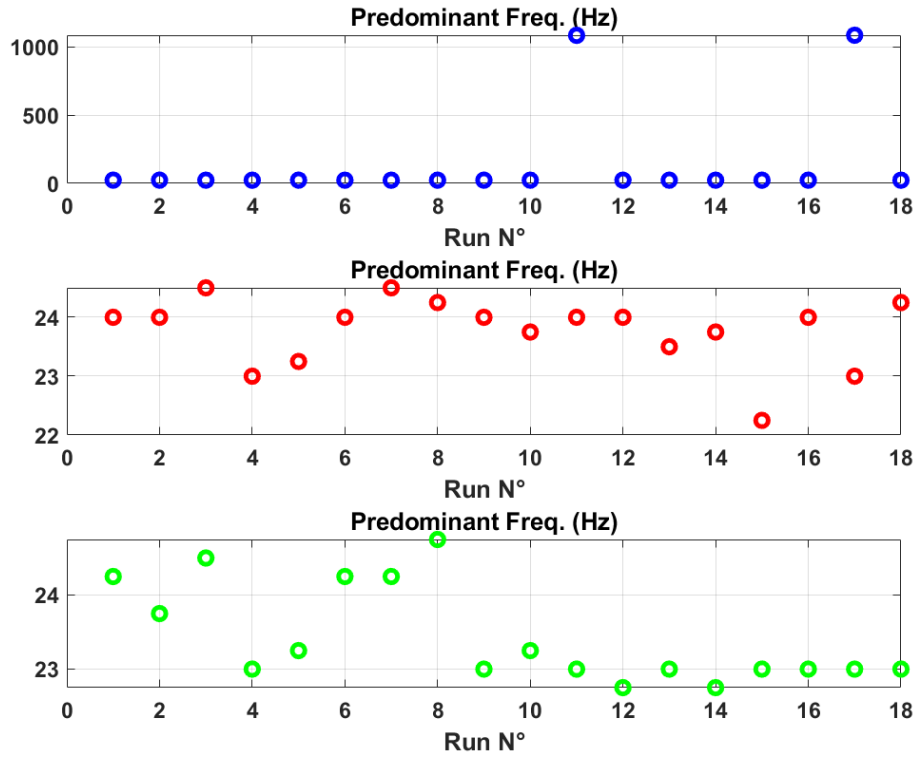
The following figures are showing the results of the PSD during the three stages of the different manoeuvres. The plots represent the frequencies where the maximum of power is measured.

In Figure 3-16, Figure 3-18 and Figure 3-20 during the 2nd and 3rd stage, the 1st and 2nd harmonic of the main rotor are the most powerful. Interestingly, a frequency of 639.6 Hz was outlined by the PSD analysis at the beginning of the run on the Fenec. This frequency doesn't correspond to the main rotor nor the tail rotor. And while close to the free turbine frequency, it doesn't exactly correspond to it. Additional investigations will be done to determine the source of this frequency.

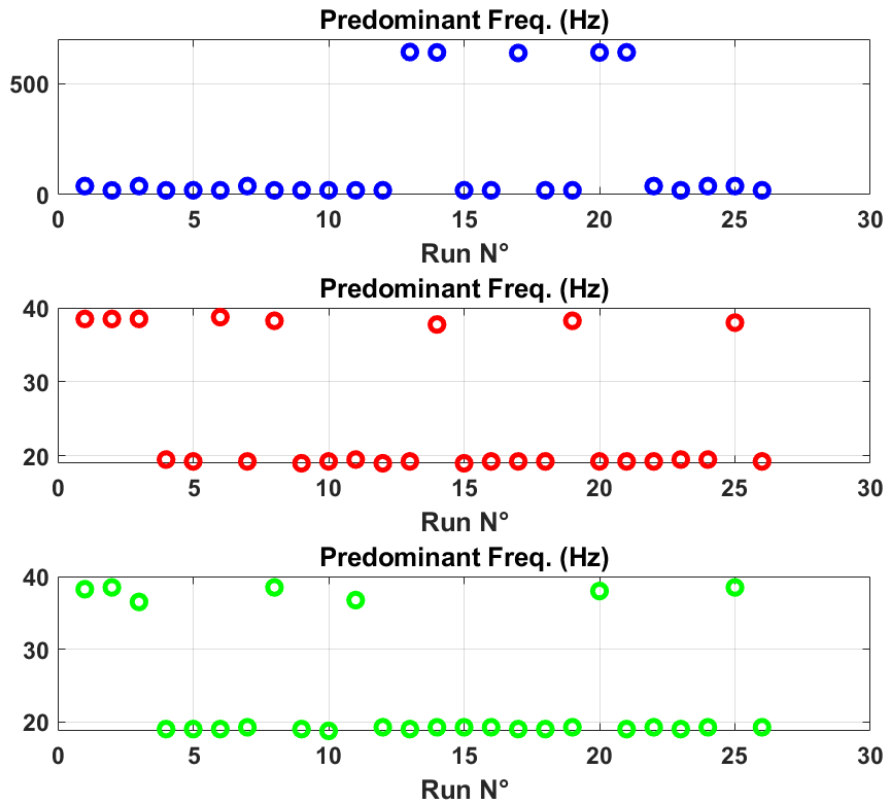
► Figure 3-16 Predominant frequencies during forward recoveries in established VRS- Fenec



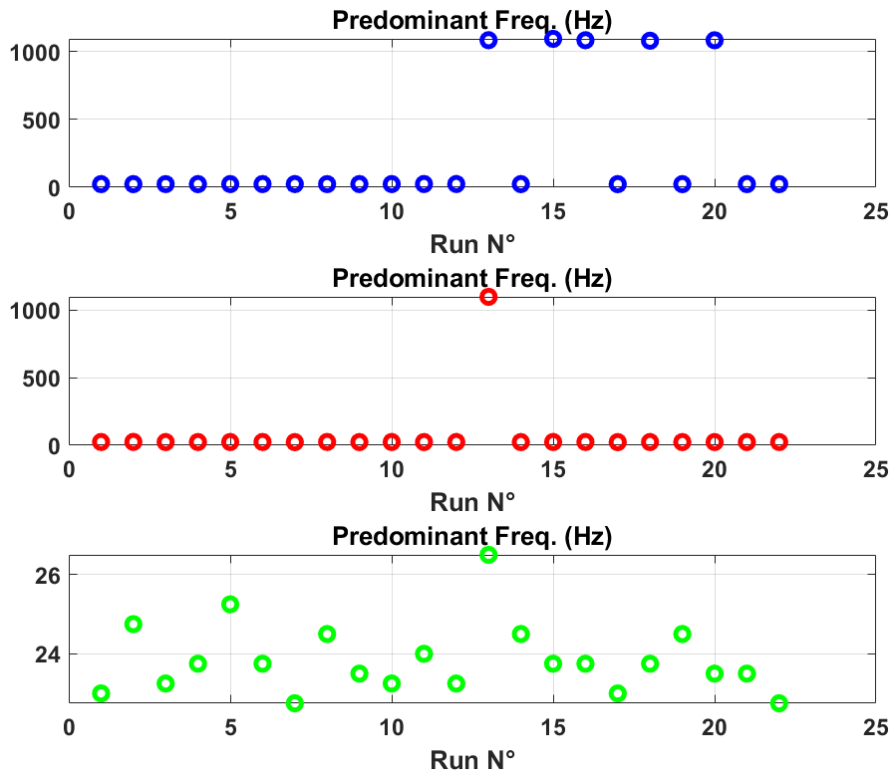
► Figure 3-17 Predominant frequencies during forward recoveries in established VRS- Dauphin



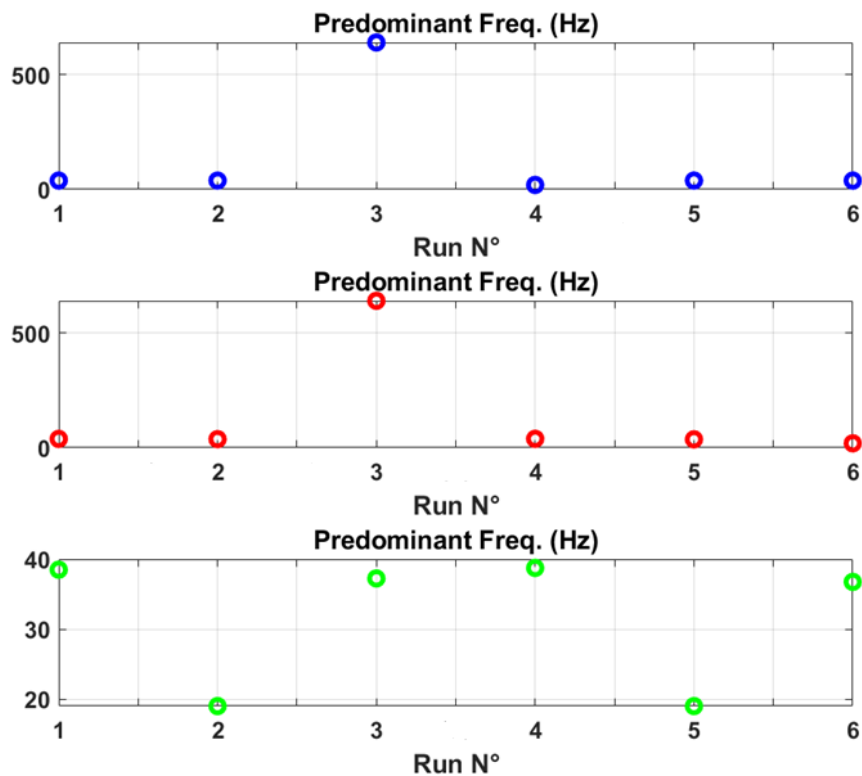
► Figure 3-18 Predominant frequencies during Vuchard recoveries in established VRS - Fenec



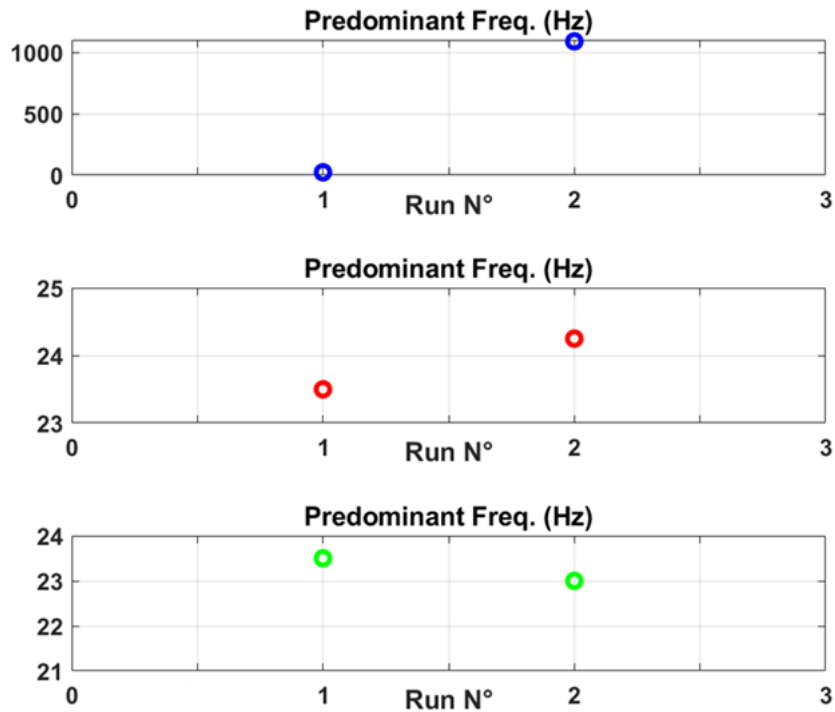
► Figure 3-19 Predominant frequencies during Vuichard recoveries in established VRS - Dauphin



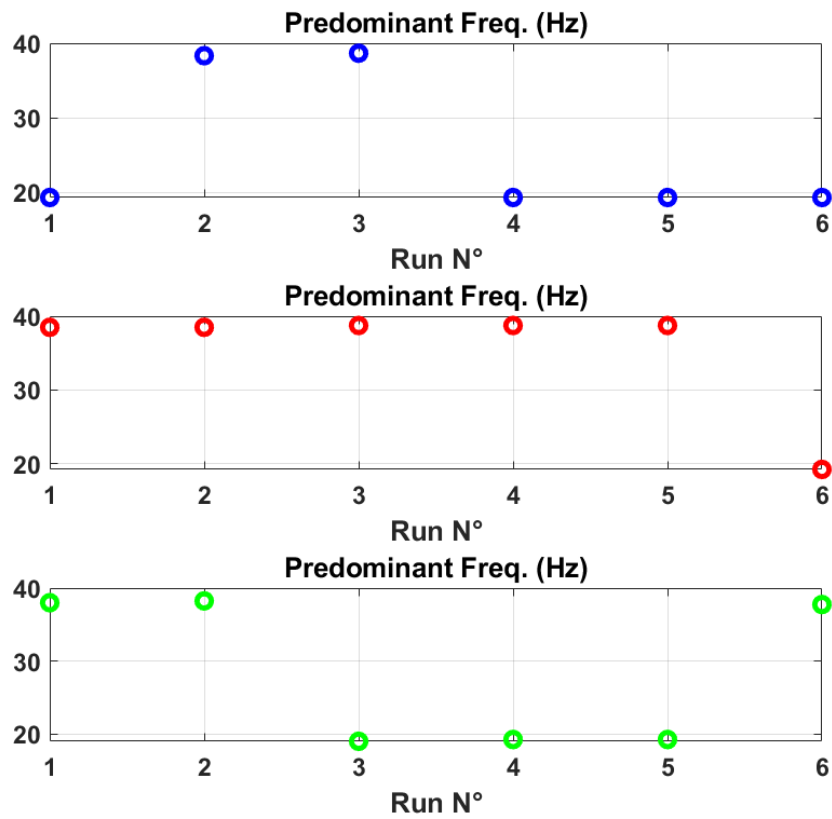
► Figure 3-20 Predominant frequencies during forward recoveries in VRS onsets - Fenec



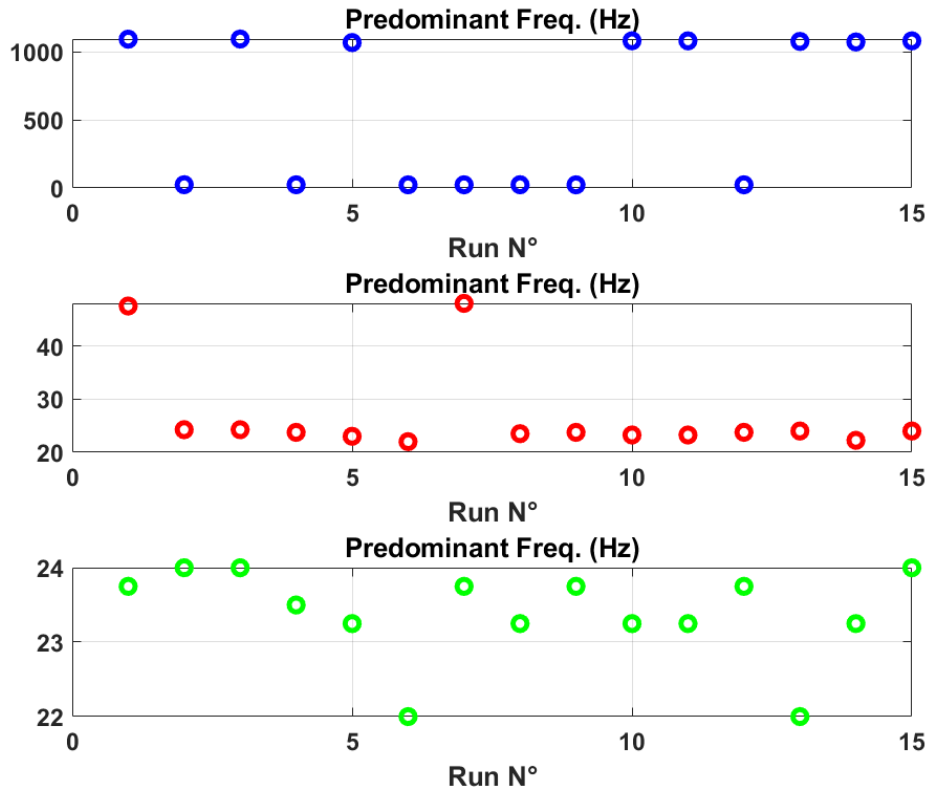
► Figure 3-21 Predominant frequencies during forward recoveries in VRS onsets - Dauphin



► Figure 3-22 Predominant frequencies during Vuichard recoveries in VRS onsets - Fenec



► Figure 3-23 Predominant frequencies during Vuichard recoveries in VRS onsets - Dauphin



3.4 Pilot feedbacks

Regarding the workload in established VRS, and for both recovery methods, the type of run (at the onsets or from an established VRS) had an unforeseen effect: maintaining the helicopter in VRS for the time required to confirm the vortex is straining for the pilots, and effectively tires them before the actual recovery even begins. Due to the attitude changes in VRS, the starting recovery position also varies in an established VRS, which adds another difficulty.

This explains why recoveries at the onsets were judged on average easier than recoveries in established vortex. For information, starting the recovery at the theoretical border of the VRS domain (i.e. at a fixed Vz around -1000 ft/min) without waiting to perceive the signs of VRS was attempted in two Dauphin runs (Runs 6.6 and 6.7) and did not improve things further.

What matters therefore seems to be how ready the pilot is at the beginning of the recovery, and not how established the vortex is. To further this, spending more than a few seconds in VRS once it has been perceived by the crew is not representative of real life, where a pilot would not actively try to stay in VRS on purpose. Therefore the need to confirm the VRS is opposed to the realism of the test points.

This reinforces the interest of developing an objective way to confirm the VRS (whether in real-time or in post analysis), such as the solution studied by ONERA and based on vibration measurements.

Alternatively, if a further analysis confirms that there are no significant performance differences between recoveries “at the onsets” versus “in established VRS” once the effect of the initial Vz is taken into account, it may be pertinent to perform future studies only with recoveries at the onsets, without confirmation of the VRS.

3.5 Conclusions on Vortex-Ring-State phenomenon

The eight flights performed during the project enabled to determine the VRS domain of the Fennec and Dauphin helicopters. These domains are comparable to those already determined in previous flight test campaigns. As shown in Figure 3-1, Figure 3-2, Figure 3-3 and Figure 3-4, a good consistency is observed between the ONERA predicted VRS domains and the actual test points.

Nevertheless, VRS domain boundaries can be different depending on the criteria used, such as pilot feedback, post-flight analysis of flight parameters or vibration level increase.

Thus, the ONERA model is very well suited when considering the Vz drop as the major criterion for VRS domain determination.

Pilots feedback remains a good indicator, as based on several parameters such as the observation of the Vz drop and associated change of the vertical acceleration, or a change in the vibration level. But the analysis of flight data generally shows that the pilot detection occurs a few seconds after the effective Vz drop initiation. Regarding the vibration level increase, it is highly dependent on the way the helicopter enters VRS and, while being a symptom of the generation of vortex rings around the rotor, it doesn't always imply a "real" VRS entry (causing a large Vz drop)

Specific analyses showed an increase of the level of vibration at the early stage of the phenomenon, and this characteristic can be used to estimate the VRS entry and exit. Once in VRS, energy is concentrated on the two first main rotor harmonics, while the maximum of energy can be observed on other frequencies outside the VRS domain. Contrary to what was expected, the maximum of vibration is reached during the recovery manoeuvres. It is almost impossible to determine if this maximum of vibration is due to the VRS or the recovery manoeuvre, and vibration investigations could be further done by changing the procedure followed in flight. Thus, in order to have a better estimation of the level of vibration inside the VRS domain, recovery manoeuvres should be initiated later, with a longer time in a fully developed VRS. But this is not an easy task, and maintaining the helicopter in VRS is straining for the pilots.

4. Recovery techniques evaluation

4.1 Recovery performance

4.1.1 Performance criteria

In order to objectively evaluate the recovery techniques, two major criteria were defined:

- Height loss: Difference between the altitude at which the recovery manoeuvre started and the altitude reached when the helicopter recovered a null/positive vertical speed.
- Recovery time: Time duration between the time at which the recovery manoeuvre started and the time at which the helicopter recovered a null/positive vertical speed.

For both recovery techniques, the pilot workload was evaluated with a method inspired from the NASA-TLX scale, and adjusted for the purpose of this evaluation. After each recovery, the pilots were asked to evaluate for each control axis (cyclic longitudinal, cyclic lateral, foot controls, and collective) their workload, and the frequency, amplitude and effort of their actions. The scale used had a 5 level range : very low, low, medium, high, very high. After each flight, these evaluations were reviewed and confirmed during the debriefing, and then checked against the control position inputs recorded by the flight test installation.

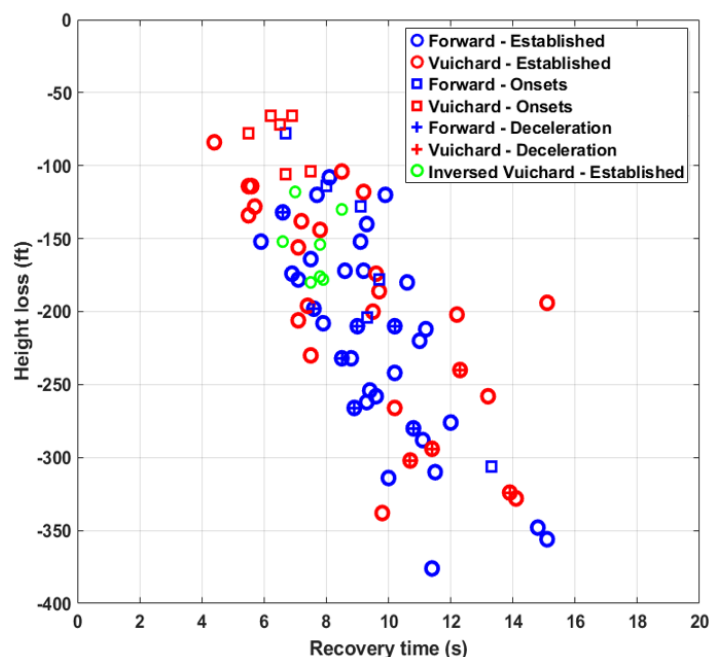
Additional analyses were performed on controls (calculation of the standard deviation) to assess the pilot activity on controls during the recovery manoeuvre.

While not strictly speaking considered as performance criteria, these parameters can bring additional information to explain the observed performance.

4.1.2 Fennec helicopter

A summary of the recovery performance observed during the Fennec test campaign is shown in Figure 4-1.

► [Figure 4-1 Fennec recovery performance](#)



The test runs are sorted based on the recovery method (Forward / Vuichard / Inversed Vuichard and Onsets/Established).

Here, and later in the document, it has to be noted that the points corresponding to the VRS onsets have been re-evaluated by ONERA thanks to the post-flight analysis of the flight parameters. Instead of being based on a subjective pilot judgment, VRS are classed as onsets when the recovery manoeuvre is initiated in the vicinity of the determined upper boundary of the VRS domain.

The height loss appears to be proportional to the recovery time, which was expected since the height loss is the integration of the vertical speed over the recovery time. In the test conditions, a first analysis shows no significant performance differences between the forward and Vuichard recoveries compared to the natural point dispersion. This observation also includes the inversed Vuichard recoveries, which is surprising since they were expected to lead to worsen performance, as the lateral motion goes against the tail rotor thrust.

As shown in table 4-1, on average, and without counting for any influencing parameter, the recovery performance with the Vuichard method appears to be slightly better during established VRS, with a mean time to recover of 9.23s (instead of 9.55s for the forward method, i.e. -0.32s or a 3.35% difference, which is of same order of magnitude than the expected uncertainty on the recovery time and therefore not significant), and a mean height loss of 199 ft (instead of 221 ft, i.e. -22 ft or a 9.95% difference).

The performance of Vuichard recovery is better when performed at VRS onsets, with a mean height loss of 82 ft (instead of 168 ft, i.e. -86 ft or a 51.19% difference).

However, the Vuichard recoveries were generally performed with a higher average torque. When limiting the comparison to a similar range of average torque during the recovery, the performance of both methods becomes similar, as shown in chapter 3.2.

The recoveries performed at VRS onsets instead of fully established VRS show better performance, as being initiated at lower rates of descent.

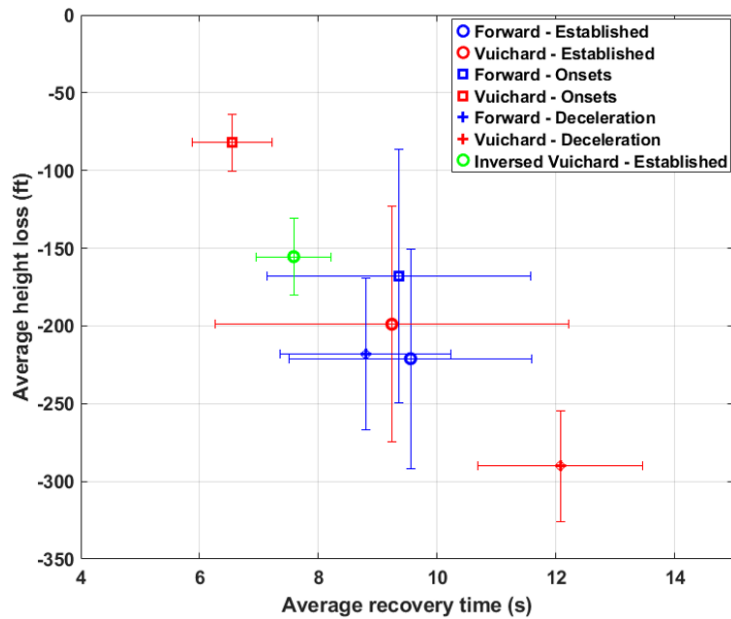
Table 4-1 Average VRS recovery performance – Fennec

Recovery method - Conditions	Average Height loss (ft)	Max. Height loss (ft)	Min. Height loss (ft)	Average Recovery time (s)	Average Vz upper limit (ft/min)	Average Vz lower limit (ft/min)	Average Torque (%)	N° of runs
Forward - Established	-221	-376	-108	9.5	-1212	-2186	58.3	34
Vuichard - Established	-199	-338	-84	9.2	-1134	-2598	68.1	26
Forward - Onsets	-168	-306	-78	9.3	-716	--	66.1	6
Vuichard - Onsets	-82	-106	-66	6.5	-537	--	61.7	6
Inversed Vuichard - Established	-155	-180	-118	7.5	-1104	-2484	70.0	7
Forward - Deceleration	-218	-280	-132	8.8	-1575	-3016	57.4	7
Vuichard - Deceleration	-290	-324	-240	12.0	-1382	-3176	64.3	4

Figure 4-2 is showing the average loss of height with respect to the average recovery time during all manoeuvres and conditions. Errorbars are representing the standard deviations of the two parameters. As this can be seen, for recovery at the VRS onset, the Vuichard manoeuvre shows better performance than the

forward one in terms of both time of recovery/height loss and standard deviations. The same is not valid for recoveries from established VRS, where the average value are comparable and the standard deviations are higher for both techniques. Inversed Vuichard recovery performance (for both metrics) is surprisingly better than the “nominal Vuichard” in established VRS. Large errorbars can be observed for recoveries from established VRS, highlighting a very large dispersion of the points as shown in Table 4-1. This is not true for inversed Vuichard manoeuvres, but this is certainly due to the very limited number of test cases.

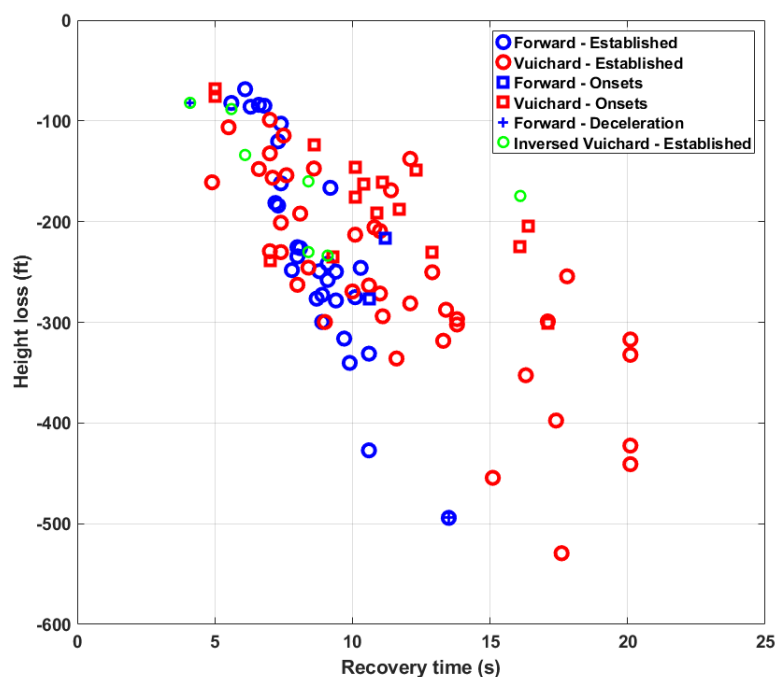
► Figure 4-2 Fennec average recovery performance



4.1.1 Dauphin helicopter

A summary of the recovery performance observed during the Dauphin test campaign is shown in Figure 4-3.

► Figure 4-3 Dauphin recovery performance



The height loss appears to be proportional to the recovery time, which was expected since the height loss is the integration of the vertical speed over the recovery time. In the test conditions, a first analysis of the performance results shows:

- no significant height loss differences between the forward and Vuichard recoveries, compared to the natural point dispersion;
- a slightly higher loss of height (-256 ft against -227 ft), as well as a slightly longer average time of recovery for the Vuichard method in fully developed VRS (11.6 s) compared to the forward method (8.53 s), which is partly explained by the time needed to recover a positive Vz after exiting the VRS and trying to come back to hover, due to the limited available power on the Dauphin.

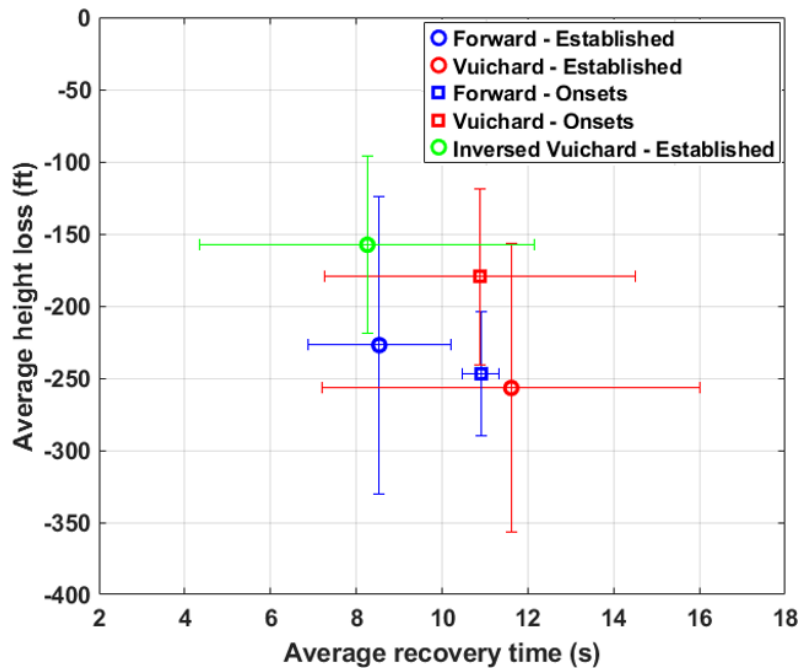
As seen on the Fennec, the performance of the 7 inversed Vuichard test runs were better for both metrics, despite a lower applied torque during the recovery, as shown in Table 4-2. While the sample size is small, this result is interesting and consistent with the pilot feedback which indicated a seemingly easier and more fluid inversed Vuichard recovery, compared to the “normal” Vuichard recovery.

Table 4-2 Average VRS recovery performance – Dauphin

Recovery method - Conditions	Average Height loss (ft)	Max. Height loss (ft)	Min. Height loss (ft)	Average Recovery time (s)	Average Vz upper limit (ft/min)	Average Vz lower limit (ft/min)	Average Torque (%)	N° of runs
Forward - Established	-227	-494	-68	8.5	-928	-2287	58.3	30
Vuichard - Established	-256	-529	-98	11.6	-921	-1981	65.2	42
Forward - Onsets	-247	-277	-216	10.9	-1051	--	58.9	2
Vuichard - Onsets	-179	-300	-67	10.8	-582	--	66.1	16
Inversed Vuichard - Established	-157	-233	-88	8.2	-903	-2241	55.9	7

Figure 4-4 is showing the average loss of height with respect to the average recovery time during all manoeuvres and conditions. Errorbars are representing the standard deviations of the two parameters. Contrary to what was observed on the Fennec, the recovery performance in established VRS with the forward method appear to be slightly better, although a very large dispersion of the points as shown in Table 4-2 and characterised here by large errorbars has to be considered. However, for the recoveries at the onset the performance are better for Vuichard recoveries than for forward ones (result to be mitigated by the very limited number of runs performed with the forward method in these flight conditions). Here again, the inversed Vuichard technique shows good performance.

► Figure 4-4 Dauphin average recovery performance



4.1.2 Performance summary

To summarize, without taking into account the effect of influencing parameters:

- On Fennec, Vuichard recoveries show better performance than forward recoveries when performed at the early stages of VRS, while the difference between both methods is small when performed in established VRS;
- On Dauphin, Vuichard recoveries also show better performance than forward recoveries when performed at the onset of VRS (although there are only two forward recoveries at the onset, so the average is not statistically significant), but show worse performance when performed in established VRS.

Besides the effect of influencing parameters, which is studied in the following chapter, a likely explanation of the relatively inferior performance of Vuichard recoveries when performed in established VRS is that the margin of power (used to reduce the rate of descent) is lower in hover than in forward translation. This effect is more noticeable when the recovery is initiated at a higher rate of descent, increasing both the height loss and the recovery time.

4.2 Influencing parameters

The analysis of the results found that several parameters can influence the VRS recovery and explain the dispersion observed:

- the vertical speed at the initiation of the vortex recovery ($t_{\text{manoeuvre}}$);
- the average torque applied during the recovery (between $t_{\text{manoeuvre}}$ and t_{vz0});
- the attitudes during the recovery (either the pitch for forward recoveries, or the roll angle for Vuichard recoveries);
- the entry conditions (and in particular the forward and lateral horizontal speeds).

4.2.1 Effect of vertical speed

4.2.1.1 Effect of vertical speed on the height loss

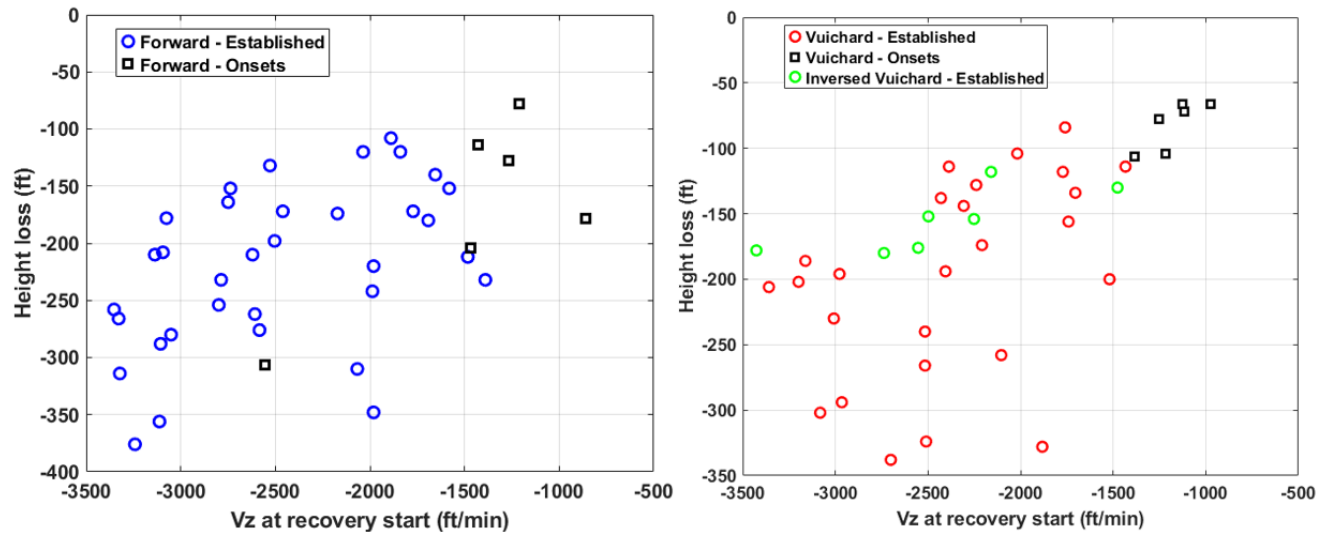
The vertical speed at the onset of the recovery was found to be one of the most important influencing parameter on the height loss, as shown in the following Figure 4-5 (Fennec) and Figure 4-6 (Dauphin) where

the left graphs represent the forward manoeuvre results, the right graphs showing the Vuichard manoeuvre results.

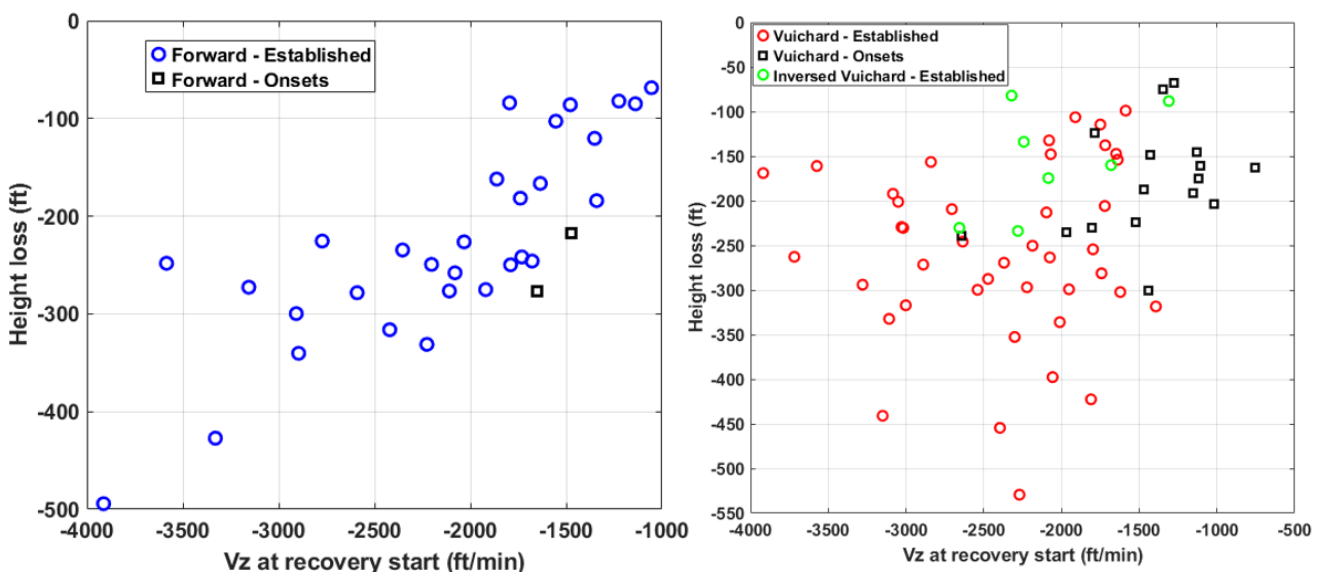
The higher the initial rate of descent, the higher the height loss on average, with a significant dispersion. This is logical since the momentum to neutralise increases with the speed.

On average, the recoveries at VRS onsets tend to occur at lower initial vertical speeds, and therefore induce smaller height losses, which was expected.

► Figure 4-5 Effect of initial Vz on height loss on Fenec



► Figure 4-6 Effect of initial Vz on height loss on Dauphin



On Fenec, Vuichard recoveries were on average initiated with a lower initial rate of descent than forward recoveries, but this is a purely random phenomenon, which would be expected to disappear if the number of test points were increased, and is independent of the test method: the planned method of recovery should not have an influence on the time at which the recovery is initiated. This uncontrolled difference in the entry parameters could partly explain the slight apparent advantage of the Vuichard recoveries in terms of height loss.

Once considering the effect of the initial Vz, there is no clear difference on the height loss tendency between both recovery methods. The important dispersion observed is more pronounced on Dauphin (Figure 4-6) for

Vuichard recoveries. This could be explained by the varying difficulty of the Vuichard maneuver on Dauphin experienced by the pilots (see §4.4.2), with an indirect effect on height loss.

Surprisingly, for inversed Vuichard recoveries the height loss is lower than what could be expected based on the vertical speed. On Dauphin this could be explained by the reduced workload experienced, but this phenomenon is not explained on Fenec.

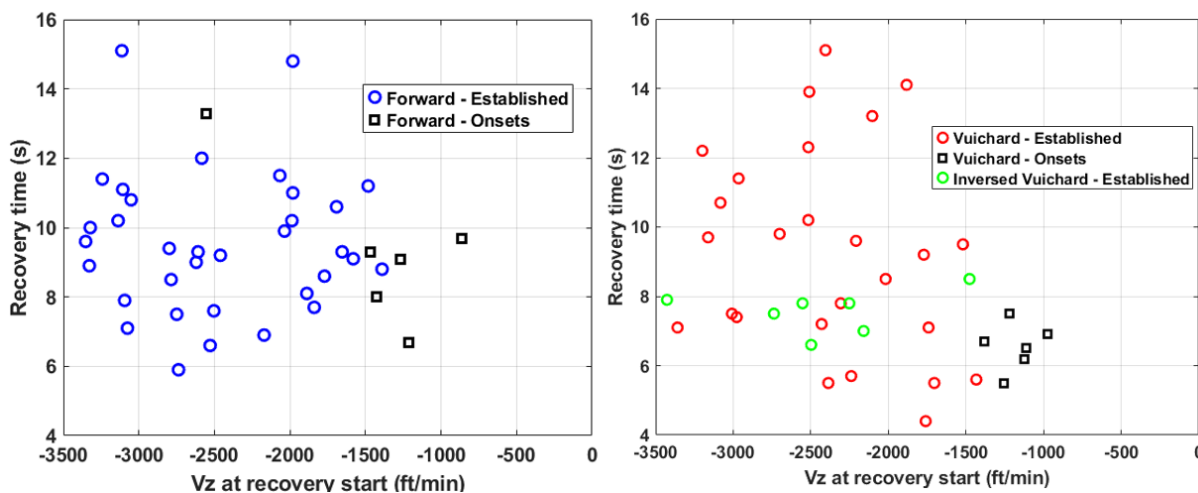
If, on average, the Vuichard recoveries at VRS onsets on the Dauphin occurred at lower initial rates of descent, this was not the case for the only two forward method runs at VRS onsets for which performance is worse.

4.2.1.2 Effect of vertical speed on the recovery time

Interestingly, opposite to the effect on the height loss, there is no clear effect of the initial vertical speed on the recovery time.

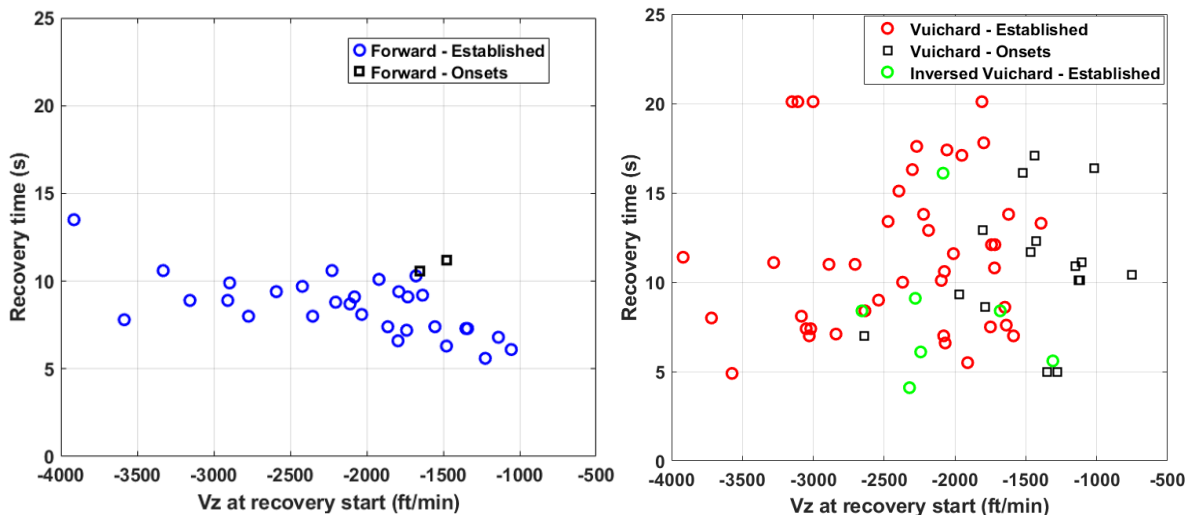
On Fenec, as shown in Figure 4-7, there is no clear effect of the initial vertical speed on the recovery time, while it can be seen that recoveries performed at onsets (at lower descent rates) lead to lower recovery time.

► Figure 4-7 Effect of initial Vz on recovery time on Fenec



On Dauphin (see Figure 4-8), the effect is clearer and appears more linear for forward recoveries (increase of about 2s over 1500 ft/min), but seems more random for Vuichard recoveries. Again, this latter observation could be explained by the varying difficulty of the Vuichard maneuver on Dauphin (see §4.4.2).

► Figure 4-8 Effect of initial Vz on recovery time on Dauphin.



4.2.2 Effect of torque

The power applied during recoveries is expressed here through the torque, as it was the first limitation reached in most test runs. Torque is defined hereafter as the one measured at the torque indicator. It is expressed in percent, with 100% corresponding to the Take-Off Power (TOP) for both helicopters. For the Dauphin, this is the sum of the two engine torques.

4.2.2.1 Effect of torque on the height loss on Fenec

For forward manoeuvres, a higher average torque applied during the recovery manoeuvre clearly reduces the height loss, as shown in Figure 4-9 (left graph).

Indeed, at an average torque of around 50%, the height loss is between -230 and -375 ft, while for average torques higher than 70% it is globally between -100 and -250 ft.

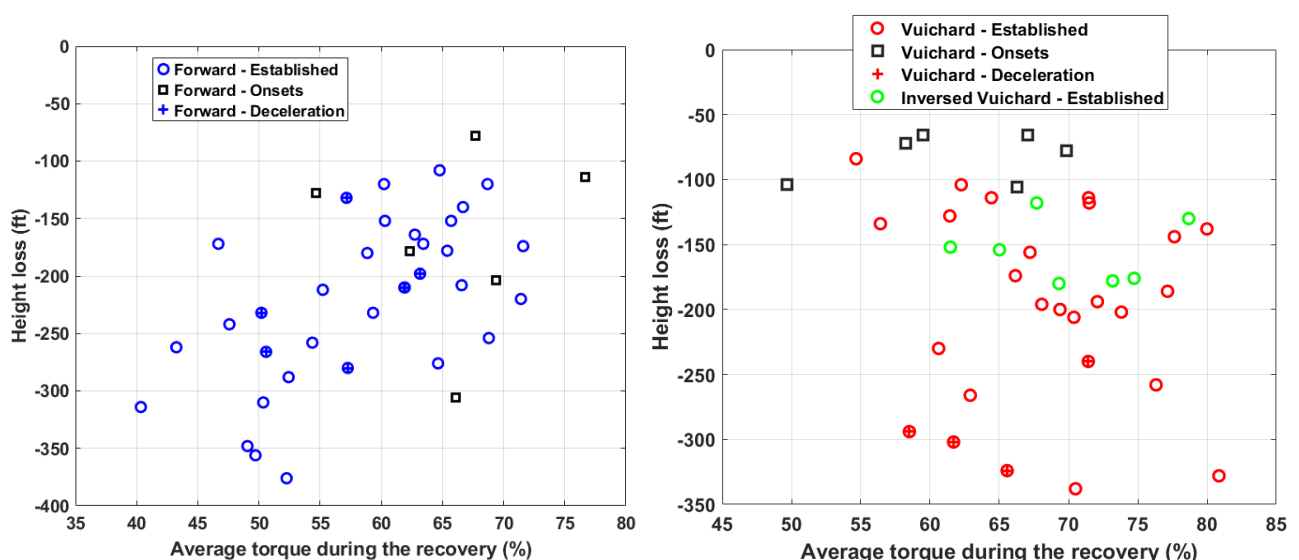
For Vuichard recoveries however (right graph), the effect is not as clear due to the strong dispersion observed, and to the narrower range of average torque observed.

The average torque applied during Vuichard recoveries (in established VRS and at onsets) was 67% (and 70.% during inversed Vuichard recoveries), while, in the same flight cases, the average torque applied during forward recoveries was 59.5 %.

It should be noted that applying too much torque has severe adverse effects on the pilot workload, as it makes it more likely to exceed the aircraft limitations or reach a control limit of authority, as explained later. Thus, it is not advisable to systematically aim for the maximum available power: a balance must be found between performance and pilot workload.

It is also important to note that the workload associated to forward recoveries performed at high torque (60-80%), while higher than at average torque, is still significantly lower than the workload associated to Vuichard recoveries performed at similar power. The main reason is because there is still only one axis to control (longitudinal cyclic) besides the power level.

► Figure 4-9 Effect of applied power on height loss on Fenec



Interestingly, if the comparison is limited to high torque values (>60%) in order to offset the effect of this influence parameter, in established VRS the average height loss becomes similar for forward and Vuichard recoveries, while at the onset Vuichard recoveries still show a lower height loss. Therefore removing the contribution of the torque seems to reduce the apparent better performance of the Vuichard recoveries without completely removing the difference observed for recoveries at the onset of VRS.

For forward recoveries, on a Fennec helicopter, the height loss is reduced by the power applied during the recovery. Therefore, when a VRS occurs close to the ground, it is recommended to apply all the power available during the recovery.

4.2.2.2 Effect of torque on the height loss on the Dauphin

On Dauphin, for forward recoveries, a higher average torque applied during the recovery manoeuvre reduces the height loss despite a strong point dispersion, as shown on Figure 4-10 (left graph). It can be seen that for average torques lower than 55%, the height losses are always greater (in absolute value) than 250 ft. For higher average torques up to 70%, a large dispersion of the points is observed, with height losses comprised between -80 ft to -420 ft. Only three points are above 70% of torque, with height losses around -100ft.

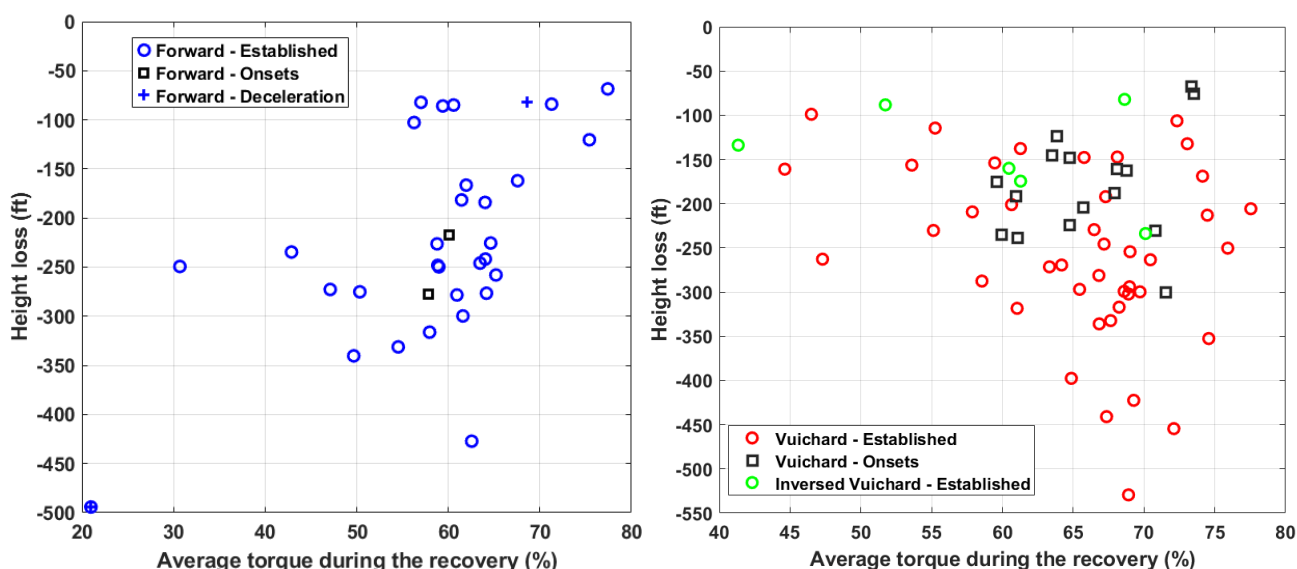
For Vuichard recoveries on Dauphin (right graph), the effect of torque is not that simple to identify due to the large dispersion of the points.

- First, the range of usable torque does not allow large changes;
- Furthermore, increase of applied torque comes with huge side effects increasing pilots' workload and point dispersion.

Indeed, it was found that reducing – or even better, delaying – the power applied during the recovery reduced the parasitic effects and the pilot workload without degrading the recovery performance (see §4.4.2.6). Trying to go back to hover also has a negative effect on the performance, as the parasitic effects (and the pilot workload) are higher than when accepting the forward motion, and as recovering a positive Vz takes longer due to a lower power margin.

Applying too much torque has severe adverse effects on the pilot workload (even more than on the Fennec), as it makes it more likely to exceed the aircraft limitations, to encounter strong parasitic effects on the yaw and pitch axis, or to reach a control limit of authority. Thus, it is not advisable to systematically aim for the maximum available power (at least not at the beginning of the recovery).

► Figure 4-10 Effect of applied power on height loss on Dauphin (All recoveries)

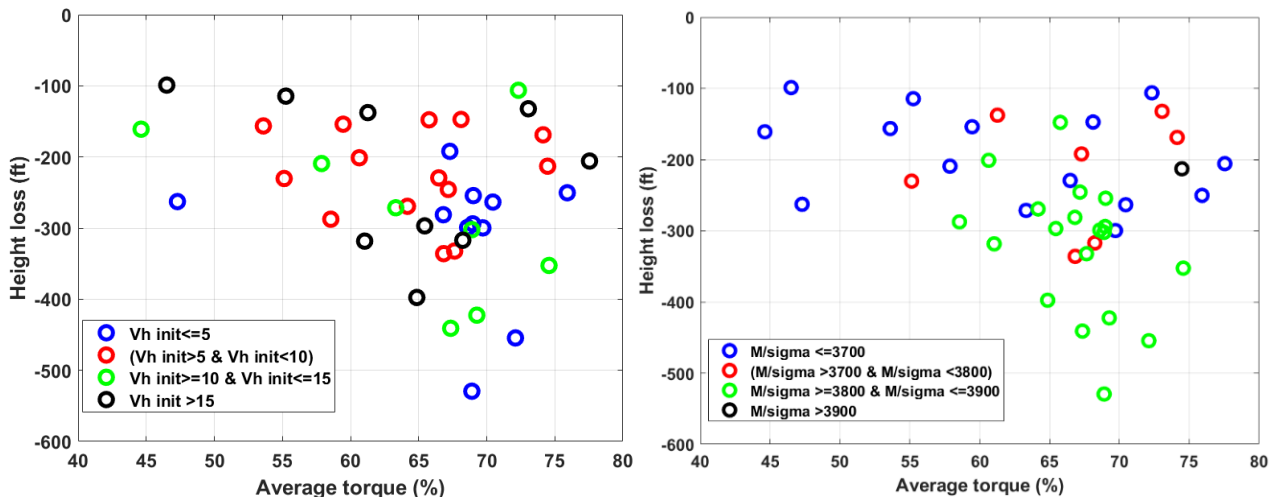


The average torque applied during Vuichard recoveries was 62% (as the Vuichard method calls for the use of all available power), while the average torque applied during forward recoveries was 58%.

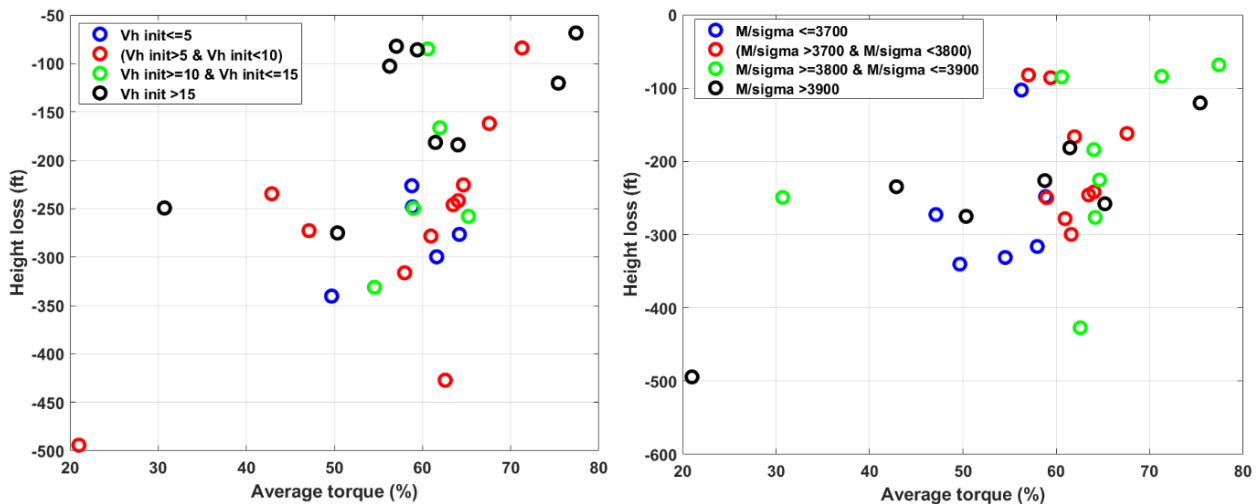
A closer study has been done to distinguish the effect of forward speed at recovery initiation and the reduced mass on global performance of both recoveries. Figure 4-11 shows the results for Vuichard recoveries, Figure 4-12 for forward recoveries, on Dauphin.

- For Vuichard recoveries, there's no clear effect of the initial forward speed, while it can be observed that higher reduced masses have a negative impact on the height loss.
- For forward manoeuvres, it seems that better performance is obtained with higher initial forward speeds, which can be explained by the vicinity of the VRS domain boundary in these conditions as this will be further detailed in §4.3.2. The reduced masses have no clear effect.

► Figure 4-11 Effect of applied power on height loss on Dauphin (Vuichard recoveries)



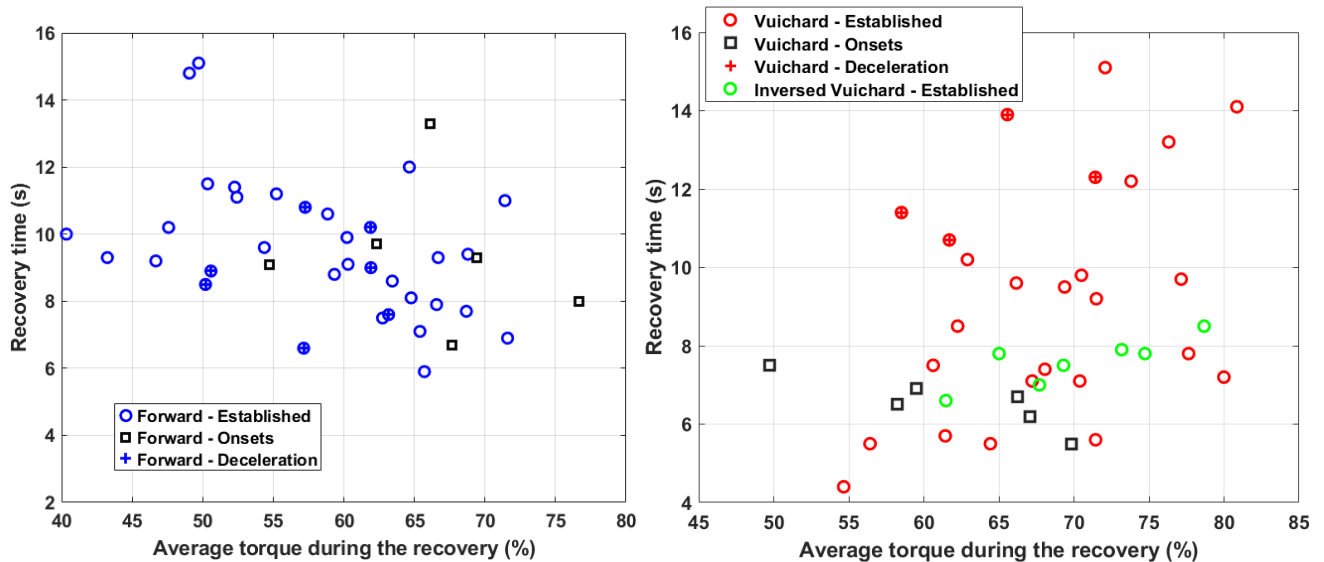
► Figure 4-12 Effect of applied power on height loss on Dauphin (Forward recoveries)



4.2.2.3 Effect of torque on the recovery time on Fennec

On Fennec, the effect of the average torque applied on the recovery time is shown in Figure 4-13. For forward recoveries (left graph), there seems to be a slight decrease of the recovery time when more torque is applied, between 8s to 15s at an average torque of 50% and between 7s to 11s at an average torque of 70%. The effect of the average torque on the recovery time seems however more random for Vuichard recoveries (left graph). This could be due the smaller range of observed torque for Vuichard recoveries (few points at low or medium power, where the recovery time could be expected to increase), and to the detrimental effect of higher torques on the handling of the aircraft.

► Figure 4-13 Effect of applied power on recovery time on Fenneck



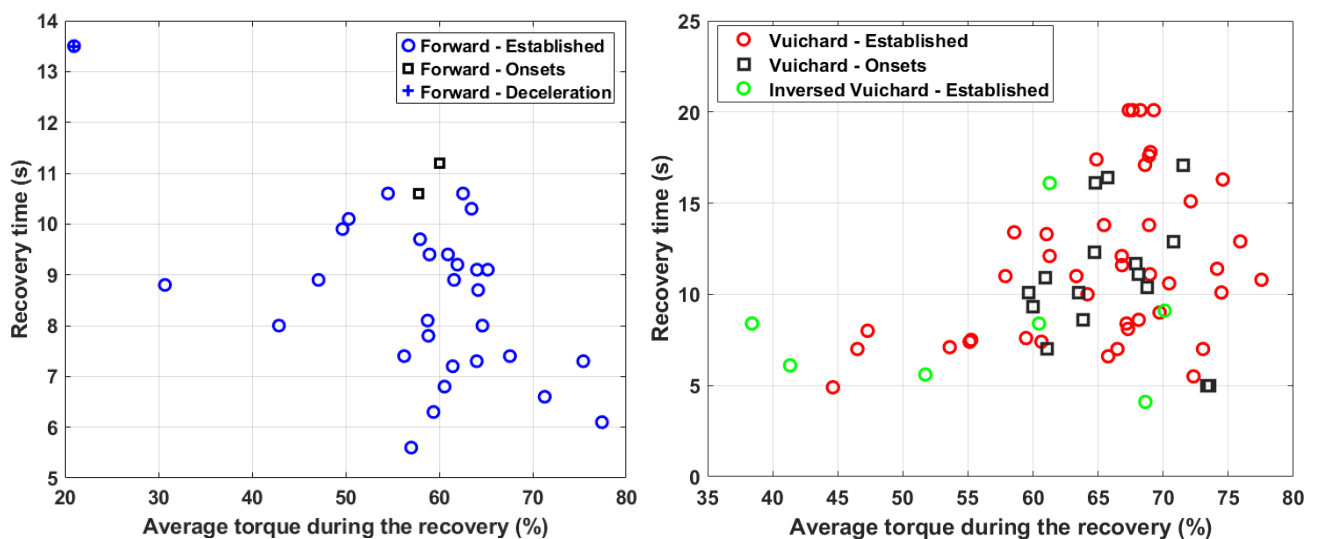
As for the height loss, if the comparison is limited to high torques (>60%), the average recovery time becomes 8.6s for forward recoveries, and 9.4s for Vuichard recoveries, with more dispersion for Vuichard recoveries.

4.2.2.4 Effect of torque on the recovery time on Dauphin

On the Dauphin, for forward recoveries (left graph), while a large dispersion is observed for average torque between 55% and 65%, there seems to be a very small decrease of the recovery time when more torque is applied (see Figure 4-14).

The effect of the average torque on the recovery time seems also more random for Vuichard recoveries (right graph). Most of the points are corresponding to high torques (between 60% and 80%) where helicopter handling is more difficult.

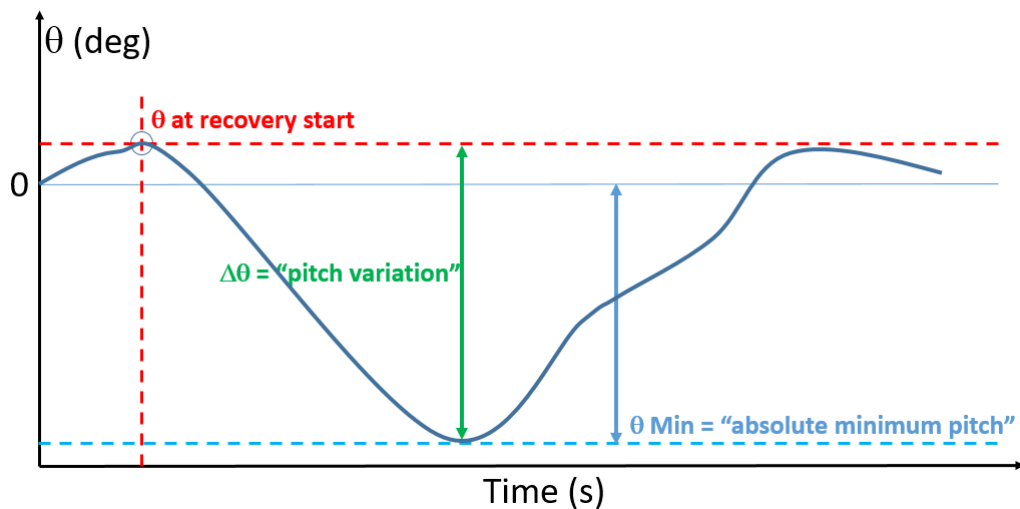
► Figure 4-14 Effect of applied power on recovery time on Dauphin



4.2.3 Effect of the pitch angle on the performance

The pitch angle is the main pilot controlled variable during a forward recovery, along with the applied power. After the first test flight, the optimal target was set for both helicopters at a pitch variation $\Delta\theta = -20^\circ$ (equivalent to an absolute pitch between -15° and -20°) as a compromise between recovery performance and pilot workload.

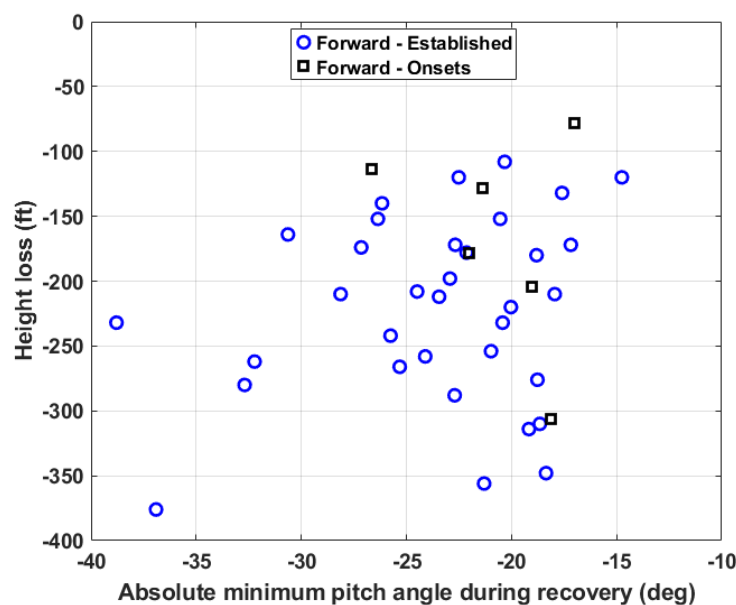
► Figure 4-15 Definition of the absolute minimum pitch angle and pitch angle variation



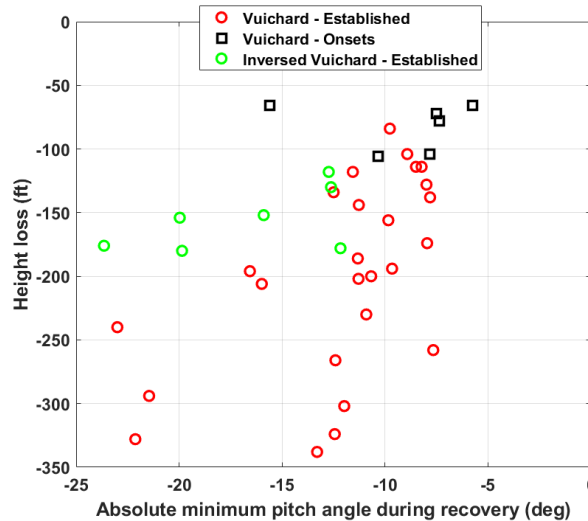
4.2.3.1 Effect of absolute minimum pitch angle on the height loss on Fenec

The effect of the absolute minimum pitch angle (as illustrated in Figure 4-15) reached during the forward recovery manoeuvre on the height loss is shown in Figure 4-16.

► Figure 4-16 Effect of absolute minimum pitch angle on height loss on Fenec (Forward recoveries)



► Figure 4-17 Effect of absolute minimum pitch angle on height loss on Fennec – (Vuichard recoveries)

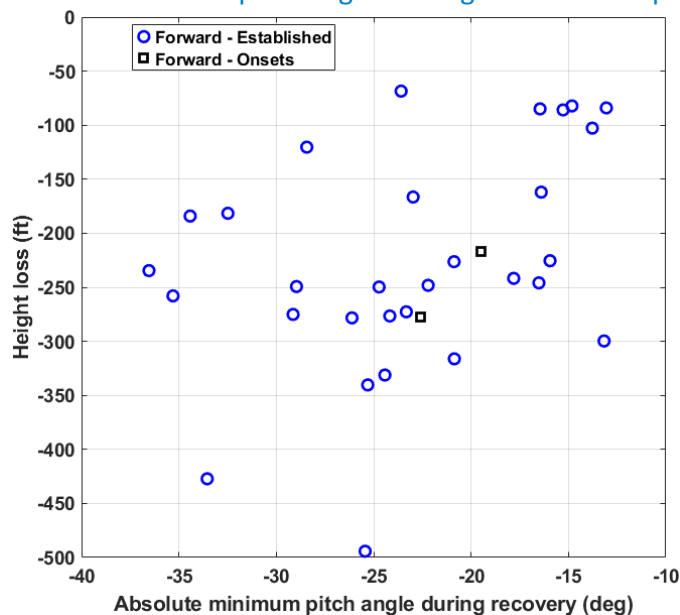


Considering forward manoeuvres, between -15° and -25° of absolute minimum pitch, the large dispersion doesn't allow to see any specific trend. But one can observe that between -25° and -30° , the height losses are slightly reduced and comprised between -140ft and -266ft . For lower absolute minimum pitch angle (lower than -30°), the 4 corresponding points show height losses between -232ft and -376ft . This could show that the optimal absolute pitch angle is between -25° and -30° . For higher angles (from -15° to -25°), the pitch angle would not be sufficient to sufficiently increase the forward speed and the height loss would be influenced by other parameters. For lower pitch angles (lower than -30°), the resulting vertical speed would have a negative impact, leading to higher height losses. Nevertheless, this conclusion has to be mitigated by the small sample of points at low pitch angle (lower than -25°).

Interestingly, a clearer trend of the increase of the height loss with the increase of the absolute pitch angle can be seen for Vuichard recoveries, which in theory should be performed without action on the helicopter pitch, as shown in Figure 4-17.

4.2.3.2 Effect of absolute minimum of pitch angle on the height loss on Dauphin

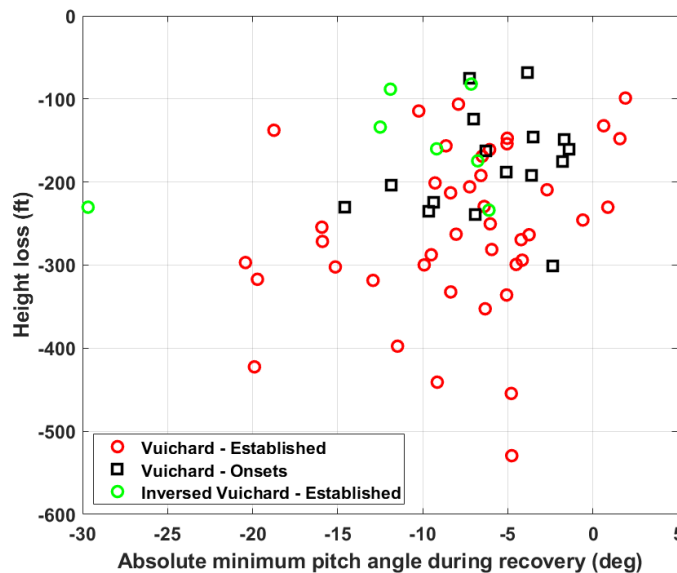
► Figure 4-18 Effect of absolute minimum pitch angle on height loss on Dauphin (Forward recoveries)



The effect of the absolute minimum pitch angle reached during the recovery manoeuvre on the height loss is shown in Figure 4-18.

Due to the strong dispersion, the tendency is unclear and would have to be confirmed through a parametric study. No real tendency can be either observed for Vuichard recoveries (see Figure 4-19).

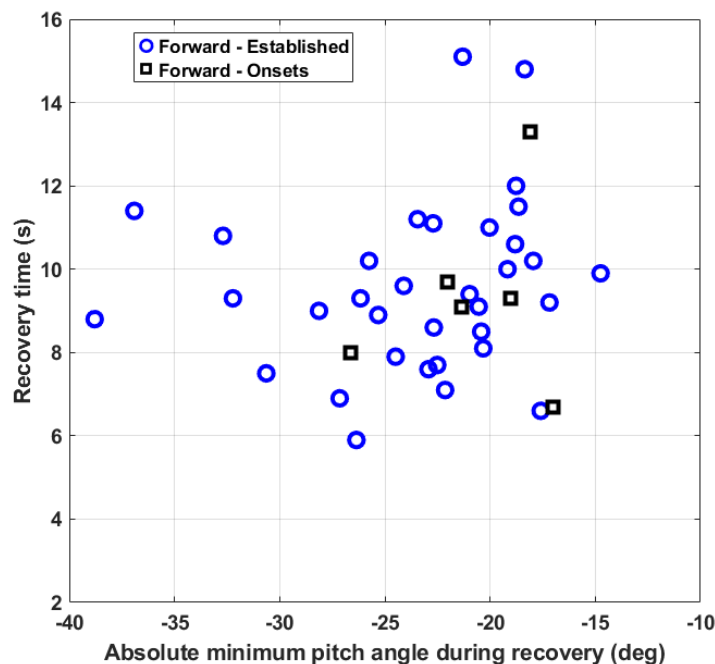
► Figure 4-19 Effect of absolute minimum pitch angle on height loss on Dauphin – (Vuichard recoveries)



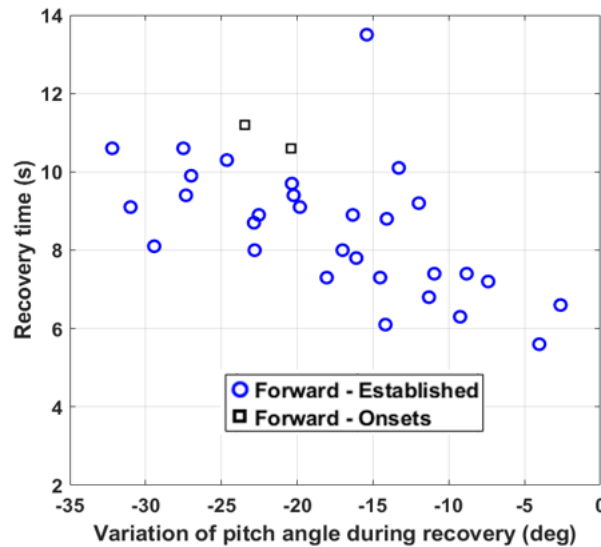
4.2.3.3 Effect of absolute minimum pitch angle on the recovery time on both helicopters

For both helicopters, the effect of the absolute minimum pitch angle on the recovery time seems relatively random, as shown in Figure 4-20 and Figure 4-21, where no clear tendency is noticeable. Nevertheless, as described before, it can be observed that on the Fenec, for pitch between -25° and -30° , the dispersion is relatively lower with lowest recovery time. This is not true for Dauphin where lowest recovery time are around -15° of pitch.

► Figure 4-20 Effect of absolute minimum pitch angle on recovery time on Fenec (Forward recoveries)



► Figure 4-25 Effect of the variation of the pitch angle on recovery time on Dauphin (Forward recoveries)

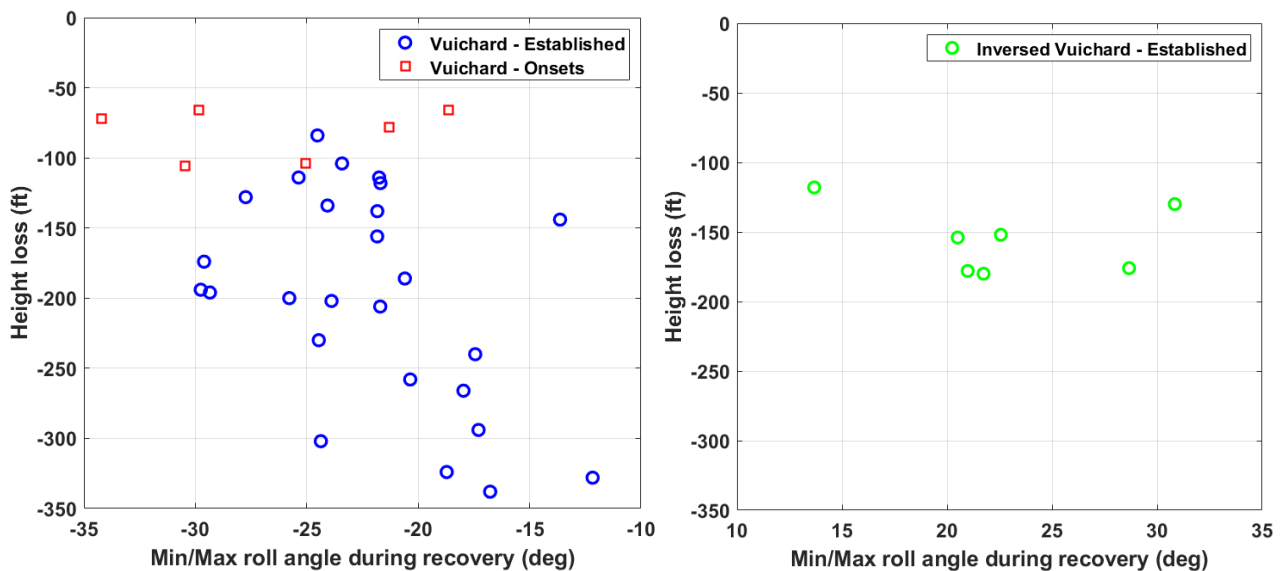


4.2.4 Effect of the variation of roll angle on the performance (Vuichard recoveries)

The roll angle is one of the main initial pilot controlled variable during a Vuichard recovery. To perform this manoeuvre, a target of $\phi = -20^\circ$ is recommended, maintained during approximately 1s.

4.2.4.1 Effect of roll angle on the height loss on Fenec

► Figure 4-26 Effect of roll angle on height loss on Fenec (Vuichard recoveries)



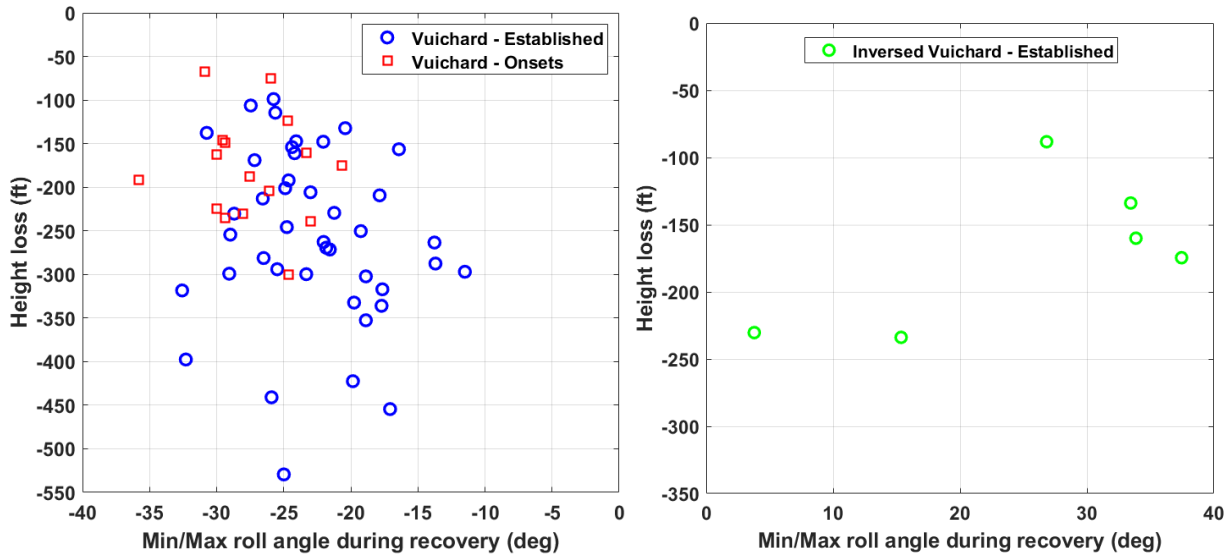
The effect of the roll angle on the height loss for Vuichard recoveries on Fenec is shown in Figure 4-26. Despite the important dispersion, there seems to be, on average, a decrease of the height loss with the increase of the roll angle in established VRS (left graph).

The runs performed at VRS onsets and the “inversed Vuichard” recoveries show no tendency.

As for the pitch angle in forward recoveries, it is possible that the effect of the roll angle is partly hidden by the effects of the initial vertical speed and of the torque.

4.2.4.2 Effect of roll angle on the height loss on Dauphin

► Figure 4-27 Effect of roll angle on height loss on Dauphin (Vuichard recoveries)



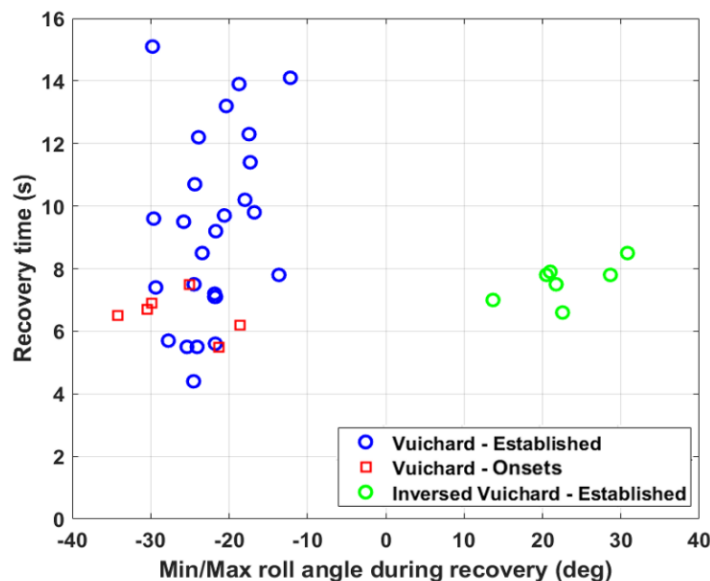
The effect on the Dauphin of the roll angle on the height loss during Vuichard recoveries is shown in Figure 4-27.

Pilots commented that the Vuichard recoveries seemed easier with roll angles of about -30° (instead of -20° as recommended), however the effect on the height loss is unclear due to the important dispersion. At the very least there appears to be no significant increase of the height loss when applying a roll angle higher than 20° in absolute value. There are not enough runs of “inversed Vuichard” recoveries to observe a clear tendency (although a slight better performance is observed at high roll angles for this small sample).

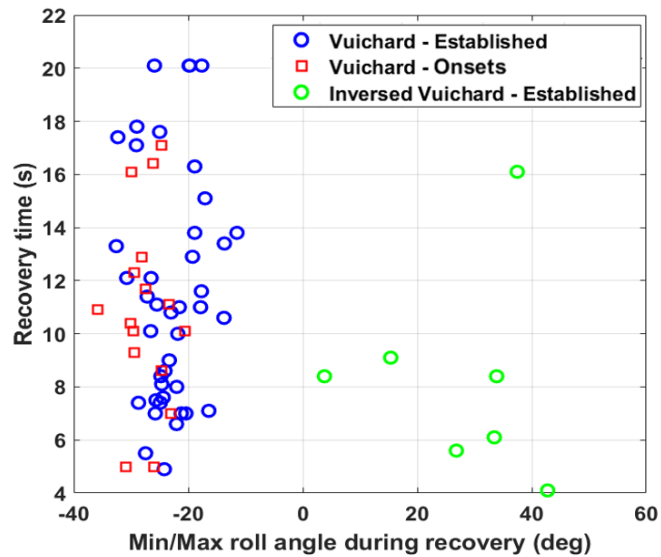
4.2.4.3 Effect of roll angle on the recovery time on both helicopters

The effect of the roll angle on the recovery time seems random for both helicopters, the points dispersion being higher than any tendency, as shown in Figure 4-28 (Fennec) and Figure 4-29 (Dauphin).

► Figure 4-28 Effect of roll angle on recovery time on Fennec (Vuichard recoveries)



► Figure 4-29 Effect of roll angle on recovery time on Dauphin (Vuichard recoveries)



4.2.5 Effect of the forward speed variation during Vuichard recoveries on both helicopters

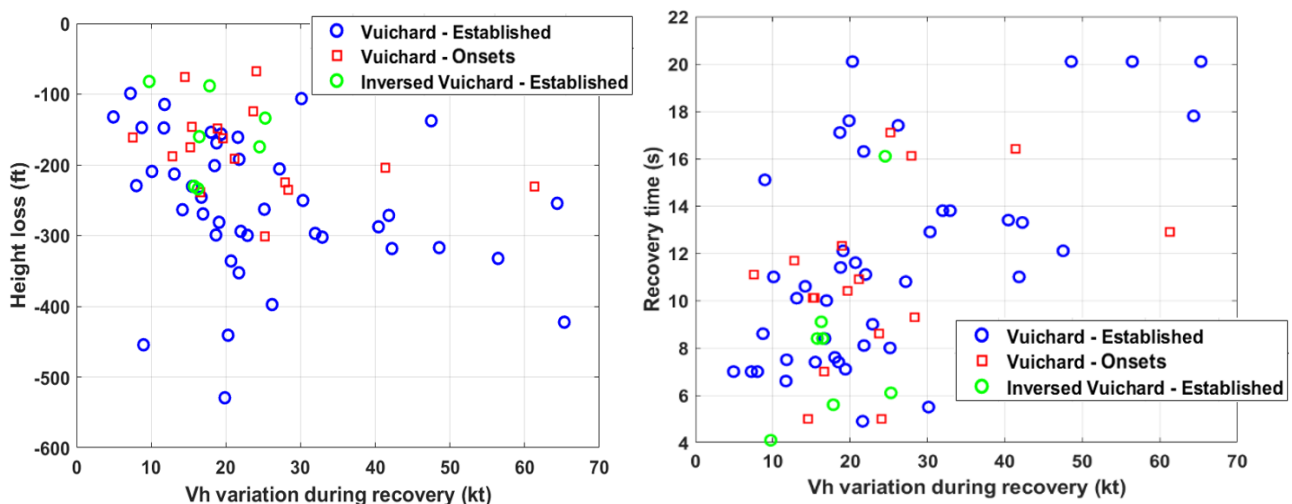
While this manoeuvre is supposed to be purely lateral, it was very difficult for the pilots to avoid any increase of the forward speed.

Figure 4-30 shows, for all Vuichard recoveries, the effect of the variation of forward speed on height loss (left graph) and on the recovery time (right graph) on the Dauphin helicopter.

It can be seen that the variations are not limited to low values, and can reach 65 kts.

Interestingly, these variations are much more limited during inversed Vuichard recoveries. The same variations can be observed in established or at VRS onsets. Globally, it seems that an increase of the forward speed variation lead to higher loss of height and longer recovery time. This could be correlated to higher pitch down attitudes, which lead to a performance deterioration. The same observations were made on Fennec data.

► Figure 4-30 Effect of the forward speed variation on performance on Dauphin (Vuichard recoveries)



4.2.6 Effect of the helicopter mass

The helicopter mass is expected to have the same type of influence as the vertical speed (as both are factors of the initial kinetic velocity), albeit with a less visible effect since its range of variation is relatively smaller (about 10% of the average mass on the Fennec, 15% on the Dauphin).

Thus, the influence of the mass on height loss and recovery time was analysed but no clear effect was noted. This can be explained by the fact that the reduced weight (M/σ where σ is the relative air density ρ/ρ_0) was maintained as constant as possible for the entries into VRS.

4.2.7 Summary of the influencing parameters

4.2.7.1 Effect of vertical speed

On both aircrafts the observed height loss increases with the initial rate of descent, with an almost linear tendency but with an important dispersion. This seems to explain the better performance of recoveries at the onset of VRS, which occur at lower rates of descent. When taking this effect into account, the performance of Vuichard recoveries are still better for recoveries at the onset on Fennec, but are worse on recoveries on Dauphin even at the onset.

The recovery time seems less predictable, with a slight increase of the rate of descent only for forward recoveries on Dauphin, but a more random distribution in the other cases.

The relative performance of Vuichard and forward recoveries are similar as for height loss, with an advantage for Vuichard recoveries at the onset on Fennec.

As mentioned in §4.1, the expected degradation of performance for inversed Vuichard recoveries was not observed. On the contrary, height loss and recovery time are better than what could be expected based on the initial V_z .

4.2.7.2 Effect of torque

The main effects of the average torque during recoveries are similar for both helicopters.

For forward recoveries, **a higher average applied torque during the recovery manoeuvre clearly reduces the height loss, with a smaller reduction of the recovery time.**

For Vuichard recovery, **the effect of the average torque on the performance is less straightforward, possibly because of the detrimental effects of a higher torque (notably, more important parasitic effects and pilot workload).**

When restricting the comparison to a similar range of average torque applied during recoveries :

- The height losses for both methods are similar for recoveries from established VRS (with more dispersion for Vuichard recoveries on Dauphin), and slightly better for Vuichard recoveries from the onset of VRS;
- The recovery time is similar on Fennec for recoveries from established VRS, while it is slightly better for Vuichard for recoveries from the onset of VRS. However on Dauphin the recovery time is clearly lower for forward recoveries than for Vuichard recoveries : this is likely because of the limited margin of power in hover which increases the time needed to neutralize the rate of descent.

Note: To deepen this first analysis, it could be interesting to investigate separately the influence of the average torque applied during the first few seconds of the Vuichard recovery (where it is expected to have a detrimental effect on the workload and parasitic motions) from its influence after the aircraft is horizontal again (where the torque is expected to reduce the time taken to reach a positive vertical speed).

4.2.7.3 Effect of the pitch angle on the performance

To summarise, in forward recoveries, the effect of the absolute minimum pitch angle:

- is undetermined on Dauphin ;
- The recovery time shows no clear tendency for both helicopters;
- For the Fennec, it seems that an absolute minimum pitch angle between -25° and -30° is optimal.

It is possible that the effect of the pitch angle is partly masked by the effects of the initial vertical speed and of the torque.

However, on Dauphin the variation of the pitch angle $\Delta\theta$ (between the recovery start and the minimum pitch angle reached during the recovery) seems correlated to both the height loss and the recovery time, which could be worth a further investigation.

It could also be interesting to consider the effect of the average pitch angle during the recovery rather than only the minimal value reached.

4.2.7.4 Effect of the variation of roll angle on the performance

The roll angle achieved during a Vuichard recovery appears to have a small positive effect on the height loss on Fennec, while the effect is undetermined on Dauphin.

For both helicopters, the effect of the roll angle on the recovery time is unclear.

At the very least, there appears to be no detrimental effect on performance of a roll angle higher than 20° , which is a useful information since found the recoveries seemed easier when performed with a roll angle closer to 30° .

4.2.7.5 Effect of the forward speed variation during Vuichard recoveries

On both helicopters, it seems that an increase of the forward speed variation lead to higher loss of height and longer recovery time. This could be correlated to higher pitch down attitudes, which lead to a performance deterioration.

4.2.7.6 Effect of the helicopter mass

The influence of the mass on height loss and recovery time was analysed but no clear effect could be noted.

4.3 Entry conditions

4.3.1 Exits at VRS onsets / established VRS

Vortex recoveries at the onsets were expected to happen at lower vertical speed (in absolute value) and with better performance. For the Fennec, quantitatively, the initial vertical speed was -626 ft/min on average for exits at the VRS onsets, versus -1173 ft/min for established VRS.

As shown in Table 4-3 for the Fennec, the recovery performance were indeed better in terms of height loss and average recovery time.

Table 4-3 Fennec performance in onsets/established VRS

Conditions	Recovery	Average Vz upper limit (ft/min)	Vz upper limit (ft/min)	Average Height loss (ft)	Height loss (ft)	Average Recovery time (s)	Recovery time (s)
Onsets	Forward	-626	-716	125	-168	7.9	9.3
Onsets	Vuichard		-537		-82		6.5
Established	Forward	-1173	-1212	210	-221	9.3	9.5
Established	Vuichard		-1134		-199		9.2

For the Dauphin, as shown in Table 4-4, the recovery performance were better regarding the height loss but worse for the recovery time.

Table 4-4 Dauphin performance in onsets/established VRS

Conditions	Recovery	Average Vz upper limit (ft/min)	Vz upper limit (ft/min)	Average Height loss (ft)	Height loss (ft)	Average Recovery time (s)	Recovery time (s)
Onsets	Forward	-816	-1051	213	-246	10.8	10.9
Onsets	Vuichard		-582		-179		10.8
Established	Forward	-924	-928	241	-227	10.0	8.5
Established	Vuichard		-921		-256		11.6

The improvement regarding height loss when exits are performed at VRS onsets can be at least partly explained by the direct influence of the initial vertical speed. But it could also be due to a less turbulent (or at least different) airflow around the rotor, as exits at the VRS onsets were in general judged slightly easier by the pilots.

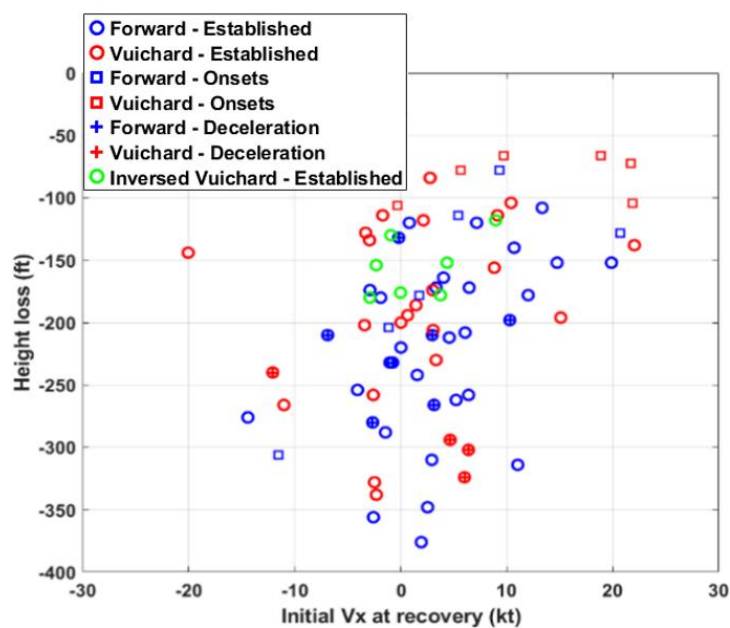
4.3.2 Influence of the horizontal speed

4.3.2.1 Influence of the initial horizontal speed on height loss on both helicopters

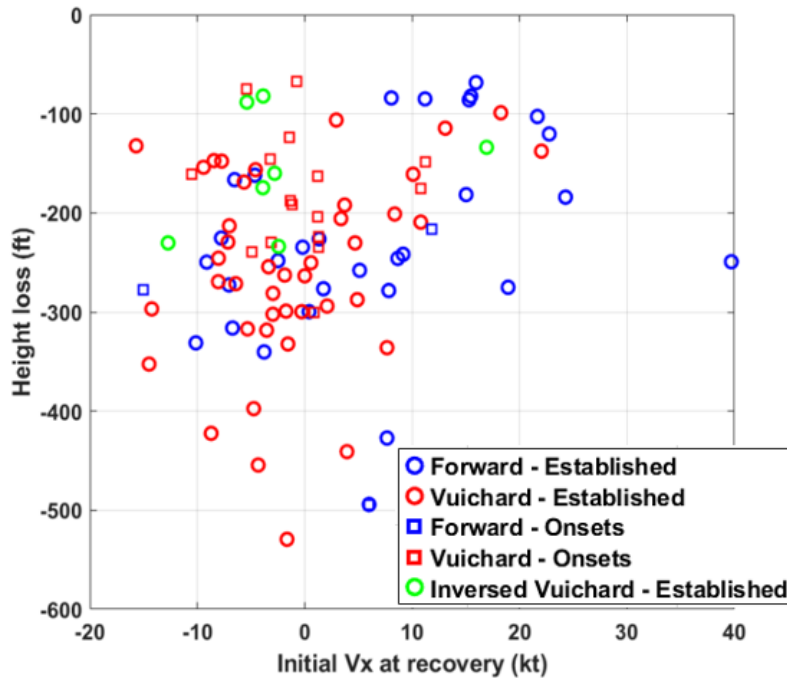
The effect of the initial forward horizontal speed (i.e. at recovery start) on the height loss seems overall positive for both helicopters, although there is an important dispersion of the points, as shown in Figure 4-31 (Fennec) and Figure 4-32 (Dauphin).

This was expected for forward recoveries, as with a forward speed the helicopter begins the recovery closer to the VRS domain boundary, but interestingly it appears to remain true for Vuichard and inversed Vuichard recoveries.

► Figure 4-31 Effect of initial Vx on height loss on Fennec (All recoveries)



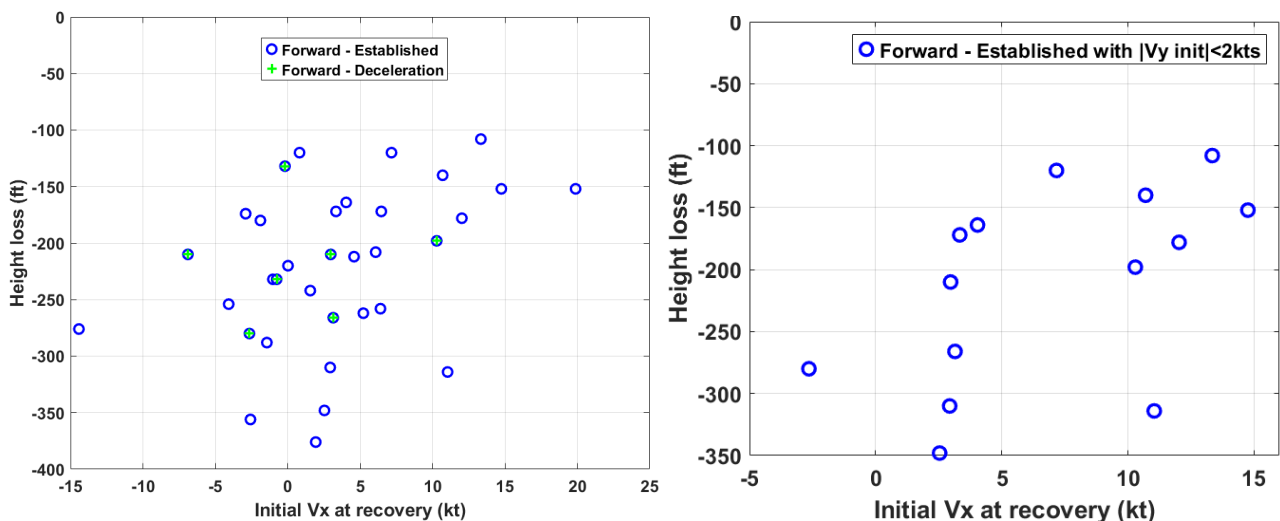
► Figure 4-32 Effect of initial Vx on height loss on Dauphin (All recoveries)

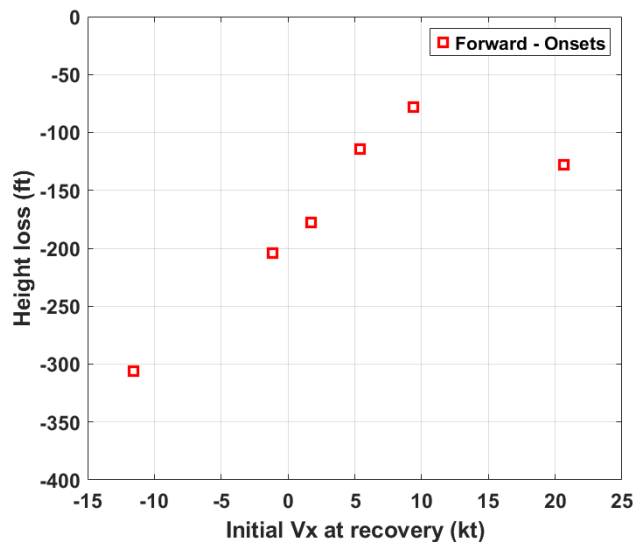


In Figure 4-33 and Figure 4-34 the effect of Vx on height loss is presented during only forward recoveries on the Fenec and the Dauphin.

Thus, it can be seen that higher values of the initial longitudinal speed Vx tend to reduce the loss of height on both helicopters. There are not enough points at negative forward speeds to clearly assess whether a negative Vx has an adverse effect on the height loss (which would be expected for forward recoveries, as the helicopter will have to cross a wider portion of the VRS domain before recovering).

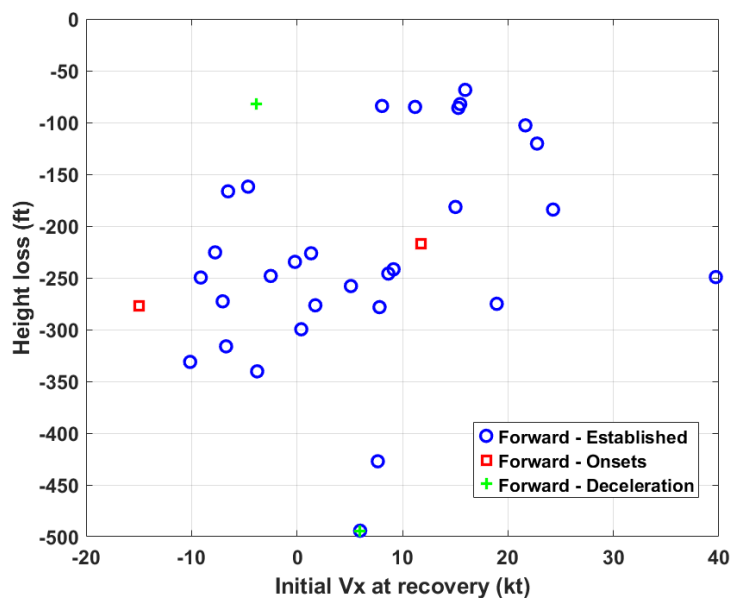
► Figure 4-33 Effect of initial Vx on height loss on Fenec (Forward recoveries)





The effect of Vx on height loss is presented during only forward recoveries on the Fenec. It can be seen that higher values of the initial longitudinal speed Vx tend to reduce the loss of height, especially when only considering the runs in which the absolute value of the lateral speed Vy at the beginning of the recovery was below 2kt (upper right graph). This trend is much clearer for exits at the VRS onsets (lower graph) while the small sample of points can be misleading.

► Figure 4-34 Effect of initial Vx on height loss on Dauphin (Forward recoveries)

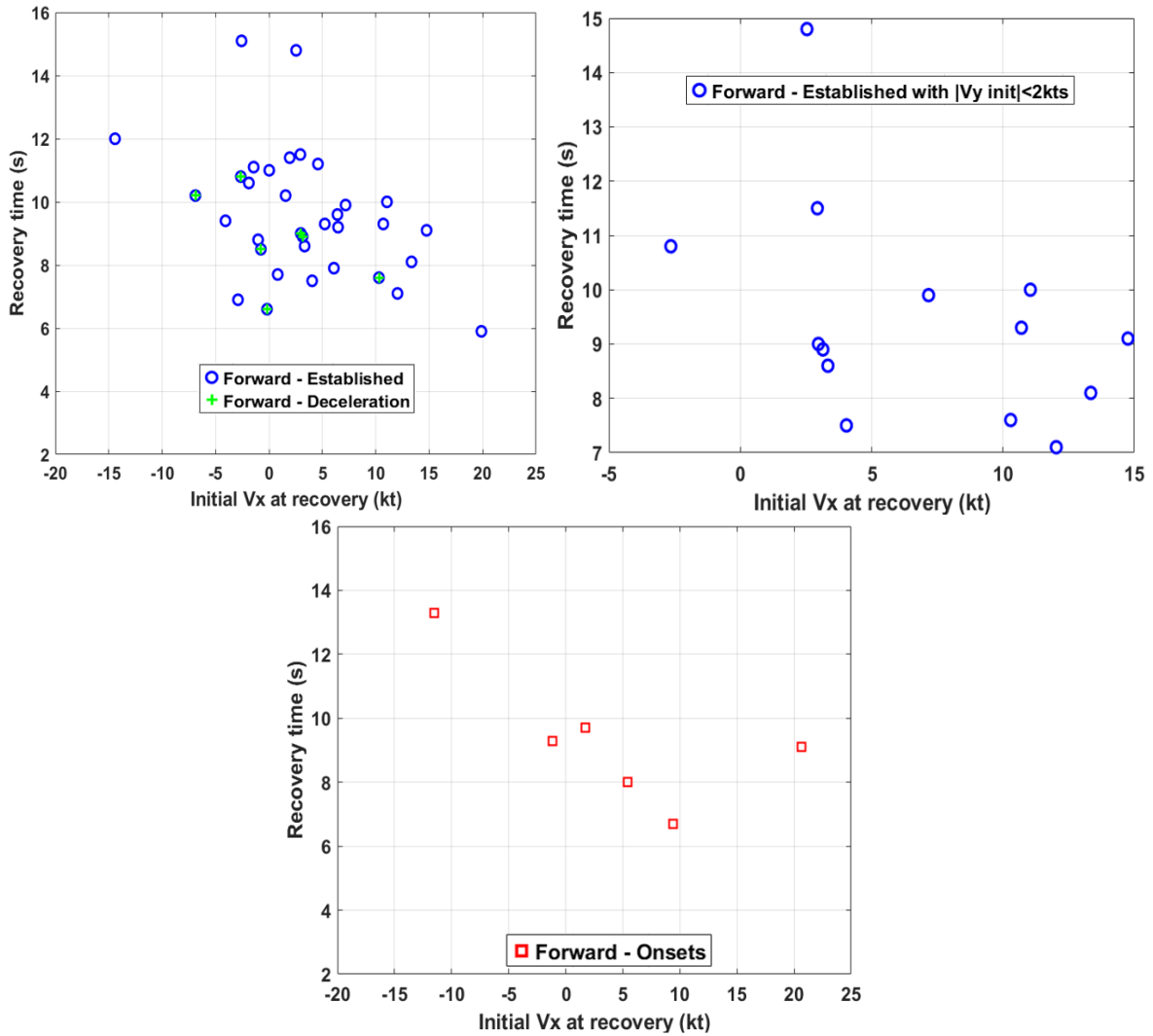


For the Dauphin, this trend is less visible, even when only considering almost pure longitudinal manoeuvres ($|V_y| < 2\text{kt}$ – not plotted in the figure)

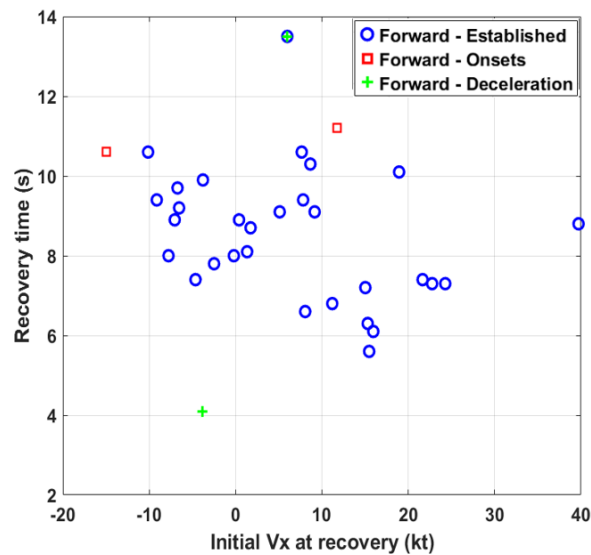
4.3.2.2 Influence of the initial horizontal speed on recovery time on both helicopters

The same trend is more noticeable on the recovery time as shown in Figure 4-35 (Fenec) and Figure 4-36 (Dauphin). For both helicopters, negative speeds seem to degrade the performance in terms of recovery duration.

► Figure 4-35 Effect of initial Vx on recovery time on Fenec (Forward recoveries)



► Figure 4-36 Effect of initial Vx on recovery time on Dauphin (Forward recoveries)

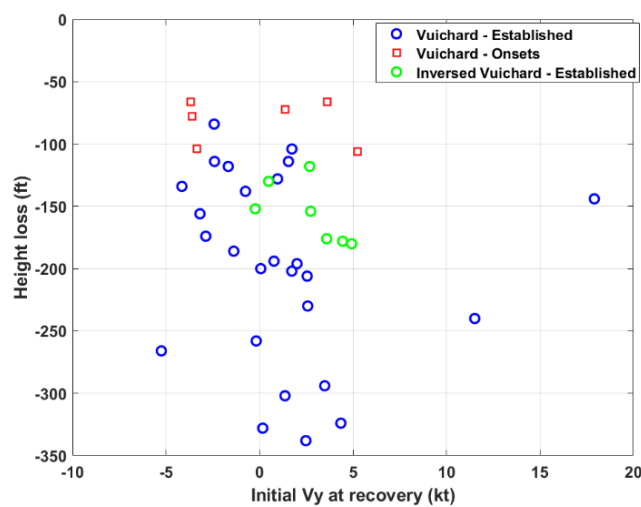


4.3.1 Influence of the lateral speed

4.3.1.1 Influence of the initial lateral speed on height loss on both helicopters

For Vuichard recoveries, the lateral speed was also expected to have an influence on the recovery. For the Fennec and exits in established VRS, as shown in Figure 4-37, on average the height loss is reduced when starting with an initial speed toward the left (negative), and conversely increased with an initial speed toward the right (positive). Indeed, except for a single outlier ($V_y = -5 \text{ kt}$, Height loss = -266), height loss is always lower than 200ft for $-5 \text{ kt} < V_y < 0 \text{ kt}$. For positive $0 \text{ kt} < V_y < 5 \text{ kt}$, height losses are comprised between 104ft and 338ft.

► Figure 4-37 Effect of initial V_y on height loss on Fennec (Vuichard recoveries)

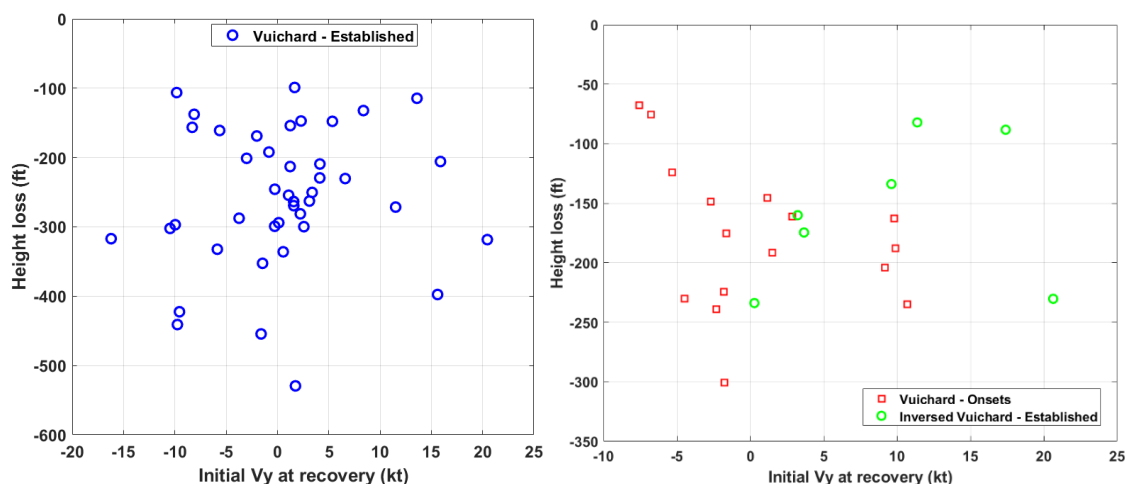


However for inversed Vuichard recoveries and for exits at the VRS onsets, there is no clear improvement due to an initial speed toward the right (positive), but this may be due to the very limited number of points (all performed with an initial speed toward the right) and to the points dispersion caused by the other influencing parameters.

For the Dauphin, as shown in Figure 4-38, for exits in established VRS (left graph), a very large dispersion of the points can be observed and no specific trend can be observed.

The height loss seems to be reduced when starting with an initial speed toward the left (negative) for recoveries performed at VRS onsets (red squares on right graph). The inversed Vuichard technique (green circles on right graph) is giving the expected tendency (reduced height loss at higher positive speeds).

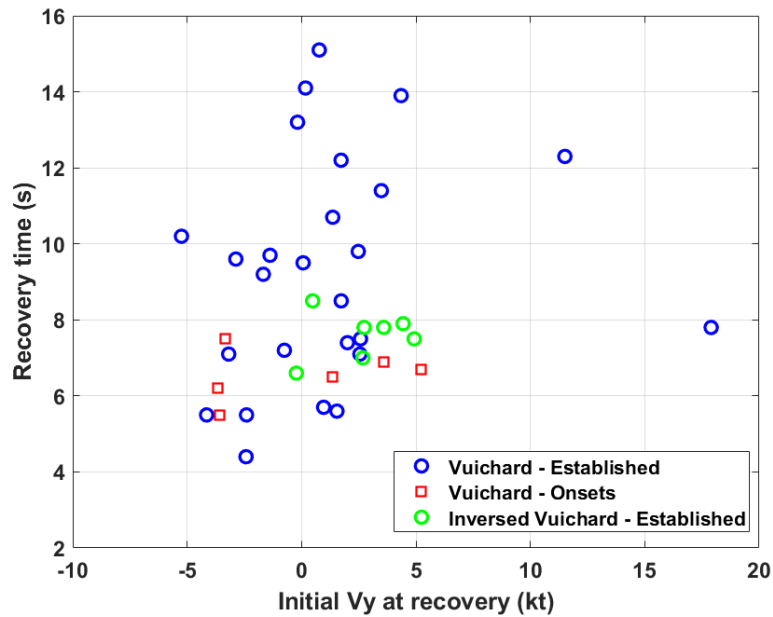
► Figure 4-38 Effect of initial V_y on height loss on Dauphin (Vuichard recoveries)



4.3.1.2 Influence of the initial lateral speed on recovery time on both helicopters

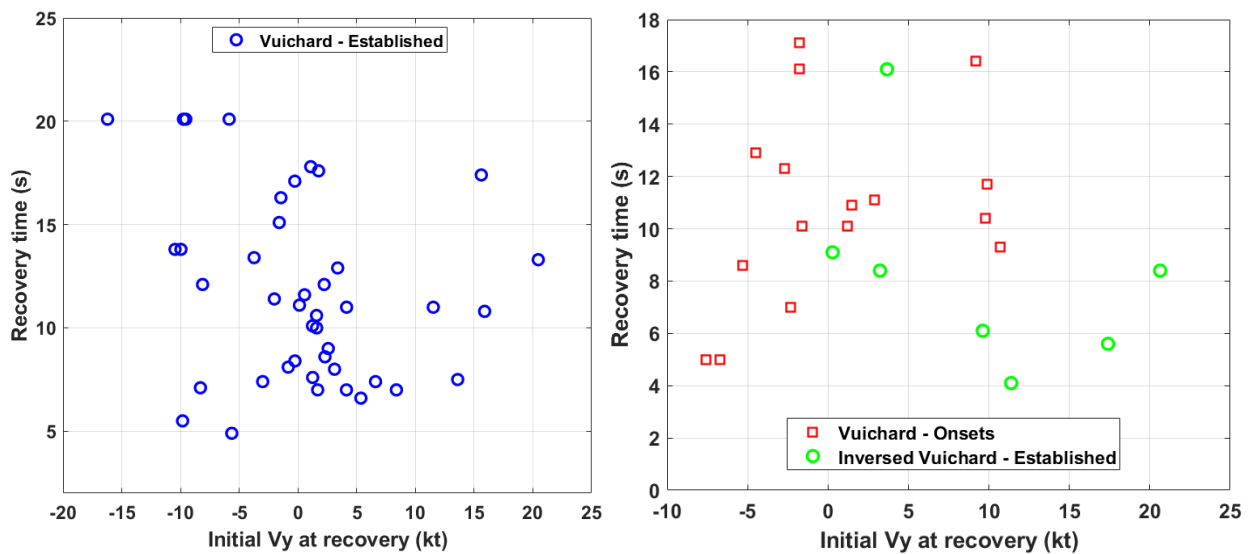
For the Fennec and exits in established VRS, as shown in Figure 4-39, on average the recovery time is reduced when starting with an initial speed toward the left (negative). For inversed Vuichard recoveries and for exits at the VRS onsets, there is no clear improvement due to an initial speed respectively toward the left or the right.

► Figure 4-39 Effect of initial V_y on recovery time on Fennec (Vuichard recoveries)



For the Dauphin, as shown in Figure 4-40, the expected effects are observed for recoveries performed at VRS onsets and inversed Vuichard recoveries (right graph). But a very large dispersion of the points can be observed for recoveries performed in established VRS without clear trend (left graph).

► Figure 4-40 Effect of initial V_y on recovery time on Dauphin (Vuichard recoveries)

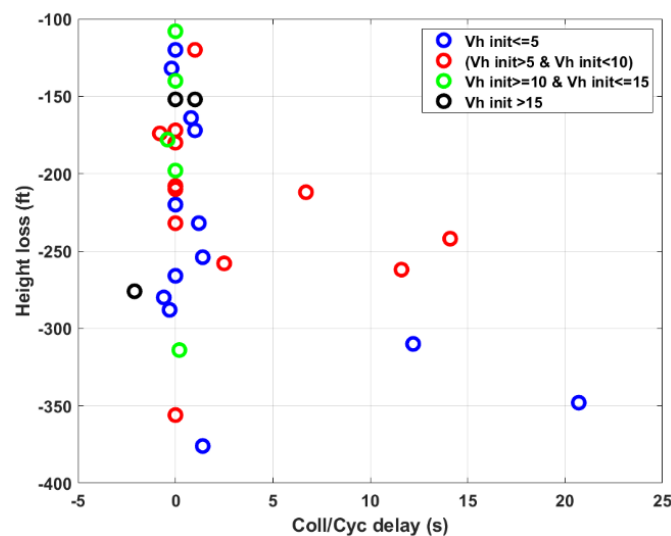


4.3.2 Effect of delayed increase of collective

4.3.2.1 Effect of delayed increase of collective on the Fenec

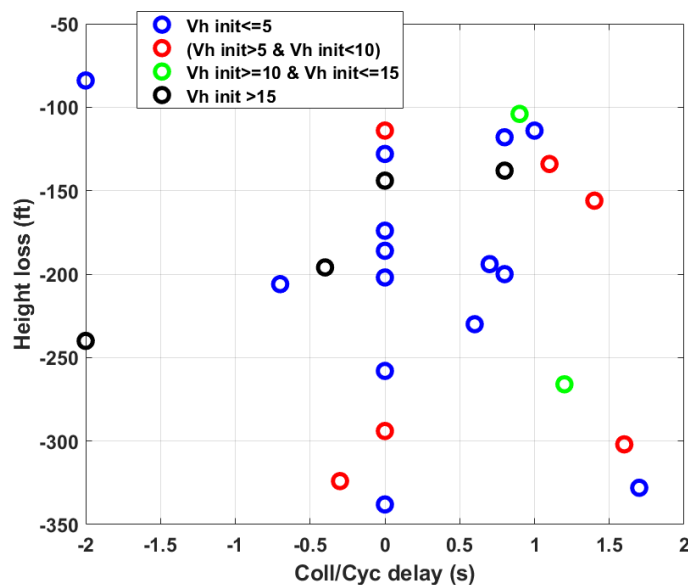
Figure 4-41 and Figure 4-42 are showing the effect of a delayed collective increase on the Fenec during respectively forward and Vuichard recoveries, and depending on the initial forward speed. “Coll/cyc delays” in the figures are defined as the time between an action on the collective and on the cyclic (longitudinal or lateral depending on the studied recovery). The delays were generally higher during the forward recovery, and it can be seen that delaying the increase of power lead to higher loss of height. Nevertheless, when the collective increase is performed before the longitudinal or lateral cyclic action (negative Coll/Cyc delays in the figures), the beneficial effect is not so clear.

► Figure 4-41 Effect of a delayed collective increase on Fenec (Forward recoveries)



As this is recommended to first apply a collective increase during a Vuichard manoeuvre, the delays were very low, and no clear tendency can be observed on Figure 4-42.

► Figure 4-42 Effect of a delayed collective increase on Fenec (Vuichard recoveries)



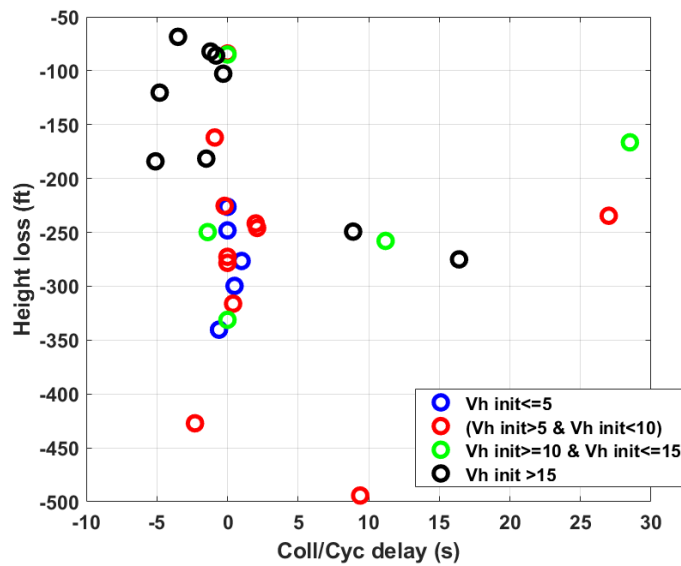
For both recovery types, the effect of a delayed collective increase seems independent of the initial forward speed.

4.3.2.1 Effect of delayed increase of collective on the Dauphin

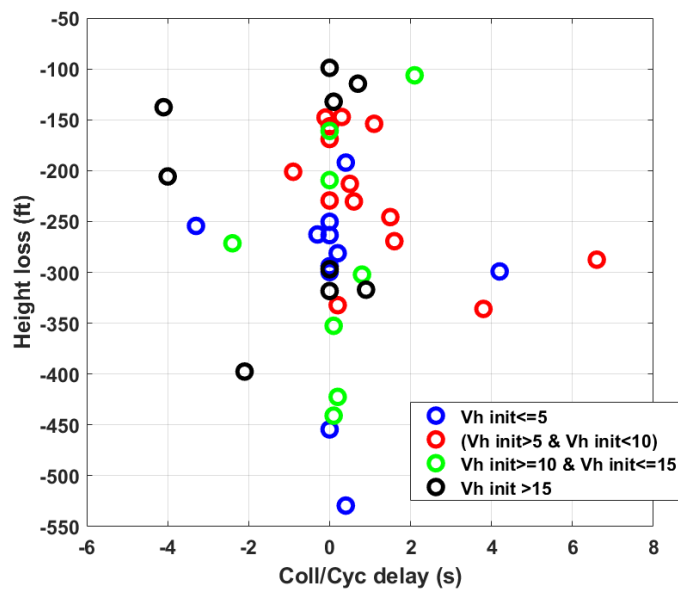
Figure 4-43 and Figure 4-44 are showing the effect of a delayed collective increase on the Dauphin during respectively forward and Vuichard recoveries, and depending on the initial forward speed.

As for the Fennec, the delays were generally higher during the forward recovery, and it can be seen that delaying the increase of power lead to higher loss of height. But contrary to the Fennec, it seems that when the collective increase is performed before the longitudinal or lateral cyclic action, a beneficial effect can be observed.

► Figure 4-43 Effect of a delayed collective increase on Dauphin (Forward recoveries)



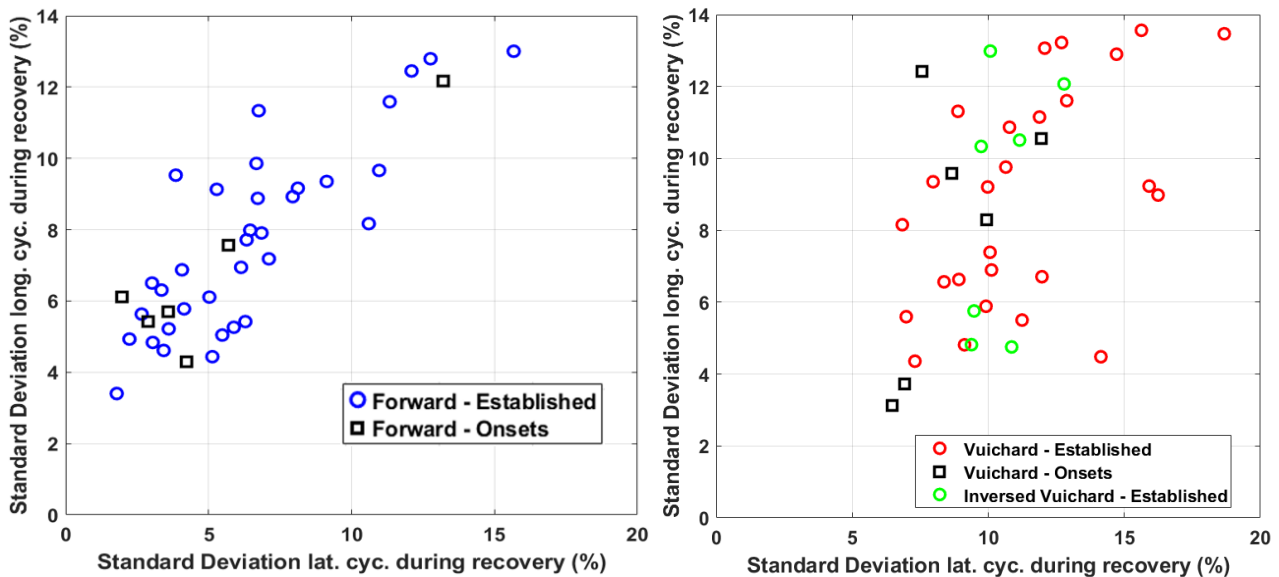
► Figure 4-44 Effect of a delayed collective increase on Dauphin (Vuichard recoveries)



4.4 Pilot feedback

Before detailing the pilot feedback, Figure 4-45 shows the standard deviations calculated on the longitudinal cyclic with respect to the lateral cyclic during all manoeuvre types. It has to be noted that pilot's activity or workload cannot be estimated through the only analysis of the standard deviations of the flight controls, but this activity on controls contributes to the general workload.

► Figure 4-45 Pilot control activities during all recoveries on Fenec



On the Fenec, the overall tendency indicates that an increase of the pilot activity on one axis lead to an increase on the other axis.

The standard deviations on the lateral cyclic, on average, are slightly higher than on the longitudinal cyclic during Vuichard recoveries, which is consistent with a lateral manoeuvre.

For forward manoeuvres, a strong correlation of the standard deviations on both axes can be observed (see left graph), an increase of the pilot's activity on one axis implying an almost similar increase on the other axis. During inversed Vuichard manoeuvres, the activity on the lateral cyclic is almost constant, around 10%, while there's a large dispersion on the longitudinal cyclic (between 4.5% and 13%). The fact that the recoveries were performed at VRS onsets or in fully VRS has no effect.

On the Dauphin, as seen on Figure 4-46, a larger dispersion of the points can be observed.

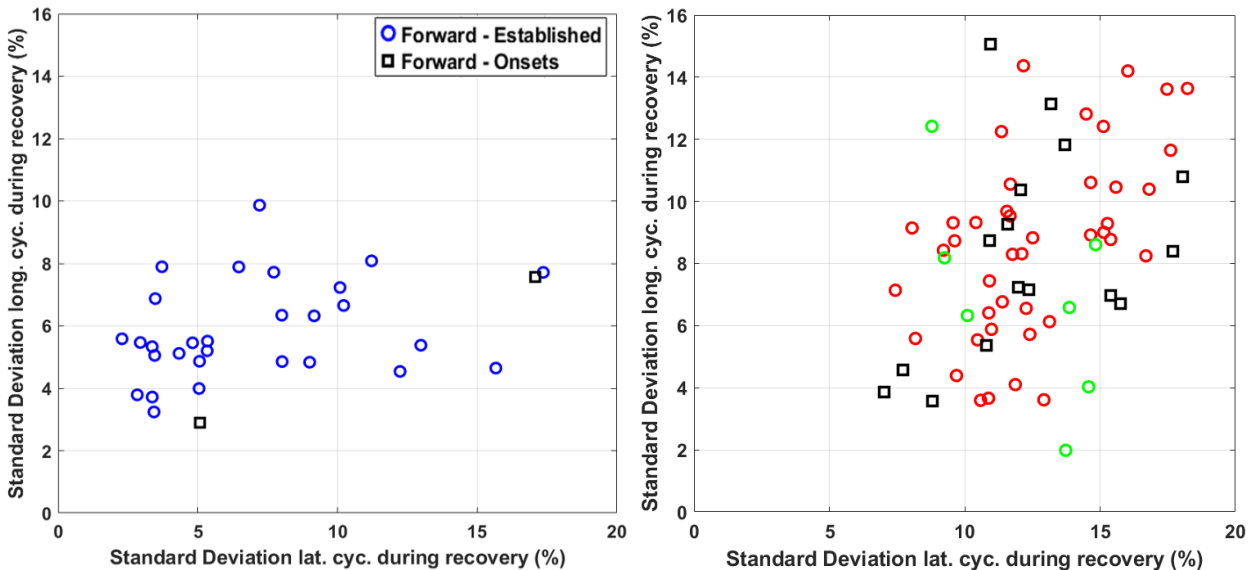
During Vuichard recoveries, the standard deviations on the lateral cyclic, on average, are slightly higher than on the longitudinal cyclic, which is here again consistent with a lateral manoeuvre. Minimum and maximum values of the standard deviations on both axes are comparable to the ones observed on the Fenec.

For forward manoeuvres, the standard deviations on the lateral cyclic, on average, are much higher than on the longitudinal cyclic, which is quite surprising for a longitudinal manoeuvre, and quite different from the results on the Fenec.

For inversed Vuichard recoveries, the standard deviations on the lateral cyclic are more dispersed (varying from 8.7% to 14.3%), with still a widespread distribution on the longitudinal cyclic (between 2% and 12.4%).

The fact that the recoveries were performed at VRS onsets or in fully VRS has no effect.

Figure 4-46 Pilot control activities during all recoveries on Dauphin



4.4.1 Pilot feedback regarding forward recoveries

4.4.1.1 Forward recoveries on Fenec

Both pilots were trained to exit VRS using forward recoveries since their initial instruction, including during their flight test training at EPNER, and were therefore familiar with this method.

Their workload during the manoeuvre was deemed as low in general, with actions mainly on one axis (cyclic longitudinal) and to a lower extent on the collective stick.

The action on the cyclic was simple and intuitive, with a simple push forward and then small corrections at a low frequency. The action on the collective was even easier, with a preset level which did not have to be changed in most cases (except with a high initial target, see further), since pushing the nose down tends to decrease the power required by the rotor.

Airbus Helicopters safety information notice n°3463-S-00 (in reference [3]) specifies to “check power and increase the collective pitch as required”, while “applying decisively forward cyclic input to gain airspeed (1-2sec)”, and then to adjust the pitch attitude to level the helicopter once a speed of 20-30 kt is achieved. There is no quantitative target for either the collective stick nor for the pitch angle.

The effect of these parameters were investigated during the first flight. The results have shown that increasing the targeted torque from 50% (hover power) up to 70% resulted in better recovery performance with little change in the workload. A further increase from 70% to 80% was detrimental as here was a sudden rise of the pilot workload, but only a marginal performance improvement.

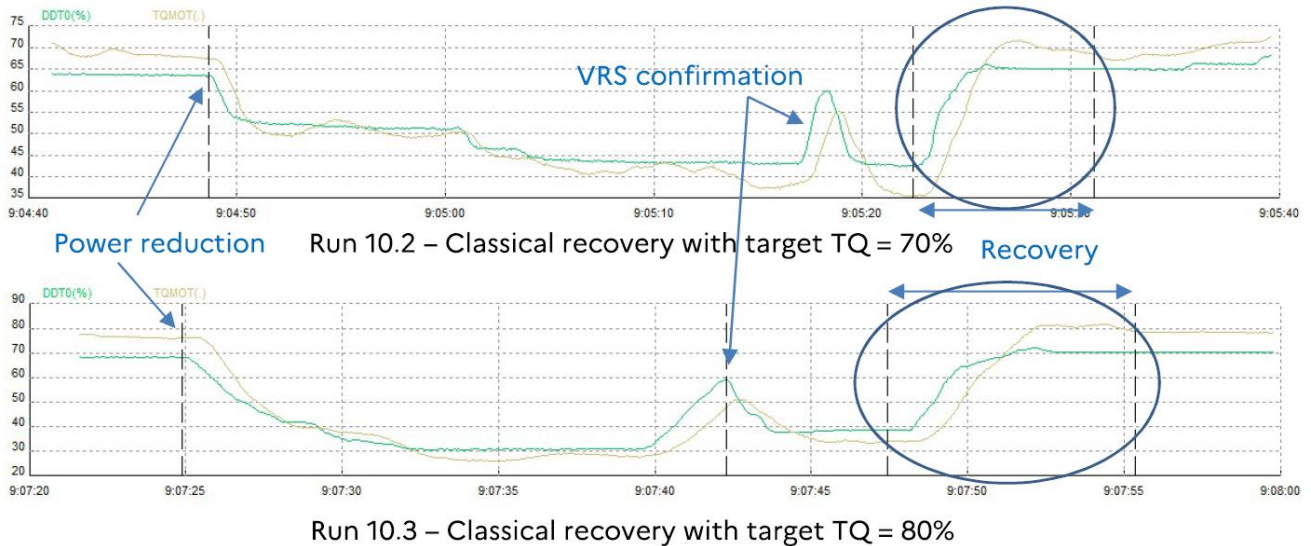
What happened in practice was that the pilot was more prudent (and slow) when increasing the power, in order not to exceed the helicopter limitations, as shown in Figure 4-47.

The target of 80% of torque is eventually reached, but with a slower dynamic : the increase of 10% of the target only translate to an increase of less than 4% of the average torque applied during the recovery, hence the small performance increase.

The pilot also had to monitor the torque increase when moving the nose back up, and had to use the foot controls with a moderate frequency to maintain the heading, which increased his workload.

In order to optimise both the recovery performance and the pilot workload, at torque target of 70% was therefore defined for forward recoveries on Fenec.

► Figure 4-47 Comparison of power increases for torque targets of 70% and 80%



Regarding the pitch applied, a target above -15° (absolute pitch angle) was considered by the pilot to be uncomfortable to pilot and too slow to exit the “unstable” part of the VRS (although this is not reflected in the previous results). It would also not be consistent with the “decisively forward input” recommended by Airbus Helicopters. On the other hand, nose-down attitudes of -30° or below were deemed inadvisable for a real VRS occurring near the ground.

Therefore the forward recoveries on Fenec were performed with a target of -20° absolute pitch angle.

4.4.1.2 Forward recoveries on Dauphin

The workload was deemed low up to a torque target of about 70%, but was evaluated as medium to high when aiming for a torque above 80% due to the risk to exceed the aircraft limitations

As with the Fenec, a target of about 70% of torque was found to be optimal to balance performance and pilot workload, along with a pitch down motion of about $\Delta\theta \sim -15^\circ$.

In these conditions, the workload during forward recoveries on the Dauphin was deemed as low in general, with actions mainly on one axis (cyclic longitudinal) and to a lower extent on the collective stick.

The action on the cyclic was simple and intuitive, with a simple push forward and then small corrections at a low frequency. The action on the collective was even easier, with a preset level which did not have to be changed in most cases, since pushing the nose down tends to decrease the power required by the rotor. There were no noticeable parasitic effects, and the fenestron appeared to play its role and remove the need to use the foot pedals to control the heading.

4.4.2 Pilot feedback regarding Vuichard recoveries

4.4.2.1 Vuichard recoveries on Fenec

Both pilots each had a training flight on the Vuichard recoveries by Mr Vuichard himself, and were then only able to train and calibrate their actions during the harmonisation flights.

They were thus less familiar with the Vuichard recovery method, which should be taken into account. It should be noted however that their increased familiarity with the Vuichard recovery method over the course of the test campaign (over 50 Vuichard recoveries shared between both test pilots) did not change their feedback on the perceived workload.

The pilots expressed a higher workload during the Vuichard recoveries, with high frequency actions on all 3 axes and on the collective to avoid exceeding the limitations, and in a short time interval. The sensations and

pilots actions differed from one Vuichard recovery to another, even for identical runs, but the typical sequence of actions was the following:

- First, inputs on both the lateral cyclic and foot pedals to initiate the motion, while increasing the power (collective). The amplitude of the actions on the lateral cyclic and foot pedals were high, with a moderate effort. In order to maintain the heading, the foot controls were close to the right stop, and this was not sufficient for a few runs (such as Run 11.3 – Flight 4, Vuichard recovery from a translation to the right, where a heading shift 15° to the left could not be prevented).

The initial increase of power also required the pilot to monitor the torque indicator, a task complicated by the small delay on the needle motion on the Fennec;

- During the translation to the left, actions with a medium to high frequency were required on the foot control to try to maintain the heading, and to a lower extent on the lateral cyclic to maintain the roll angle;

- When putting the helicopter back to a horizontal attitude, the pilot had to work with a high frequency on the lateral cyclic and foot controls to try to stabilise the roll and yaw angles. He also had to act quickly on the longitudinal cyclic to counteract a nose-down parasitic motion of the helicopter (with an average of about $\Delta\theta=10^\circ$ despite the pilot actions). Meanwhile, he had to closely monitor the power to avoid an overtorque.

There was a peak in the workload both at the start of the manoeuvre and when the roll angle was brought back to zero, due to the proximity to the aircraft limitations and to parasitic effects.

The cyclic lateral activity was variable from one test run to another, and seemed on average more important for recoveries from established VRS than at the onsets. Exits at the VRS onsets were overall judged easier to perform by the pilots. This could be explained by the difficulty to maintain a stable attitude while confirming the VRS, which tires the pilot even before the recovery is started, and by a more random initial position (of the aircraft and of the cyclic stick) due to the turbulent and unpredictable conditions encountered in established VRS.

Recoveries with a forward speed (either because it was the entry condition, or because the nose down parasitic motion was not completely balanced) were also judged to be easier to pilot, with more intuitive actions on the cyclic stick.

Pilots felt that the Vuichard manoeuvre allowed a quick return to hover about half the time (when the pilot managed to counteract the pitch-down parasitic effect quickly enough). Nevertheless, this statement is not validated when analysing the flight data as shown in Table 4.1, where it can be seen that the recovery duration is 30% lower (6.5s instead of 9.3s for forward manoeuvre) only for recoveries at VRS onsets. In established VRS, the duration are almost the same.

4.4.2.2 Inversed Vuichard recoveries on Fennec

Regarding the “inversed” Vuichard recoveries, performed by translating to the right, the observations were similar with the following additions:

- It was even harder to maintain the heading, especially at the start and the end of the translation. The foot pedals activity was higher than for a translation to the left;

- Strong attitude changes both on the pitch and roll axis, and a pendulum motion on the roll axis, required a high activity on the cyclic stick;

- Stronger vibrations were heard and felt by the crew during the recoveries;

- The pilot reported peculiar sensations on the controls and on the aircraft reaction, which could be linked to unusual parasitic actions (effect of the tail rotor for example);

- The recoveries were again judged easier at the VRS onsets.

It should be noted that during the Vuichard recoveries, the helicopter take-off power limitations were often approached despite their attentive monitoring by the evaluator pilot, and even when keeping a margin against the maximum available power called for by the procedure (to anticipate the torque increase when the roll angle is brought back to zero).

In operational conditions, for a pilot with normal skills immediately using all available power at the start of the recovery, there would be a high risk to exceed the aircraft limitations.

During the last flights, the test pilots did try to pre-calibrate some actions (such as the amount of foot on the right pedal required to keep the heading constant) to make the recovery easier, but found that the variations observed from one Vuichard recovery to another (even for identical entry conditions) did not allow them to correctly anticipate the required actions. A few Vuichard recoveries were judged fluid and easy, and even allowed to come back quickly to hover, but this was not reproducible even for successive set of points in identical conditions. This non-homogeneity of the Vuichard recoveries is a significant factor of the high workload on Fennec, as the test pilots felt that after they initiated the motion they had to react to a succession of unpredictable reactions of the aircraft: in their words, they “reacted more than they controlled”.

Overall, the lateral motions of the Vuichard recoveries were also deemed less “intuitive” than the forward motion of forward recoveries by both test pilots, as their natural instinct (consistent with the emergency procedures in case of failure in hover) is to increase speed toward V_y by moving forward.

4.4.2.3 Vuichard recoveries on Dauphin

Overall, the pilots encountered difficulties and a high workload during Vuichard recoveries due to the strong and sudden attitude changes encountered during the recovery, which had to be corrected by actions on all 4 control axis (cyclic longitudinal and lateral, collective, and foot pedals). The feedback is similar to what was observed on the Fennec flights, but with worse parasitic effects and attitude changes (very likely due to the effect of the fenestron during the lateral translation), and less power margin, which results in a higher workload and more risks to exceed the aircraft limitations.

More in detail:

- During the initial increase of power and simultaneous lateral translation toward the left, a parasitic yaw motion toward the left was observed, which had to be countered by an action on the right foot pedal to maintain heading. A parasitic nose-down motion was also noted at the end of the translation, which had to be countered by an action on the longitudinal cyclic. Meanwhile, fluctuations in power (torque and NG) had to be closely monitored to avoid exceeding the limitations: for this reason the pilots kept a margin compared to the requirement to use “all the available power”. A first power peak was usually observed in the middle of the roll;

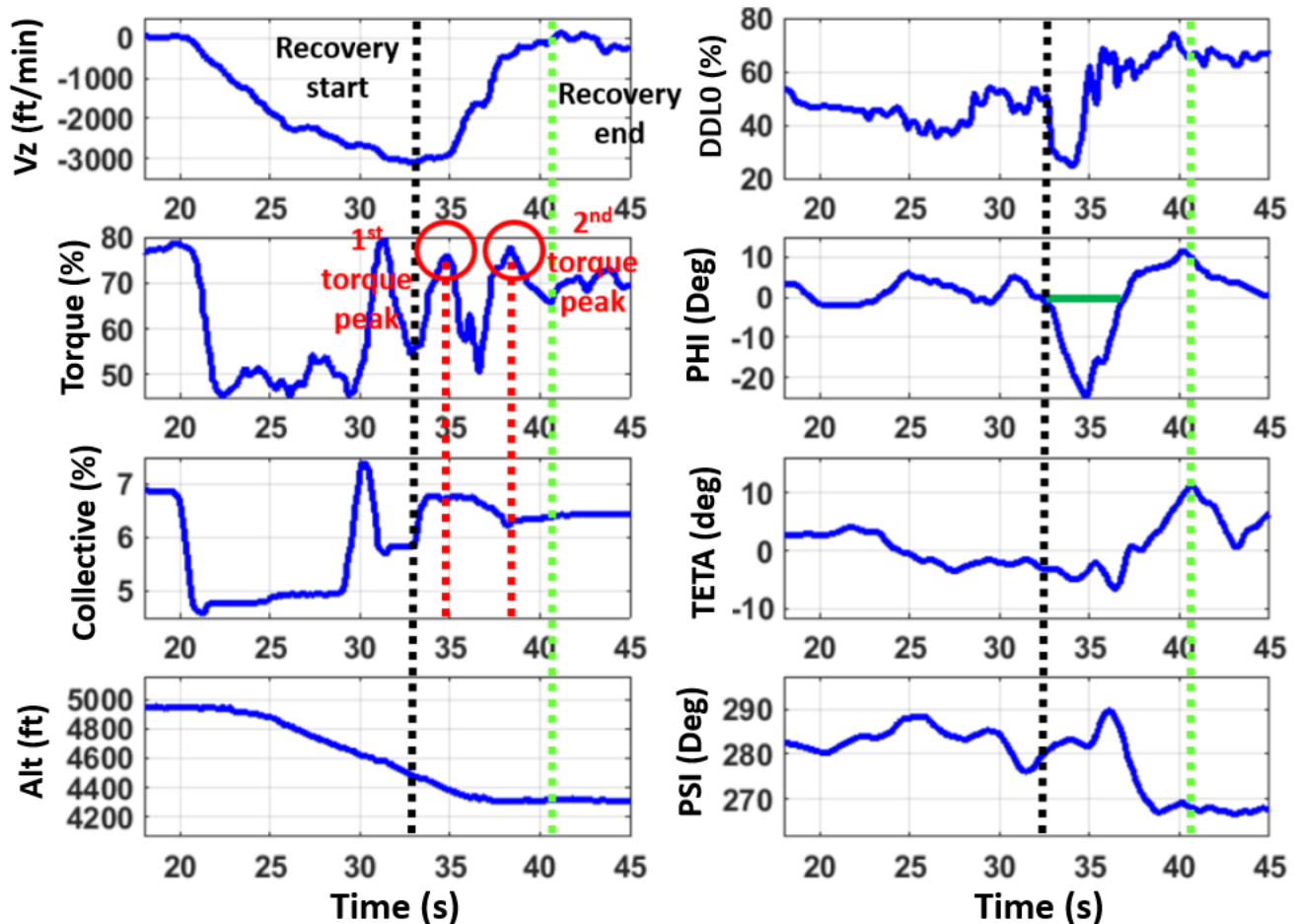
- When putting the rotor back to an horizontal position, actions were required on the cyclic (both axis) and foot pedals to maintain the heading and keep the helicopter flat, while closely monitoring the power level to manage a second peak of power. As shown in Figure 4-49, this second peak, often higher than the first, occurred despite slightly decreasing the collective, and was only caused by the actions on the cyclic and foot pedals to stabilise the aircraft attitudes. The parasitic yaw motion (likely due to the effect of the lateral speed on the rudder/fenestron) was maximal at this stage:

due to the proximity with the limit of authority on the right pedal and to the speed of these changes, heading changes of -20° on average and up to -50° were observed despite the pilot actions.

The pilots’ actions and workload on each axis were:

- On the lateral cyclic: an initial impulsion of moderate to high amplitude to start the roll (sometimes close to the left cyclic stop). The motion was hard to calibrate, because of a perceived “lag time” between the pilot action and the aircraft reaction (which was not noticed on the longitudinal axis and may be due to the fenestron), and the pilots felt they had to “accept” the roll angle reached. A roll angle above the recommended 20° and closer to 30° was judged more comfortable by the pilots without degrading the recovery performance. Then actions with moderate amplitude and high frequency were required to bring the rotor flat again, and stabilise it. The associated workload on this axis was moderate, and more easily accepted since it was an intentional motion;

► Figure 4-48 Example of Vuichard recovery from established VRS



- On the longitudinal cyclic: actions on this axis were mostly performed to correct the nose-down parasitic effect. They started in the middle of the roll, with actions of moderate amplitude and moderate frequency, although quite variable from one run to the other. The pilots judged fighting the nose down motion and the associated speed increase “not instinctive”, as in case of failure the procedure usually recommends to increase the speed toward V_y or V_{TOSS} . The associated workload was moderate to high, the unpredictability of the required actions being the main factor in this workload. It should be noted that accepting the forward speed without acting on the commands to come back to hover significantly decreased the actions required on this axis;
- On the foot controls: actions on this axis were mainly performed to counter the parasitic yaw motion while trying to maintain heading. These corrective actions were performed at a high amplitude (often close to the right stop), and with a low to moderate frequency. The associated workload was moderate to high, again because of the unpredictability of the required actions, which prevented the pilots from usefully anticipating the required motions. In other words, the issue was not the number of actions to be performed, but being unable to anticipate when and how much foot to apply. Exiting with a forward speed (not trying to return to hover) significantly decreased the actions and workload on this axis, probably because when moving forward the fenestron was acting as intended as a rudder to stabilise the trajectory;
- On the collective: after the first increase of power, actions were performed at a low to moderate amplitude and frequency. However the pilot had to closely monitor the power limitations, which could be exceeded either through the effect of the other controls (mainly the foot pedals) or because of the

fluctuations encountered (probably because of the airflow changes). The associated workload was high, again mainly because pilots had to watch carefully the power indicators to know if and when it was necessary to reduce the power level. In practice, the second power peak occurring after the end of the roll was particularly deceptive, as it was indirectly caused by actions on the foot pedals and lateral cyclic (which were themselves varying from one run to another and therefore unpredictable). Despite the margins taken by the evaluators and their focus on the power level, interventions of the safety pilot to block or even lower the collective stick were frequent (about a third of the Vuichard recoveries).

In summary, the high workload of the Vuichard recoveries was caused by:

- The strong and sudden attitude changes and the actions on controls required to correct them;
- The unpredictability of the parasitic effects, which varied from one run to another (even for similar entry conditions) and prevented pilots from efficiently anticipating their actions. Pilots felt that after their initial impulse, they had to uncomfortably manage a succession of unpredictable reactions of the aircraft;
- The proximity to power limitations, which required several interventions by the safety pilot despite the margins taken by the evaluator. In operational conditions, for a single pilot with normal skills immediately using all available power at the start of the recovery (as the methods prescribe), there would be a high risk to exceed the aircraft limitations.

The workload evaluation remained unchanged even after the familiarisation of the pilots, which occurred over the test campaign (and over a hundred Vuichard recoveries on Fennec and Dauphin spread between both pilots). Additional training is therefore not expected to significantly change the workload, which is generated by the longer and more complex sequence of actions, by the number of controls/axis on which to act, and by the unpredictable parasitic effects.

As a positive point, returning to hover after a Vuichard recovery could be fast when the pilot managed to control the aircraft attitude changes.

For both forward and Vuichard methods, recoveries at the onsets were overall judged easier than recoveries from an established the vortex. At the onsets, the pilot starts to work intensely only at the beginning of the recovery, which is performed from a reproducible (or more “calibrated”) commands positions. Whereas in established vortex, the workload is high as soon as the VRS is detected and during the time needed to perform the collective check, while using the cyclic (both axis) and foot pedals to try to maintain a stable attitude. Pilots felt therefore less available for the actual recovery, which in addition started from more random attitudes and commands positions.

4.4.2.4 Inversed Vuichard recoveries on Dauphin

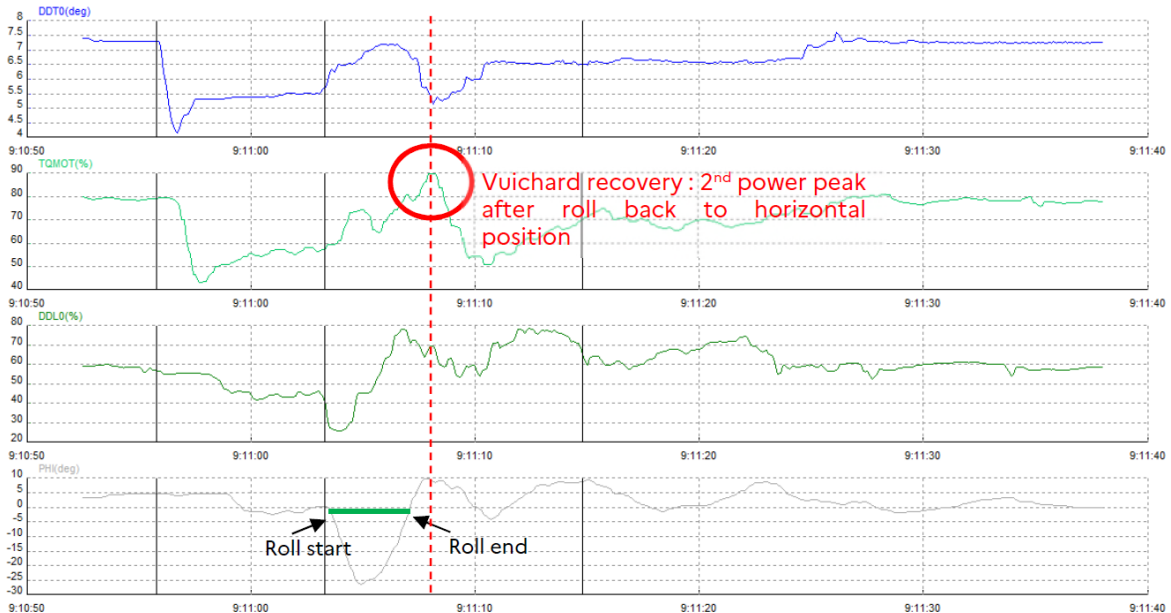
Inversed Vuichard recoveries (exit toward the right) were performed carefully as the experience on Fennec had shown that the workload was higher than for Vuichard recoveries, and with stronger attitude changes.

Curiously, the observations on Dauphin are different: during the five inversed Vuichard runs, the attitude changes were not as sharp as during Vuichard recoveries (possibly because of slower actions by the pilot, or because of a lower average torque applied), and the workload was not as high. Surprisingly, the recovery performance were also better.

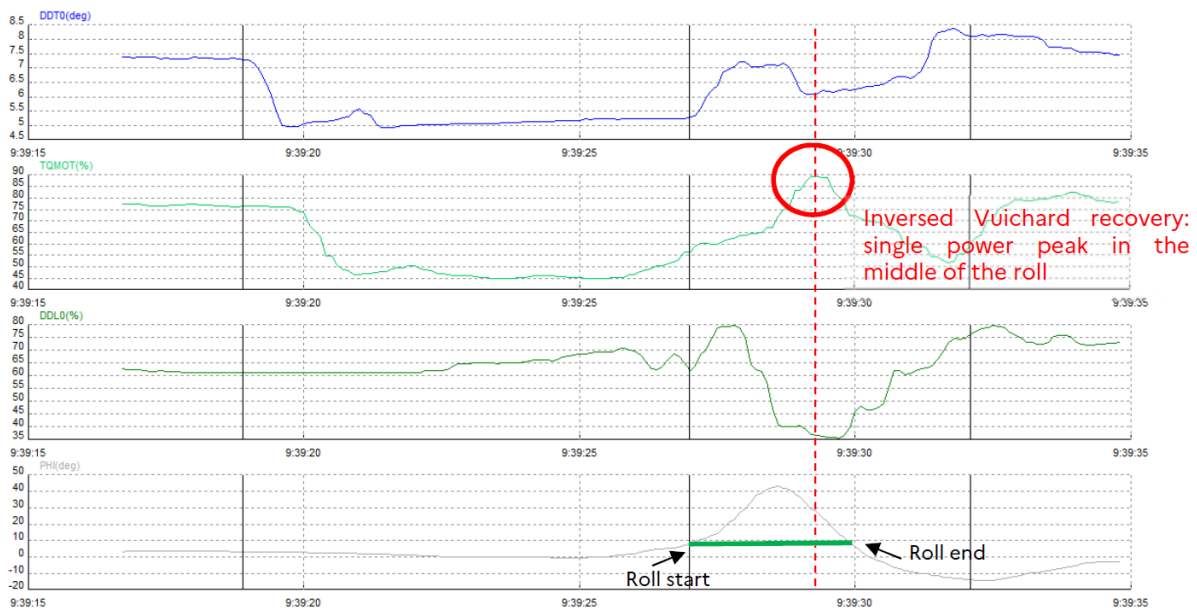
However the pilot felt he had even less control on the roll angle reached than during Vuichard recoveries: he had to “accept” the roll angle reached after his initial impulse, although this may be explained by the limited number of inversed Vuichard runs and therefore less experience to calibrate the motion.

Monitoring the power limitations was easier because once the power peak following the initial roll toward the right was passed, there was no second peak after the rotor was brought back to a horizontal position (see Figure 4-49 and Figure 4-50). On the contrary, the power level decreased slightly when the helicopter was rolling back (to the left) toward an horizontal position. This reduced the risk to exceed limitations and partly explains the lower workload.

► Figure 4-49 Example of power peak after a Vuichard recovery at the onsets



► Figure 4-50 Example of power peak after an inversed Vuichard recovery at the onsets



This shows that performing a Vuichard recovery “on the wrong side” does not have major drawbacks on a Dauphin, neither for recovery performance nor for the risk of limitations exceedance.

4.4.2.5 Possible improvements: exit with forward speed

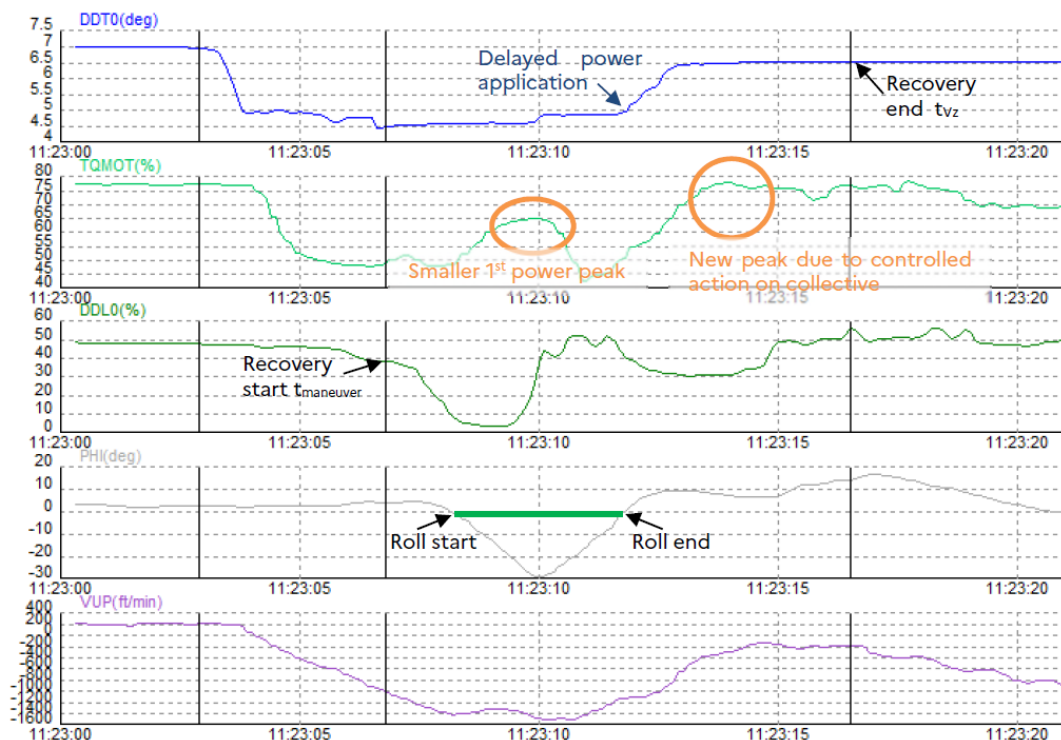
The effect of several small changes to the Vuichard recovery on the workload and performance was evaluated. Since it was noted in the first flight that at the end of Vuichard recoveries the helicopter was often exiting with a forward speed due to the pitch down parasitic effect, a few test runs were performed by instructing the pilot to accept this forward speed instead of fighting it to come back to hover, while the others were performed with the instruction to try to come back to hover. The idea was that with a forward speed the fenestron would help maintain the heading and reduce the need to act on the foot pedals, instead of introducing a yaw motion during a lateral translation from hover.

Indeed, in the runs where the forward speed was accepted, the workload on the longitudinal cyclic was significantly reduced, along with the workload on the pedals in the second part of the recovery (once the forward speed was enough for the Fenestron to fully play its role). It also reduced the amplitude of the second power peak and therefore reduced the risk of a limitation exceedance. A small improvement of the height loss with the exit speed was also noticed (which could be due to the better climb performance with a forward speed compared with hover).

Obviously, this variant could only be performed in the absence of obstacles in the forward sector, and removes one of the main benefit of the Vuichard recoveries, which is to come back to hover quickly after a small lateral translation.

4.4.2.6 Possible improvements: reducing or delaying the applied power

► Figure 4-51 Example of delayed power application on a Vuichard recovery at the onsets



While the Vuichard method calls for the application of all available power at the beginning of the recovery, this application of power on a Dauphin both increases the risk of limitation exceedance, and worsen the parasitic effects encountered (which in turn require corrective actions which increase the power needed).

A few test runs were performed by reducing the initial power applied (which in practice meant increasing the margin taken by the evaluators). There was less workload on the collective axis (due to the lower risk to exceed limitations), and a lower amplitude required on the right pedal at the beginning of the roll. However, the overall workload was not significantly reduced, and there was a high likelihood to reenter VRS at the end of the translation, as the power applied was not sufficient to maintain hover.

Another variant was therefore tested during the last flight, this time by delaying the application of power (see Figure 4-51 for example). In practice, the translation was performed without moving the collective (maintaining a torque of about 50%), and only applying power after the rotor was flat again, when it was needed to maintain hover and bring the rate of descent back to zero. Six runs were performed with a delayed power application, and confirmed that the workload was deemed more acceptable in this case: the pilot had one less axis to control during the first phase of the recovery, did not have to monitor the power level as closely, and had less parasitic effects to manage. During the second phase of the recovery, he could focus on the collective to eliminate the

rate of descent. There was no significant change in the recovery performance, therefore the trade-off seems interesting.

Recommendation: Executing a Vuichard recovery after a VRS entry on Dauphin involves a high workload for the pilot. In operational conditions, due to the low power margin and to the important and unpredictable power level, there would be a high risk to exceed limitations for a pilot with normal skills. The requirement to apply all the available power from the start therefore seems unsuitable for Dauphin helicopters. However, delaying the power increase at the end of the translation reduces the pilot workload and the risk to exceed limitations, without degrading the recovering performance.

Therefore, in case of VRS entry on Dauphin, it is recommended to apply the Vuichard recovery method only if a forward recovery is unadvisable (due to the presence of obstacles in the forward sector for example), and to delay the power increase after the end of the translation, once the rotor is back to an horizontal position.

4.4.3 Analytic comparison

In addition to the pilot feedback, a specific data processing has been carried out on pilot controls in order to estimate the pilot control activity during the recovery procedures. As stated in 4.1.1, pilot workload or activity on controls were not considered as efficiency criteria, but can be used to further explain the differences of performance between recovery techniques.

4.4.3.1 Fennec

Table 4-5 provides the calculated average standard deviations of the pilot commands during the recoveries on the three axes: Standard DDLO (Roll axis), Standard DDM0 (Pitch axis), Standard DDNO (Yaw axis). The average standard deviation of the helicopter attitudes (φ , θ , ϕ) are also presented, as well as the average standard deviation of the rotor RPM.

Table 4-5 Average VRS recovery performance – Fennec

Recovery method - Conditions	Average Standard deviation DDLO (%)	Average Standard deviation DDM0 (%)	Average Standard deviation DDNO (%)	Average Standard deviation φ (deg)	Average Standard deviation θ (deg)	Average Standard deviation ϕ (deg)	Average Standard deviation Rotor RPM
Forward - Established	6.46	7.70	6.12	2.77	6.74	4.63	1.53
Vuichard - Established	11.30	8.87	6.47	9.20	3.45	5.40	2.10
Forward - Onsets	5.26	6.87	3.43	1.62	6.01	2.45	1.65
Vuichard - Onsets	8.58	7.95	9.77	12.20	3.99	6.02	2.73
Inversed Vuichard - Established	10.49	8.74	5.84	9.51	4.24	5.75	1.92
Forward - Decelaration	7.57	8.67	6.09	2.62	6.42	4.5	1.63
Vuichard - Decelaration	14.96	12.96	6.77	7.41	4.26	4.28	1.95

Recoveries at VRS onset also required a lower pilot workload on cyclics compared to recoveries in established VRS, for both helicopters. The average standard deviations on pilot controls are always higher during the Vuichard recovery. While this can be expected on the lateral axis, it can also be shown on the longitudinal and yaw axes, highlighting the strong cross-couplings involved in this manoeuvre.

The standard deviations of the pitch and roll angle are, higher during Forward and Vuichard recoveries respectively, which is expected as being the predominant axis of the respective procedures. The heading variations are slightly higher during Vuichard recoveries, which can be also explained by the strong cross-couplings involved in this manoeuvre. Average STD of the rotor RPM are very similar between both techniques, while being slightly higher in Vuichard recoveries.

4.4.3.2 Dauphin

Table 4-6 presents the results obtain on the Dauphin.

Table 4-6 Average VRS recovery performance – Dauphin

Recovery method - Conditions	Average Standard deviation DDL0 (%)	Average Standard deviation DDM0 (%)	Average Standard deviation DDN0 (%)	Average Standard deviation φ (deg)	Average Standard deviation θ (deg)	Average Standard deviation ϕ (deg)	Average Standard deviation Rotor RPM
Forward - Established	7.54	5.97	4.52	3.38	8.16	18.75	3.95
Vuichard - Established	12.59	8.65	5.50	9.66	4.09	13.15	3.63
Forward - Onsets	11.08	5.22	2.25	2.98	7.33	3.00	4.90
Vuichard - Onsets	12.37	8.31	6.78	10.76	3.24	17.19	2.87
Inversed Vuichard - Established	12.16	6.87	6.75	13.26	6.25	6.89	4.57

When considering established VRS (only two runs were done at VRS onsets in forward manoeuvre which is not statistically representative), the average standard deviations on pilot controls are always higher during the Vuichard recovery. While this can be expected on the lateral axis, it can also be shown on the longitudinal and yaw axes, highlighting the strong cross-couplings involved in this manoeuvre. The average standard deviation of the helicopter attitudes (φ , θ , ϕ) are also presented, as well as the average standard deviation of the rotor RPM. The standard deviations of the pitch and roll angle are higher, during Forward and Vuichard recoveries respectively, which is expected as being the predominant axis of the respective procedures. The heading (ϕ) variations are globally higher than on the Fennec, which can be also explained by higher cross-couplings on this machine. There's no clear trend regarding the average Standard deviations of the rotor RPM, very similar between both techniques, but the values are higher than observed on the Fennec.

4.5 Summary

For both recovery methods and helicopters, a number of influencing parameters affect the performance, notably the initial vertical speed and the average torque applied during the recovery.

4.5.1 Fenec

In the test conditions, and even when trying to standardise the VRS recoveries, an important dispersion was observed on the height loss (66ft - 376 ft) and recovery time (4.4-15.1s).

When considering these effects, performance in term of height loss and recovery time are similar between Vuichard and forward recoveries. Nevertheless, for recoveries from the VRS onset on Fenec, Vuichard method shows slightly better performance than the forward one.

The effects of the identified influencing parameters on Fenec are summarised in the tables below:

Table 4-7 Effect of the identified influencing parameters on Fenec

Effect of:	On: Height loss	On: Recovery time
Vertical speed at manoeuvre start	Clear increase	Neutral
Average torque	Clear decrease (Forward) Neutral (Vuichard)	Small decrease (forward) Neutral (Vuichard)
Minimum pitch below – 15° (forward recoveries)	Increase	Neutral
Pitch variation (forward recoveries)	Undetermined	Undetermined
Maximum roll (Vuichard recoveries)	Decrease	Neutral
Initial Vx (forward)	Decrease (forward & Vuichard)	Decrease (forward)
Initial Vy (left)	Decrease (Vuichard)	Small decrease (Vuichard)

Several parameters have a noticeable effect on the height loss, which is relevant when assessing the risk of a ground collision. The recovery time is less susceptible to influencing parameters, with a few exceptions, and its distribution seems more random.

The torque applied has a clear positive effect on the height loss for the forward recovery methods, and can be directly controlled by the pilot. Therefore, when a VRS occurs close to the ground in a Fenec it is recommended to apply all the power available during a forward recovery.

The pilot workload was judged low to medium in forward recoveries, with pilot inputs mostly observed on the longitudinal cyclic only after an initial action on the collective.

The workload was however judged high in Vuichard recoveries, due to the number and partial unpredictability of the actions required on the controls.

In Vuichard recoveries, inputs were observed on both cyclic axis, on the collective while monitoring the power, and on the foot pedals to try to maintain heading, with a nose down parasitic effect in the second part of the recovery. The variations observed from one recovery to another, even for similar sets of entry conditions, did not allow the pilots to usefully anticipate the required actions. The Vuichard recoveries were also overall judged

less intuitive than forward recoveries by the test pilots, who are usually trained to regain speed by moving forward in case of failure occurring in hover. These assessments did not change with the increased familiarity with the method over the course of the test campaign.

Additionally, in operational conditions and with normal piloting skills, due to the power fluctuations during the lateral motion there would be a risk to exceed the aircraft power limitations during a Vuichard recovery on the Fennec.

Additional test runs are recommended to perform a complete parametric study to confirm the list of influencing parameters and quantify their effect on the recoveries performance.

4.5.2 Dauphin

In the test conditions, while trying to standardise the VRS recoveries and as observed on the Fennec, an important dispersion was observed on the height loss (67ft - 529 ft) and recovery time (4.1-17.8s).

For both recovery methods, a number of influencing parameters affect the performance, notably the initial vertical speed, the average torque applied during the recovery, and the initial horizontal speed, although their effects tend to be less clear on Dauphin than on Fennec due to a higher point dispersion.

When considering these effects, performance in term of height loss and recovery time are similar between Vuichard and forward recoveries. Several parameters have a noticeable effect on the height loss, which is relevant when assessing the risk of a ground collision. The recovery time is less susceptible to influencing parameters, with a few exceptions, and its distribution seems more random.

The effects of the identified influencing parameters on Dauphin are summarised in the table below:

Table 4-8 Effect of the identified influencing parameters on Dauphin

Effect of:	On: Height loss	On: Recovery time
Vertical speed at manoeuvre start	Clear increase	Increase (Forward) Neutral (Vuichard)
Average torque	Clear decrease (Forward) Undetermined (Vuichard)	Small decrease (forward) Neutral (Vuichard)
Minimum pitch below – 15° (forward recoveries)	Undetermined	Neutral
Pitch variation (forward recoveries)	Clear increase	Clear increase
Maximum roll (Vuichard recoveries)	Undetermined	Neutral
Initial Vx (forward)	Decrease	Decrease
Initial Vy (left)	Decrease	Decrease

The pilot workload was judged low to medium in forward recoveries, with pilot inputs mostly observed on the longitudinal cyclic after an initial action on the collective.

The workload was however judged high in Vuichard recoveries, due to the number and partial unpredictability of the actions required on the controls.

The Vuichard recoveries were also overall judged less intuitive than forward recoveries by the test pilots - who are usually trained to regain speed by moving forward in case of failure occurring in hover – and less comfortable due to the sudden attitude changes often experienced.

These assessments did not change with the increased familiarity with the method over the course of the test campaign. Additionally, in operational conditions and with normal piloting skills, due to the power fluctuations during the lateral motion there would be a risk to exceed the aircraft power limitations during a Vuichard recovery on the Dauphin.

Since delaying the power increase at the end of the translation significantly reduces both the workload and the risk of limitation exceedance without significantly degrading the recovery performance, it is recommended to apply the Vuichard recovery method on a Dauphin helicopter only if a forward recovery is unadvisable (due to the presence of obstacles in the forward sector for example), and to delay the power position.

A summary of the pilots' workload for forward recoveries is shown in Table 4-9 and for Vuichard recoveries in Table 4-10. Ratings are based on the definition provided in §4.1.1.

Table 4-9 Workload during forward recoveries on Dauphin

Controls	Worload	Frequency	Amplitude	Effort
Cyclic longitudinal	MEDIUM	LOW	LOW to MEDIUM	LOW
Cyclic lateral	VERY LOW	VERY LOW	VERY LOW	NONE
Pedals	LOW ¹	LOW ¹	LOW	LOW
Collective	LOW ¹	LOW	MEDIUM	LOW

Table 4-10 Workload during Vuichard recoveries on Dauphin

Controls	Worload	Frequency	Amplitude	Effort
Cyclic longitudinal	LOW (start) MEDIUM (end)	LOW (start) MEDIUM (end)	LOW (start) MEDIUM (end)	LOW
Cyclic lateral	MEDIUM	MEDIUM to HIGH	MEDIUM	MEDIUM
Pedals	HIGH ²	MEDIUM	HIGH	HIGH
Collective	HIGH ³	MEDIUM	MEDIUM	LOW

¹ MEDIUM if high torque

² Due to proximity to control stop and watching power limitations

³ Due to watching power limitations

Additional test runs are recommended to perform a complete parametric study to confirm the list of influencing parameters and quantify their effect on the recoveries performance.

Other metrics for the recovery performance, such as the distance travelled by the helicopter from the beginning to the end of the recovery, could be pertinent and worth investigating.

4.6 Lessons learnt

In order to determine more accurately the VRS domain boundaries, dedicated flights would have to be performed with the following procedure:

- For the upper part of the domain (zone A): set and maintain the horizontal speed V_h , and pilot a rate of descent of -500 ft/min initially (instead of a power level). Maintain this rate of descent for at least 30 seconds. If the aircraft does not enter VRS, climb back to the initial altitude and modify the rate of descent in decrements of about 100 ft/min; Once the rate of descent associated to the VRS boundary for this speed has been determined, start again for a different speed, exploring the 0-30kt.
- For the knee (right part, zone B): set a rate of descent and an initial horizontal a few knots above the predicted boundary. Maintain for at least 30 seconds. If the aircraft does not enter VRS, climb back to the initial altitude and decrease the horizontal speed (either using fixed decrements, or proceeding by dichotomy). Once the horizontal speed associated to the VRS boundary for this rate of descent has been determined, start again for a different rate of descent, exploring a range of about - 800 ft/min to -3300 ft/min.

This process would of course be very time consuming, with a realistic number of VRS entries of about 5 to 10 per hour (instead of 20 to 25 with the method followed in this test campaign).

5. Numerical approach

5.1 Summary

Many studies have been conducted on the VRS phenomenon, but the representativeness of flight mechanics models for prediction of the vortex ring boundaries, and their capability to reproduce the helicopter behaviour during VRS and recovery manoeuvres is still questionable. Therefore, developing fast numerical models able to reproduce this specific aerodynamic rotor regime and validating their representativeness compared to flight tests is an important task to perform trainings in real-time simulator.

The research project also aimed at evaluating the prediction of VRS with simulation methods. Therefore, off-line simulations were compared against the flight test data gathered from the eight flights performed during this project. Additionally, simulator trials were realised in the ONERA research simulator in order to evaluate the representativeness of two different VRS models through piloted simulations. The objective being to highlight the potential shortcomings of the VRS models and thus the reservations to be taken into account when the vortex phenomenon and associated recovery techniques are evaluated through simulations. Results were synthesised in a paper that was submitted to the European Rotorcraft Forum in September 2024 (reference [4]).

The purpose of this paper was to evaluate the correctness of flight mechanics code and VRS models and reproducibility of recovery techniques.

In this study, we focussed on two fast VRS models, enabling real-time simulations and shortly presented hereafter:

- The first one was developed by ONERA and consists in an induced velocity model based on an adaptation of the momentum theory in steep descent. It will be called “OA VRS model” later in this document.
- The second one is representative of VRS models used in training simulators, and consists in an artificial rotor thrust reduction occurring when the helicopter model enters a predefined VRS domain in terms of forward and vertical speeds seen in rotor frame. It will be called “ATR VRS model” later in this document.

It was not planned to use more complex methods such as rotor free wake models or even less CFD computations. Free wake models are certainly a good way to reproduce VRS conditions as computing a more realistic rotor wake. Nevertheless, performing a strong coupling between flight mechanics and rotor wake model remains a challenging task especially to reproduce VRS flight cases for which it is mandatory to control, or at least, to stabilise the helicopter model. In addition, performing real-time simulations with these models is still impossible.

Two helicopter models were tested, a Fennec AS-550 and a Dauphin AS365N, corresponding to the machines operated by DGA-EV. Off-line simulation comparisons were mainly done with the Fennec model while simulator trials involved both helicopter types.

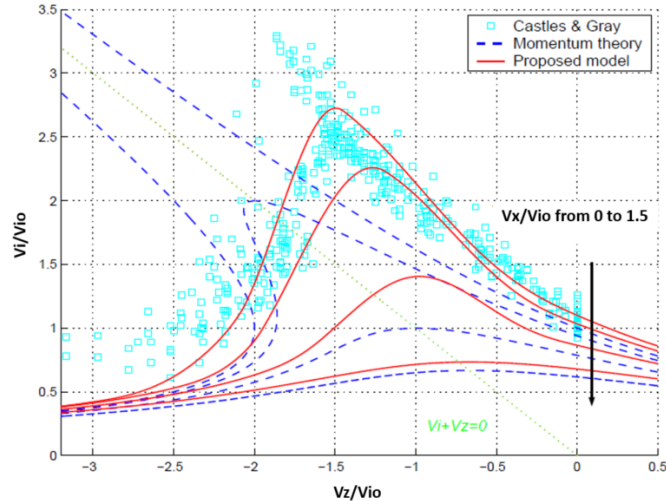
5.2 VRS models

5.2.1 ONERA VRS model description

Simulations have been performed with the Airbus Helicopters flight mechanics code HOST, integrating a specific induced velocity model developed by ONERA in the 2000s and detailed in references [5, 6]. As shown in Figure 5-1, showing the evolution of the induced velocity with respect to the vertical speed at different forward speed (all being normalised by the induced velocity in hover V_{io}), this model mainly consists in linking the branches

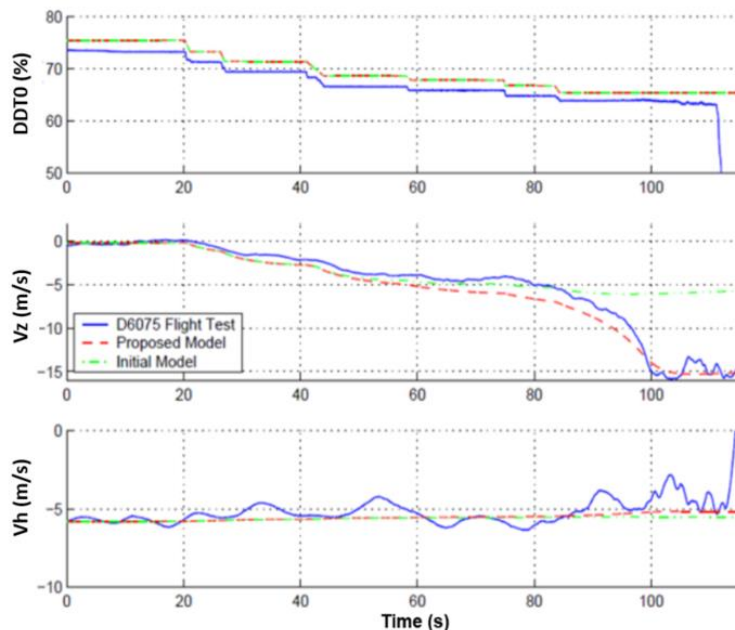
of the momentum theory between climb/level flight and very high descent rates corresponding to the wind-mill brake state. This model was tuned to match to available induced velocity measures taken from publications and from a dedicated flight test campaign performed by ONERA and DGA-EV in the 2000s.

► Figure 5-1 ONERA induced velocity model in steep descent



Previous papers (references [5, 6]) presented comparisons between the OA VRS model and Dauphin flight test data as shown in Figure 5-2. In this example, successive collective (DT0) decreases were performed while maintaining the horizontal speed (V_h). At around 85 s, a slight collective decrease generates the characteristic drop of vertical speed (V_z). Absolute vertical speed values in simulation and in flight are a bit different, but the drop is well captured by the model, leading to a similar minimum value of -15 m/s (-2950 ft/min). As this will be discussed later, most of the comparisons were performed in “stabilised and smooth” VRS entries, i.e. slight successive collective decreases, at constant forward speed. This model was thus partially validated against flight data and demonstrated its ability to reproduce VRS entries. But while this model is able to correctly capture the drop of vertical speed, questions still arise about the representativeness of the vertical speed response due to a collective pitch increase realised in fully developed VRS as well as the ability of this model to well represent the helicopter behaviour during recovery techniques.

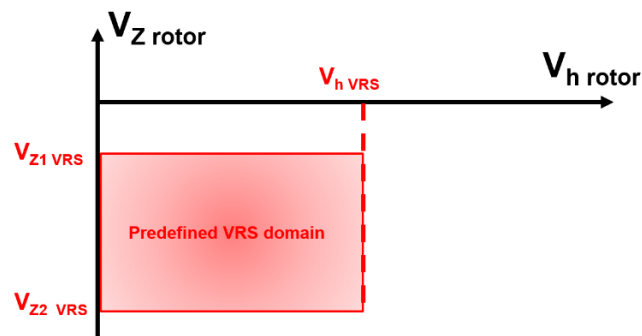
► Figure 5-2 ONERA induced velocity model ability to reproduce VRS entry in “steady” conditions



5.2.2 ATR VRS model description

Another VRS model has been also assessed. Contrary to the ONERA model, it is not based on an adapted induced velocity model in descent but on an artificial rotor thrust reduction.

► Figure 5-3 ATR VRS model domain



In this model, VRS is reproduced by an artificial drastic decrease of the rotor thrust if the helicopter enters a predefined VRS domain (defined in terms of forward and vertical speeds) as illustrated in Figure 5-3. A predefined percentage of lift loss is set and applied depending on the speeds seen by the rotor with respect to a predefined VRS domain. The major disadvantage of this approach remains the need of experimental data and/or pilot evaluations to tune the different parameters defining the VRS domain (i.e. forward and vertical speeds defining the VRS domain).

In addition to the thrust reduction, cyclic efficiency reduction can be set while pitch and roll angle variations are generated in order to represent the characteristic increase of vibrations felt during the VRS phenomenon. Following parameters were set during this study:

- Percentage of thrust reduction: 60%
- Low threshold of cyclic efficiency: 5%
- V_h VRS: 10 kts
- V_{Z1} VRS 1: -850 ft
- V_{Z2} VRS 1: -3250 ft

► Figure 5-4 ATR VRS model inducing pitch and roll angle variations

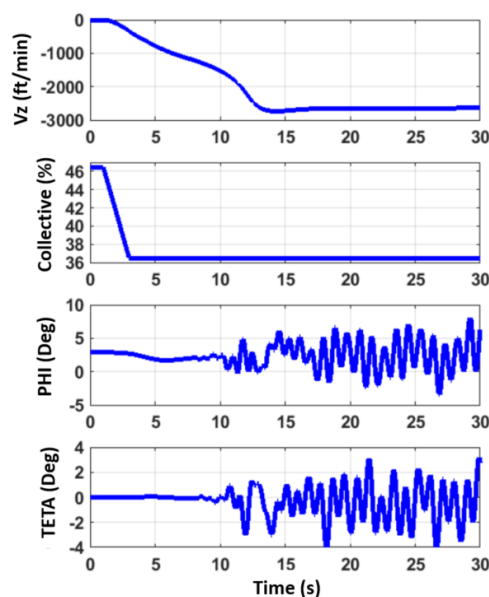


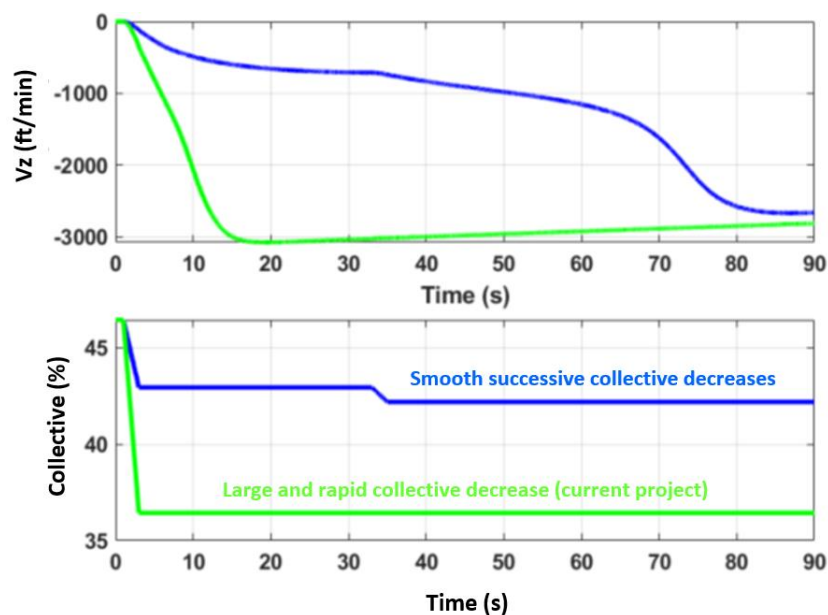
Figure 5-4 is representing a VRS entry through the reduction of the collective in off-line simulation, where the ATR model generates periodic pitch and roll angle variations of relatively large amplitudes: $\pm 5^\circ$ on roll, $\pm 3^\circ$ on pitch.

If this clearly indicates a change in the helicopter behaviour to the pilot, one will see further in the paper that these oscillations are not representative of the VRS phenomenon, at least for the two types of helicopter studied, and even prevented to properly assess the Vuichard recovery technique in the ONERA simulator.

Important note: This model was used at ONERA without any tuning from pilot(s), as this is always done when it is integrated into FFS simulators. The main objective of such a type of model is to reproduce major symptoms of the VRS phenomenon (increase of the descent rate, vibrations, reduction of cyclic efficiency) but it does not intend to be fully representative. Another objective being to allow the pilots to quickly and “easily” in the VRS during training sessions.

5.3 Differences between current and previous flight test campaigns

► Figure 5-5 Two collective decreases strategies



In the different previous flight test campaigns performed by DGA-EV and ONERA, as shown in Figure 5-2, VRS entries were mostly realised through successive slight collective decreases in order to “slowly” reach the VRS domain from the upper boundary. (The “knee” of the VRS domain was determined in the same way than in the current project, i.e. by decreasing the airspeed in a pre-established descent).

As previously outlined, in this test campaign, pilots were lowering the collective more rapidly to be sure to enter VRS at each run and more quickly, enabling the realisation of more test cases in a flight.

The difference between both strategies is represented in Figure 5-5 thanks to two simulations.

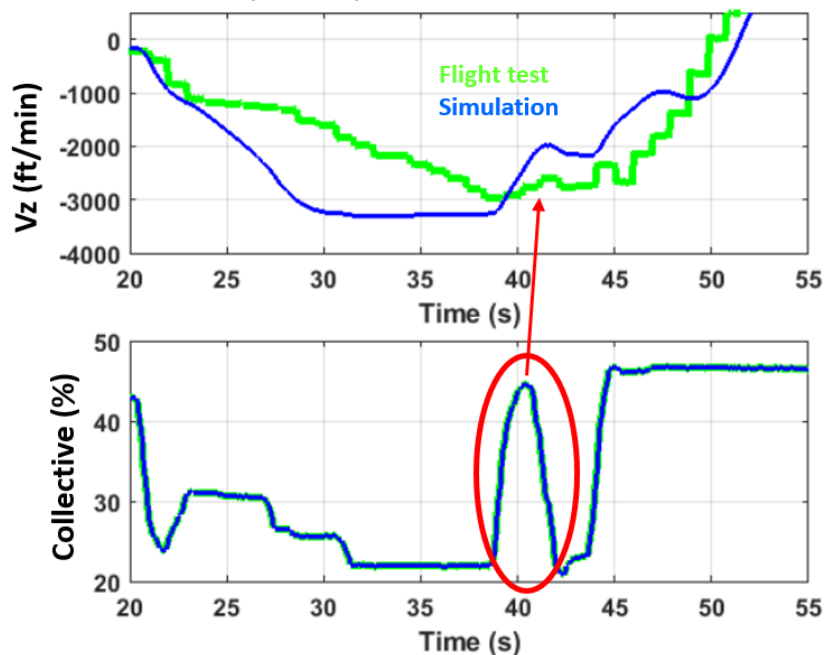
The blue curve corresponds to slight successive decreases of the collective, leading to a VRS entry at around 60s, and at a vertical speed V_z of -1175 ft/min. This strategy was applied in the previous flight test campaigns performed by DGA-EV and ONERA. The green curve then corresponds to the procedure applied during the EASA flight tests, with a large collective decrease directly leading to the lower boundary of the VRS domain ($V_z = -3000$ ft/min). This comparison clearly shows that, when analysing the V_z data, the V_z drop (as defining the VRS entry) can be more easily identified when the collective is smoothly and gradually decreased. When collective is largely and quickly reduced, V_z drop (i.e. VRS entry) is hidden by the rapid rate of descent increase due to the

large collective reduction. Specific post-treatment analyses are then required (as described in §3.1.1) to determine the VRS entry.

In addition, once in a supposed fully developed VRS, pilots were increasing the collective to verify that there was only a very limited impact on the vertical speed. This effect was already verified in previous flight tests and is a characteristic of the phenomenon.

Figure 5-6 shows the V_z and the collective level during a fully developed VRS flight on the Fenec helicopter. The green curves are the flight data while the blue ones are the results of a simulation.

► Figure 5-6 Collective increase in fully developed VRS



During the simulation, the variations of the collective are followed, the variation of the vertical speed being the result of the OA VRS model in this case. After the collective decrease at 20s to enter VRS, the pilot managed to reach and hold a torque of 40%. Compared to simulation, it can be observed that the collective variations after the first decrease slowed the increase of the rate of descent during the flight test. The helicopter reached a V_z of -3000 ft/min in 38s while a V_z of around -3200 ft/min is reached in 30s in the simulation. At 38.5s, the pilot increased the collective by 22.6% in less than 2s and then re-decrease it to its previous level. This collective increase had almost no impact on the helicopter vertical speed (392 ft/min of variation) while this generates of variation of 1272 ft/min in simulation. This flight test run clearly shows that once in a fully developed VRS, an increase of the collective is inefficient but doesn't worsen the situation. In this case, the OA VRS model is not representative of the vertical speed response due to a collective variation. At 43.5s, the pilot performed a forward recovery by increasing the collective and pitching down the helicopter to increase the forward speed.

Finally, compared to the previous flight test campaigns, test runs were performed with either a recovery initiated at the first signs of VRS (recovery at vortex onsets), or once the VRS was fully established.

5.4 Strategy to follow flight test data

The flight mechanics code HOST used at ONERA, while implementing official helicopter data packages from Airbus Helicopters, has not been tuned to match flight test parameters like it is done for training simulator. Using the recorded pilot controls as inputs would lead to the divergence of the simulation, especially in such complex manoeuvres, and specific strategies have been applied to follow flight data.

Thus, pre-developed flight control laws or auto-pilot modes were used to either follow the helicopter airspeeds or attitudes. A Translational Rate Command law (TRC) has been tuned to follow the longitudinal and lateral speeds of the helicopter in simulation, or to impose pre-defined speeds for parametric studies.

When the goal is to reproduce recovery techniques from flights, the controls are switched to an Attitude Hold mode (ATT) enabling to follow the helicopter pitch and/or roll angles. The heading was managed by either the TRC or the ATT mode.

As the vertical speed drop is the major characteristic of the VRS phenomenon, the vertical axis was always left free. Therefore, same collective variations were applied in simulation than in flight, while the absolute values were different.

Considering this control strategy, as it has to be noted that the results of the simulations are therefore not representative of the helicopter response except on the vertical axis, the other axes being constrained by a flight control law or an auto-pilot mode.

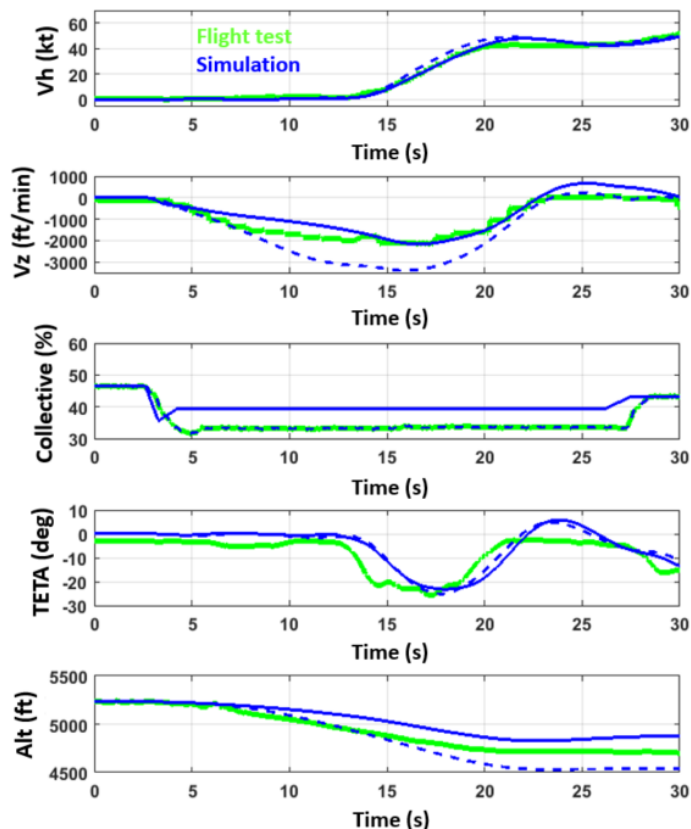
5.5 RESULTS

While four flights were performed on both Fennec and Dauphin helicopters, the comparisons between simulations and flight tests were only done on the Fennec model.

5.5.1 Forward recovery in fully VRS with and without collective increase

In a general manner, an increase of the loss of height is observed when the collective is not increased during the forward recovery. In flight, only considering the Fennec helicopter and recoveries performed in vertical descent and established VRS, the observed average loss of height without collective increase is 283 ft, while it is 184 ft with a collective pull-up.

► [Figure 5-7 Forward recovery without collective increase](#)

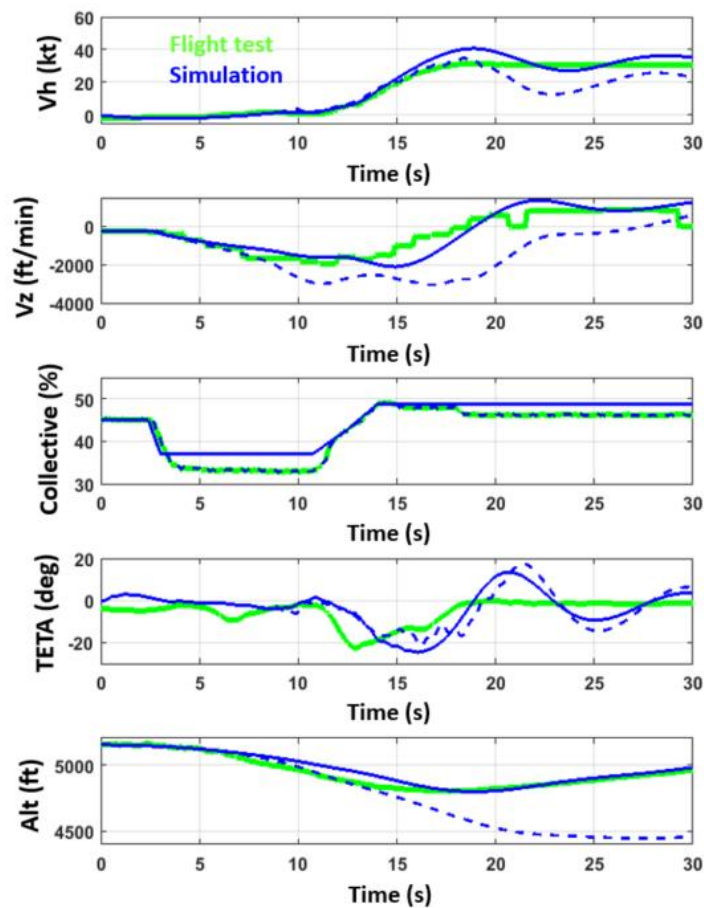


In Figure 5-7, a comparison is done between flight data (green curve) and two simulations. The blue dotted line corresponds to a simulation where collective variations applied in flight are exactly reproduced. As already shown, following the same collective variations lead to much higher vertical speed (more than -3000 ft/min compared to -2000 ft/min in flight). The blue solid line shows the results of a simulation where the collective variations have been modified to better match with the vertical speed. In simulation, the loss of height with similar collective variation is around 452 ft while it is 272 ft with adapted collective variations. It was equal to 225 ft in flight.

It has to be noted that, while the pitch down is produced later in both simulations, forward speeds are comparable to the flight test.

The same comparison is done in the following Figure 5-8 where the collective increase is applied simultaneously with the pitch down attitude.

► Figure 5-8 Forward recovery with simultaneous collective increase and pitch down attitude



Here again, adapting the collective variations is needed to better reproduce the Vz drop. It can be seen that the pitch down performed at the same time than the collective increase (at 11s) lead to a slight descent rate re-increase in both simulation cases while this is not observed in flight. In simulation, the loss of height with similar collective variations is around 490 ft while it is 203 ft with adapted collective variations. It was equal to 114 ft in flight.

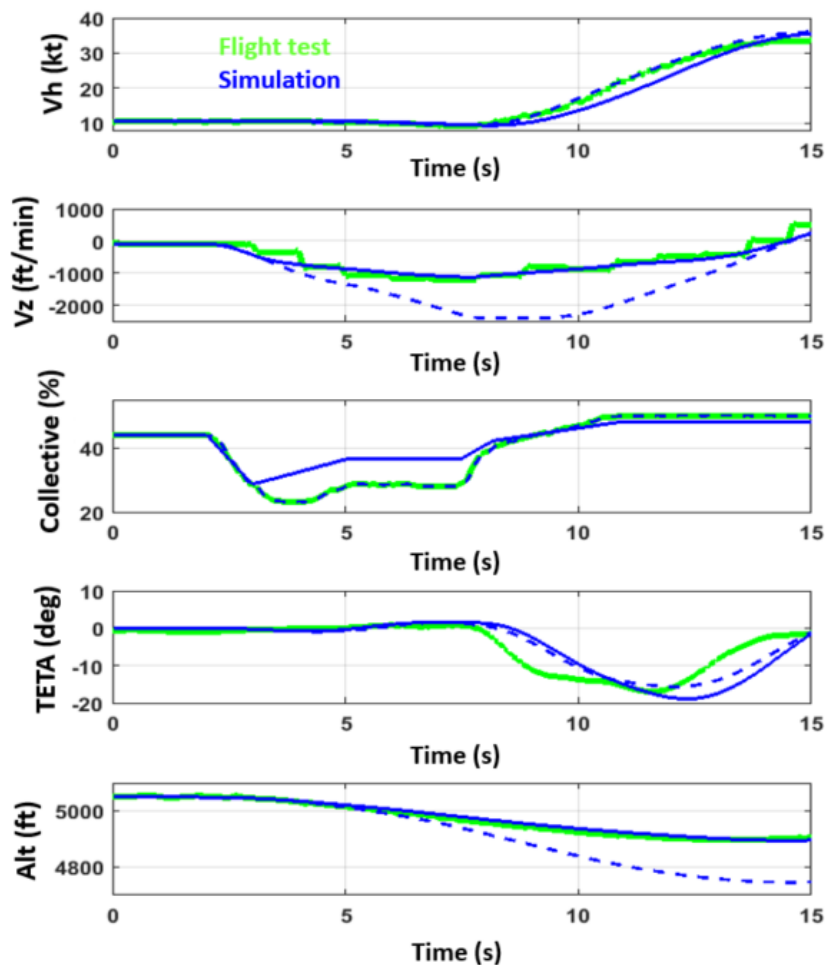
5.5.2 Forward recovery at VRS onsets

The following Figure 5-9 shows comparisons between simulations and flight test where the recovery was initiated at VRS onsets, corresponding to a vertical speed of -1200 ft/min. Once again, it is necessary to adapt

the collective inputs to better match the vertical speed reached in flight. In that case, the height loss is 84 ft, compared to 70 ft in flight and 193 ft in simulation with same collective variations.

The analysis of the flight test data showed that the vertical speed at the onset of the recovery is one of the most important influencing parameter on the height loss. The higher the initial vertical speed (in absolute value), the higher the height loss on average, with a significant dispersion. On average, the recoveries at VRS onsets tend to occur at lower initial vertical speeds, and therefore induce smaller height losses, which was expected.

► Figure 5-9 Forward recovery at VRS onsets



Simulations are able to reproduce the effect of the initial (at recovery initiation) Vz on the height loss. Nevertheless, it requires the tuning of the collective axis to better match with flight data.

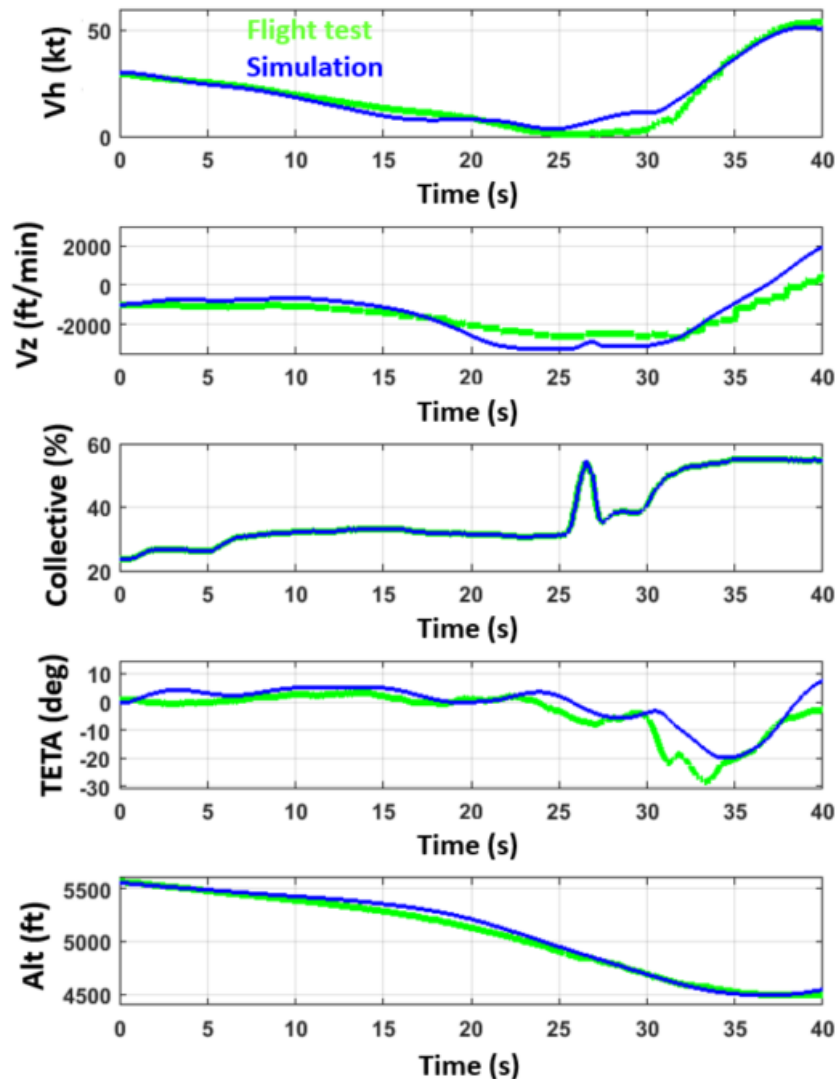
5.5.3 Forward recovery in decelerated flight

A total of 16 VRS entries in decelerated flights were performed to determine the “knee” of the VRS domain and to evaluate the recovery techniques in such a condition.

Figure 5-10 shows the comparison of flight data and a simulation where the collective variations reproduce the ones in flight. Although the flight parameters are mostly well captured in simulation, it is interesting to see that, here again, the collective increase at 27s, to evaluate if the VRS is fully developed, has a very limited impact on the vertical speed in flight while it is larger in simulation. In this case, there was no need to modify the collective

to match the flight data. The height loss in flight was 203 ft and a very comparable value is obtained in simulation: 198 ft.

► *Figure 5-10 Forward recovery in decelerated flight*



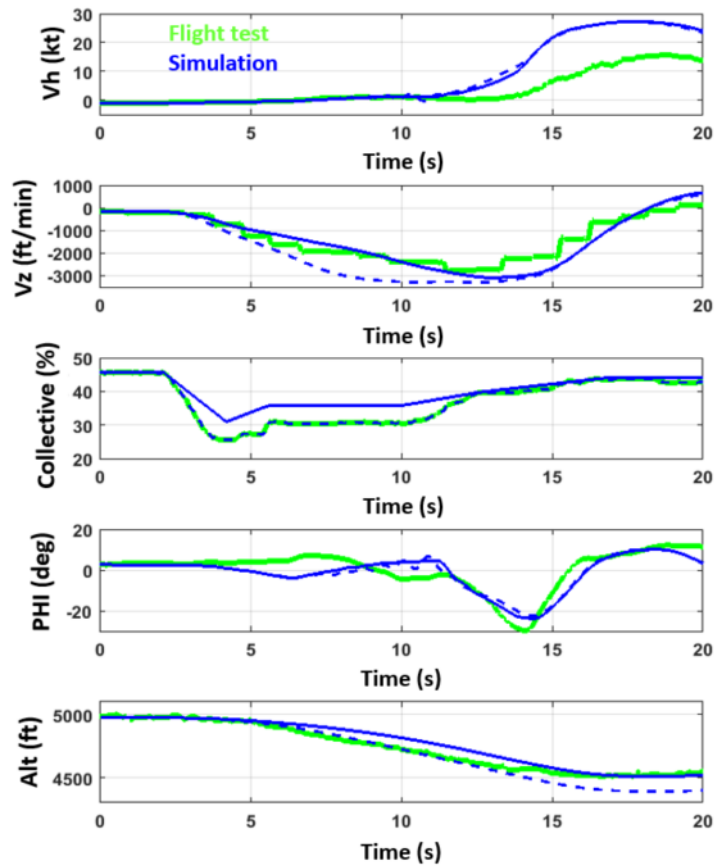
5.5.4 Vuichard recovery in fully VRS

The Vuichard recovery is simulated in the following Figure 5-11. In order to enter the VRS as in flight, modifying the collective inputs is still mandatory. Instead of applying a pitch down attitude, a roll angle variation on the left is performed as the Fenec helicopter rotor turns clockwise. As recommended, the power increase is applied prior to the lateral motion.

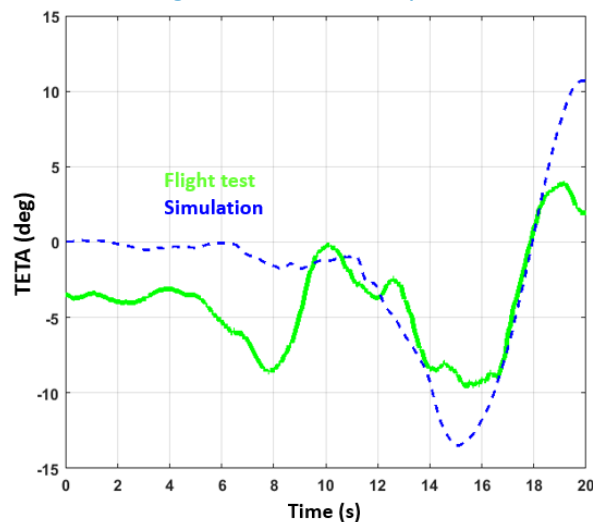
The height loss observed in flight was 153 ft while it is much higher (306 ft) in simulation, even with the corrected collective. Additional tuning of the collective could improve the simulation results.

Moreover, as shown in Figure 5-12, the pitch angle variations are higher in simulation (minimum value of -14°) than in flight (minimum value of -9.4°), certainly contributing to a longer increase of the vertical speed and thus a higher loss of height.

► Figure 5-11 Vuichard recovery in fully developed VRS



► Figure 5-12 Pitch angle variation during Vuichard recovery

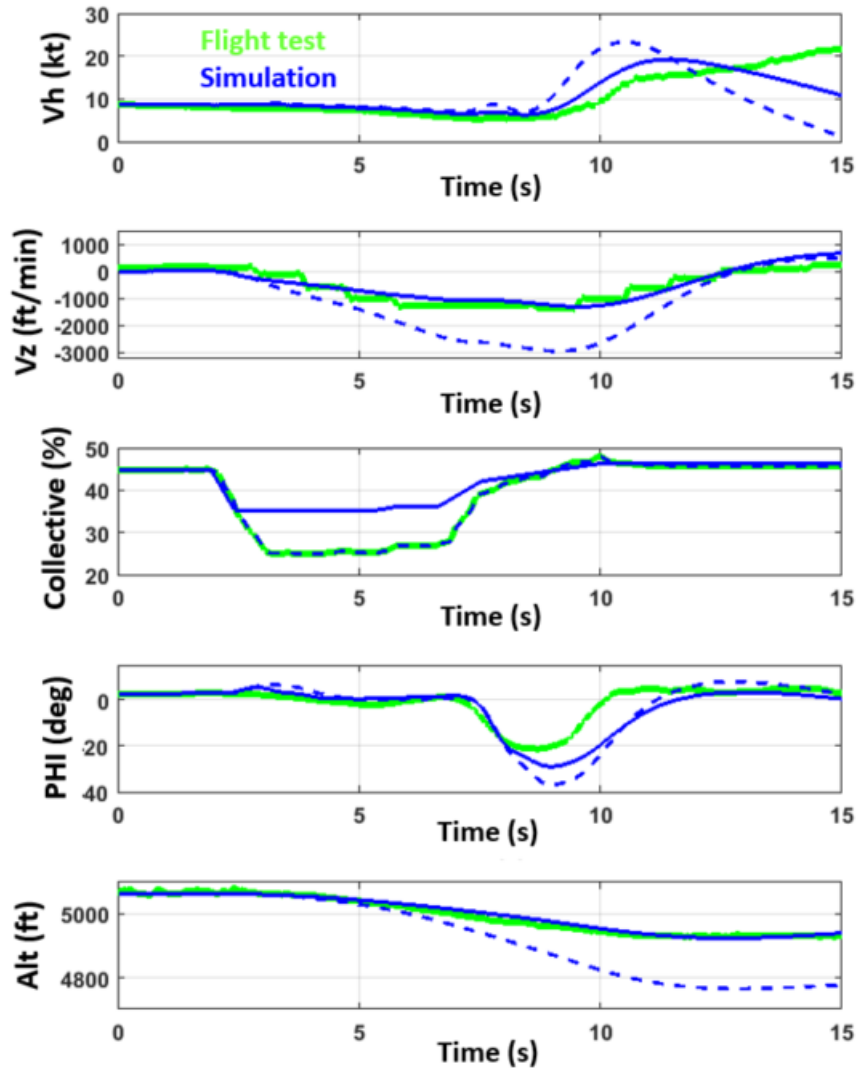


5.5.5 Vuichard recovery at VRS onsets

The Vuichard recovery has also been simulated when performed at the VRS onsets as this can be seen on Figure 5-13. Following the flight test collective lead to large discrepancies between simulation and flight data, but the adaptation of the collective variations largely improve the simulation results. An ATT mode is used in the simulation to follow helicopter attitudes. Nevertheless, the maximum roll angle variation is higher (+30°) in

simulation than in flight (+20°) and it takes a longer time to be brought back to 0°. This ATT mode should be further tuned to better match the roll angle variations observed in flight.

► *Figure 5-13 Vuichard recovery at VRS onsets*

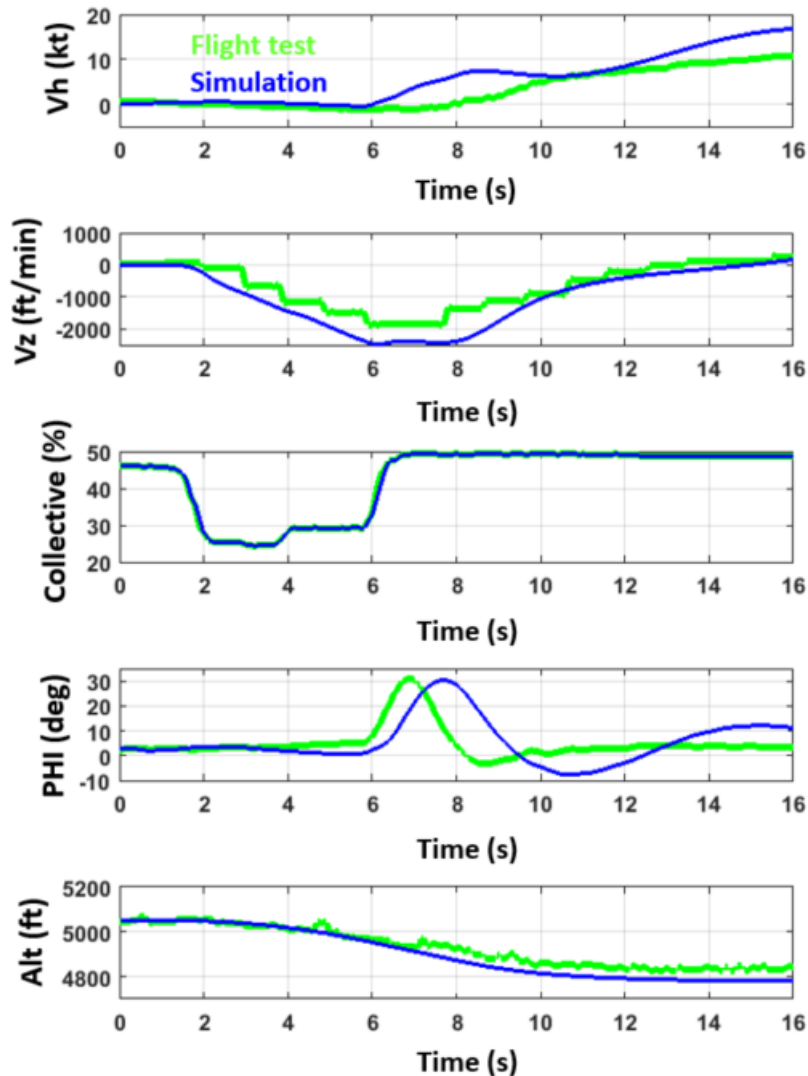


As already experienced with forward recoveries, the efficiency of the procedure is much higher when fulfilled at VRS onsets, with a limited loss of height in flight (67.27 ft) and 92 ft in simulation.

5.5.6 Inversed Vuichard recovery in fully VRS

During the entire flight test campaign, 12 inversed Vuichard recoveries were performed (7 on the Fenec and 5 on the Dauphin). A comparison is shown in Figure 5-14 between flight data from a Fenec run and a simulation. In this example, the simulated collective corresponds to the collective variations applied in flight. The roll angle variation, done on the right here, is simultaneously done with the collective increase at 5.8s. Contrary to what is observed in the previous case, the roll angle variation is the same in simulation than in flight (+30°), but a delay of 1s can be seen with here again a longer time to come back to 0°.

► Figure 5-14 Inversed Vuichard recovery at in fully developed VRS



While simulated response of the vertical speed, and roll angle variation could be improved to better follow flight data, the loss of height or relatively similar with respectively 141 ft in flight and 179 ft in simulation.

5.6 Summary of comparisons between simulation results and flight data

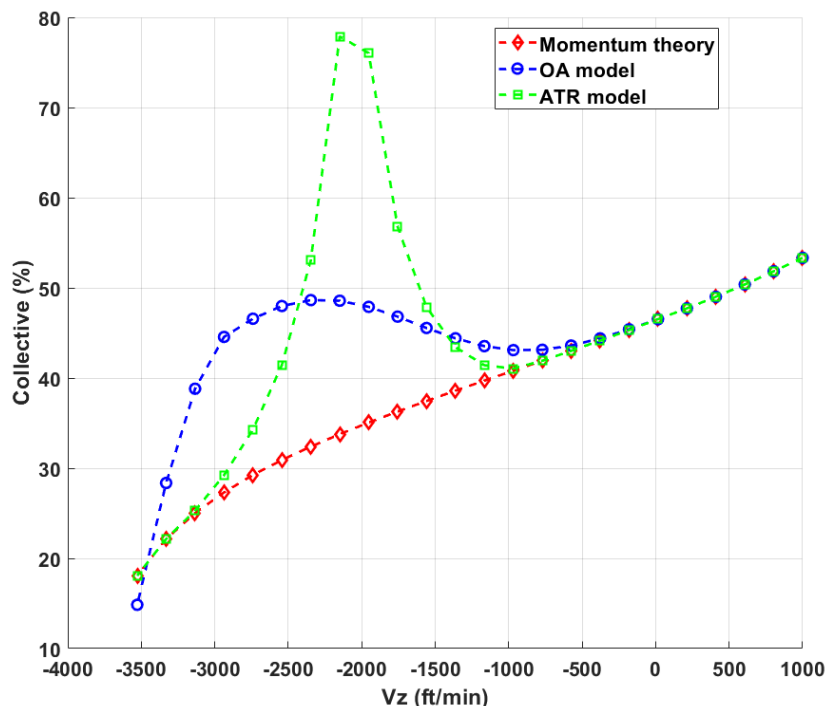
Comparisons between flight test data and results of simulation are showing relatively good agreement. The OA VRS model is able to reproduce VRS entries and recovery techniques in different conditions. The loss of height, which remains a major effectiveness criterion for evaluating recovery techniques, is comparable to the one observed in flight, but this generally requires a tuning of the collective pitch effect on the vertical axis.

As observed in flight, the flight conditions at which the recovery is initiated have a very large effect on the performance of the procedure, especially the vertical speed. For that reason, even before trying to simulate (and even more, to evaluate) recovery techniques through simulations, it is necessary to ensure that the VRS entry is well reproduced by the flight mechanics code.

In our case, this implies to modify the level of collective applied in simulation compared to the one applied in flight. A large part of the discrepancy between level of collective and resulting vertical speed is certainly due to the induced velocity model used. As explained in sub-chapter 5.2.1, the OA VRS model modifies the induced velocity in descent. As a result, this changes the relation between collective pitch and vertical speed. As this

will be detailed in next chapters, VRS is characterised by the generation of a hysteresis in the collective pitch/ V_z curve. In flight, this is characterised by the possibility to reach different vertical speeds with the same level of collective.

► Figure 5-15 Comparison of induced velocity models in descent



As an illustration, trim computations have been done and comparisons between different induced velocity models in vertical flight are presented in Figure 5-15, from a climb speed of +1000 ft/min to a descent rate of -3500 ft/min. The momentum theory is shown here in red curve. As already known, this theory is not adapted to steep descent and provides a monotonous relation between collective and vertical speed. It means that a collective value always implies a vertical speed in any conditions.

The OA VRS model modifies the induced velocity in descent which cause a change in the collective/ V_z curve as this can be seen on the blue curve. Collective/ V_z curve is similar to the momentum theory in climb and down to around -600 ft/min, but for higher descent rates, a hysteresis appears and the level of required collective re-increases (as the induced velocity), to finally decrease down to very high descent rates, towards the autorotation and wind-mill brake state branch.

In green on the figure, the ATR model also presents this hysteresis. Being also based on the momentum theory in these computations, the collective/ V_z curve is similar to the momentum theory in climb and down to around -1000 ft/min and below -3100 ft/min. Between these vertical speed values, the amount of required collective is much higher than with the OA model, reaching nearly 80% at $V_z = -2200$ ft/min.

In addition to the potential difference in the control mixing between pilot collective and blade pitch between the flight mechanics model and the real helicopter, this can explain why, depending on the collective decrease applied at the beginning of the run to quickly reach the VRS, results of simulations and flight test can be different. For instance, starting from hover (Collective = 46%), a reduction to 30% would lead to a RoD of around -3200 ft/min with the OA model, -2950 ft/min with the ATR model, and -2600 ft/min with the momentum theory. This also clearly shows the effect of the induced velocity model on the resulting vertical speed, and the need to have tuned models in such flight conditions.

Linked to the representativeness of the induced velocity model, the effect of a collective increase in fully developed VRS is also different between simulation and flight and a parametric study based on simulations will be detailed in next chapters.

As already mentioned, as using the pilot controls as inputs is almost impossible, a strategy had to be developed to follow helicopter attitudes. In our case, a tuning of the ATT mode gains could be done to better follow the attitude variations.

Helicopters are well known to present cross-couplings in every axis. Nevertheless, cross-coupling considerations are certainly not sufficiently taken into account during studies on VRS and more particularly recovery techniques evaluations, that all require large and rapid attitude variations. The strategy used during these off-line simulations prevented the analysis of these effects as helicopter attitudes were not resulting from pilot controls. Nevertheless, simulator trials performed by one pilot and further detailed showed the lack of representativeness of the flight mechanics code in this domain. This project has been an opportunity to fully assess the impact of these couplings on the pilot's workload and the effectiveness of the recovery techniques, while helicopters operated by DGA-EV have semi-rigid rotors and cross-coupling effects are certainly minored compared to rigid rotors.

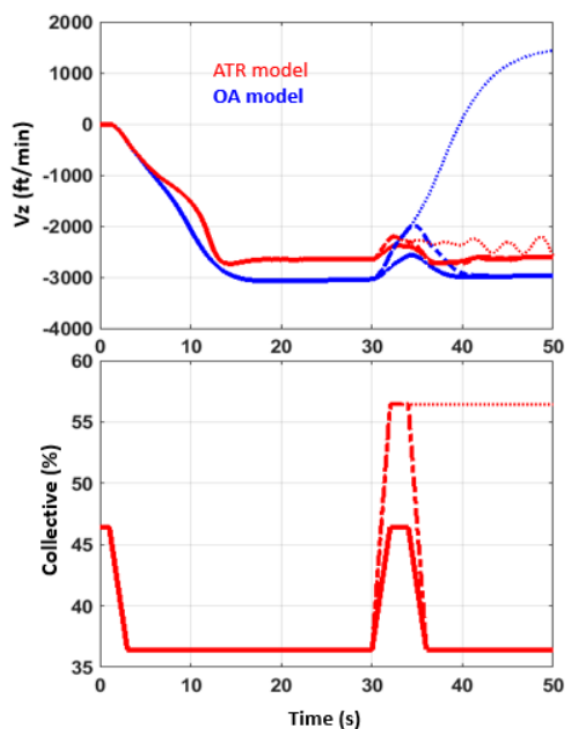
Finally, pilot's workload can obviously not be assessed through off-line simulations. Flight test analyses clearly outline the large impact of the pilot's workload on the efficiency of the recovery manoeuvres. Both manoeuvres involving inter-axes actions and cross-couplings effects, reducing the workload always improves the efficiency of recovery. Taking into account the pilot's workload is thus mandatory to properly evaluate these techniques, which here again requires representative flight mechanics code and real-time piloted simulations.

5.7 Off-line parametric studies

5.7.1 Collective efficiency in fully developed VRS

As introduced previously, collective increase showed a larger effect on the vertical speed in simulations compared to flight data.

► [Figure 5-16 Comparison of collective increase in fully developed VRS](#)



In order to investigate this discrepancy, several off-line simulations (see Figure 5-16) were performed with both OA and ATR induced velocity/VRS models. A large collective decrease was first done as in flight to reach VRS, and different collective increases were then applied. First, 10% increase (solid line) and 20% increase (dashed lines) during a limited time, and finally a maintained 20% of collective increase (dotted lines).

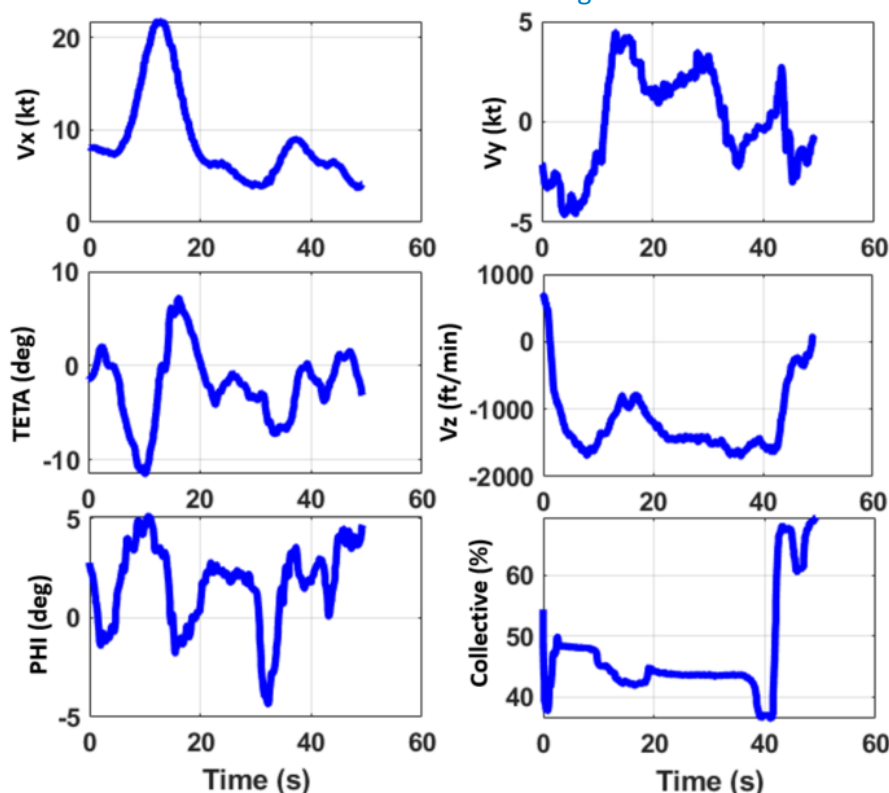
As previously explained thanks to Figure 5-15 showing trim computations, the Vz response according to collective variation is highly dependent on the induced velocity/VRS model used. With the OA model, applying and maintaining a large increase of collective leads to overpass the hysteresis and high positive vertical speeds can then be reached. This is not the case with the ATR model, as generating a much stronger hysteresis curve. Only an application of more than 80 % of collective would allow to overpass the hysteresis which will never be done in real flight, as this would certainly cause over-torque. As done in flight, a temporary collective increase generates a temporary reduction of the descent rate in both cases, while it is too strong with the OA model as shown in the previous comparisons with flight data. The ATR model is more representative, inducing a much limited response of the vertical speed and even more, preventing its re-increase with a maintained collective pull-up.

5.7.2 Collective efficiency at VRS onsets

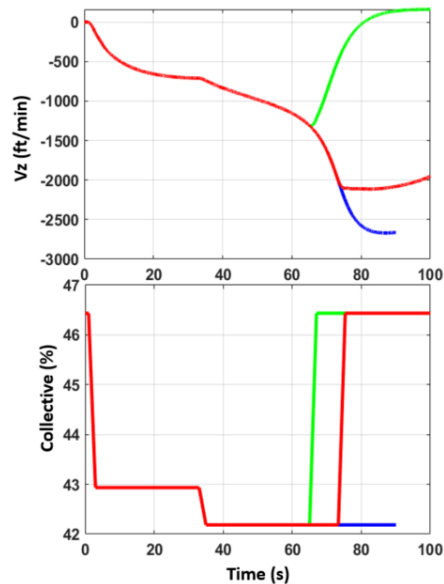
Once in a fully developed VRS, raising the collective has a limited effect of the vertical speed. This characteristic was used in flight to verify that the VRS was effectively established. But during some runs, this verification was done at relatively low rates of descent.

In Figure 5-17, a test run on the Fennec helicopter is shown, where a collective increase was performed at 41s without any action on the other axes. The vertical speed at that moment was -1560 ft/min, the longitudinal speed around 6 kts and the lateral speed was null, corresponding to a VRS onset. While no other action on the cyclic was done, this collective increase had a major effect on the rate of descent which decreased to zero in less than 8s. The resulting total loss of height being of 76 ft only.

► Figure 5-17 Effect of collective increases at VRS onsets in flight



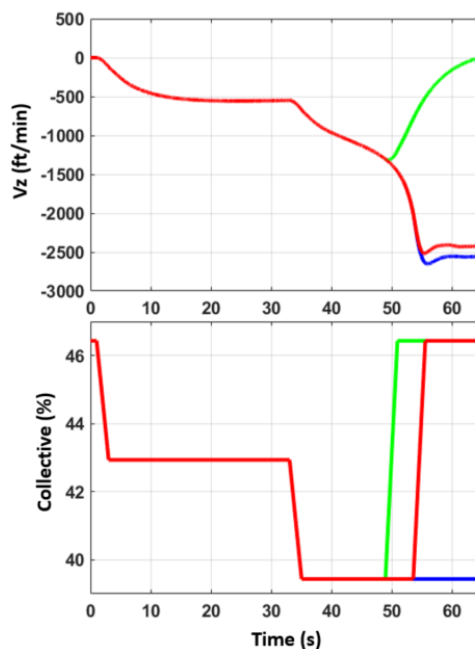
► Figure 5-18 Effect of collective increases at VRS onsets in simulation with the OA VRS model



Some simulations were done in order to evaluate the capability of the VRS models to reproduce this outcome. The OA VRS model was first assessed Figure 5-18 showing, in blue curve, successive collective decreases leading to a fully established VRS and where no action is undertaken to exit. A vertical descent is performed in this example. The green curve shows a collective increase up to the initial collective value, performed at a RoD of -1307 ft/min (at 65s). As this can be seen, the drop of Vz is just initiated, well corresponding to a VRS onset. The effect on the vertical speed is immediate, the hover being reached at 80.8s and a total loss of height of 158 ft. Another simulation was done (red curve) where the collective increase was applied at a higher rate of descent (-2075 ft/min). In this condition, the same collective increase was not able to recover from VRS, stabilising the RoD to -2000 ft/min.

The same simulations were realised with the ATR VRS model (shown in Figure 5-19) and very comparable results can be noticed.

► Figure 5-19 Effect of collective increases at VRS onsets in simulation with the ATR VRS model



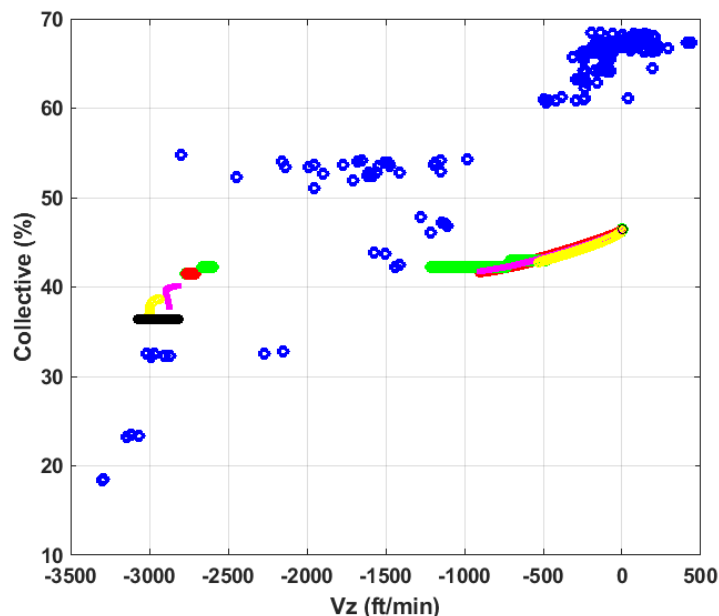
When no action is undertaken, the RoD stabilised at -2500 ft/min for a collective decrease of -7%. When the collective is increased at 48.9s, at a RoD of -1300 ft/min, the VRS is exited and hover is reached in 15.7s (in 15.8s with the OA model), with a loss of height of 114 ft. As observed with the previous VRS model, a collective increase at a RoD equal to -2000 ft/min doesn't allow to recover, the RoD stabilising at -2400 ft/min.

As a conclusion, both VRS models are able to reproduce recovery if power increase is carried out at VRS onsets. In these conditions, as observed in flight, the only application of a collective increase seems sufficient to get out of the phenomenon. Nevertheless, this must not to be considered as a fully-fledged recovery technique and an increase of the speeds (longitudinal or/and lateral) remains mandatory to be sure to get away from the VRS domain. But this demonstrates that, very close to the VRS domain, at VRS onsets or even in case of VRS suspicion, the first action to take is certainly a raise of collective pitch.

5.7.3 Collective versus vertical speed

As already observed in previous flight test campaigns, in the current one and discussed in reference [1], the relation between level of collective and vertical speed is modified in VRS. In Figure 5-20, the blue points are taken from the first Fennec flight performed in the framework of this project, and correspond to the level of collective plotted with respect to the vertical speed in "stabilised" conditions. Actually, these points are plotted when during a run, and function of time, the variation of the vertical speed is lower than 75 ft/min, the collective variation is lower than 1%, and for forward speeds between -5kts and +5kts. While not exactly corresponding to trim computations as shown in Figure 5-20, it can be clearly seen than below -1000 ft/min down to -3000 ft/min, the collective/Vz curve is no more monotonous and several very different descent rates can be reached with the same level of collective.

► Figure 5-20 Collective vs Vz in stabilised flight test cases



In climb and vertical descent down to -500 ft/min, a dispersion exits but the average collective/Vz curve is monotonous. This is also the case for descent rates higher than -3000 ft/min.

The different coloured plots in the figure have been generated in the same conditions but processing data from 5 different simulations. Except for the bias in terms of collective level (20% in hover), the same characteristic is observed, i.e. several achievable vertical speeds for a given level of collective.

Considered as a criterion, this characteristic could be also used to define the VRS domain of a helicopter.

5.7.4 Delayed collective application during recoveries

As discussed in sub-chapter 5.5.1, an increase of the loss of height is noticed when the collective is not increased during the forward recovery.

In Figure 5-21, four simulations were completed to evaluate the effect of an anticipated (blue curve), a simultaneous (red curve), or a delayed (by 10s for green curve, 20s for magenta curve) increase of the collective in a forward recovery in vertical descent and fully developed VRS. For all cases, the pitch angle variation applied was -10° .

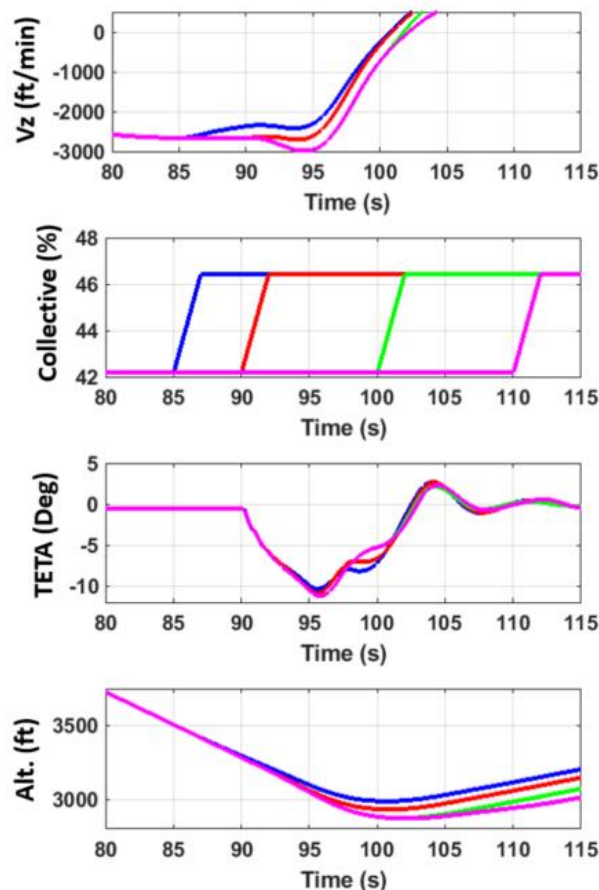
The respective loss of height observed in simulations are given hereafter:

Collective -5s:	308 ft
Collective 0s:	352 ft
Collective +10s:	412 ft
Collective +20s:	413 ft

In this case, an anticipated collective increase improve the efficiency of the procedure (in terms of height loss) but this result must be taken with reservations. It has been previously shown that an increase of the collective in VRS has an over-estimated effect on the vertical speed when using the OA induced velocity/VRS model.

It can be seen again on the Figure 5-21, that when applying the collective increase 5s prior to the pitch down attitude (blue curves), the descent rate is already reduced when the recovery manoeuvre is initiated, leading to a reduced loss of height. In flight, such an effect would probably not be observable, or highly minored.

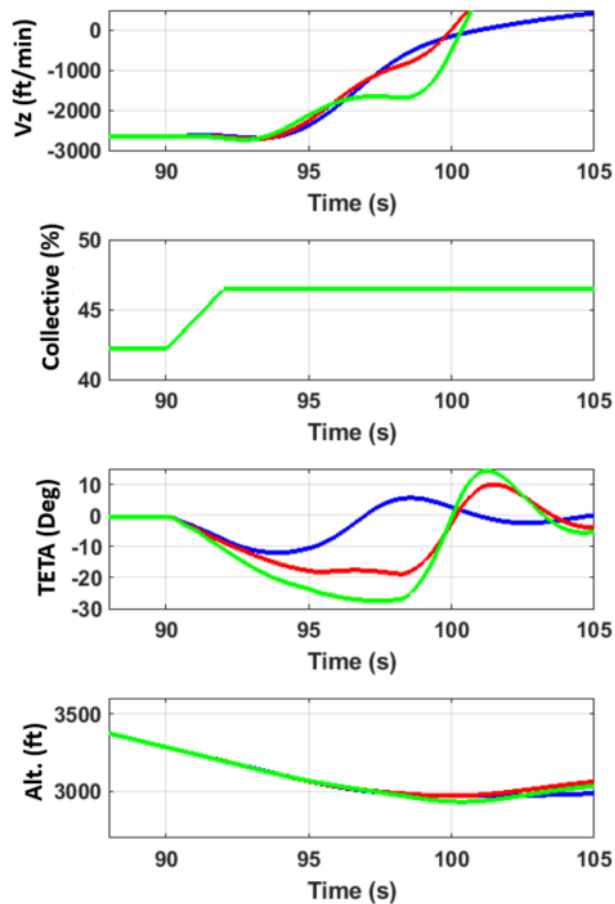
► Figure 5-21 Effect of delayed increase of the collective on height loss in forward recovery



5.7.5 Pitch attitude in forward recovery

A parametric study has been performed to evaluate the effect of the pitch angle variation on the loss of height during a forward recovery in vertical descent. Three simulations are shown in Figure 5-22 where the minimum pitch angle reached were -12° , 19° and -27.5° . The corresponding loss of height measured are 313.6 ft, 314.3 ft and 352.6 ft.

► Figure 5-22 Effect of the pitch angle on the height loss



As well as in simulation, the analysis of the flight data showed that, in forward recoveries and fully developed VRS, higher nose down attitudes tend to worsen the height loss.

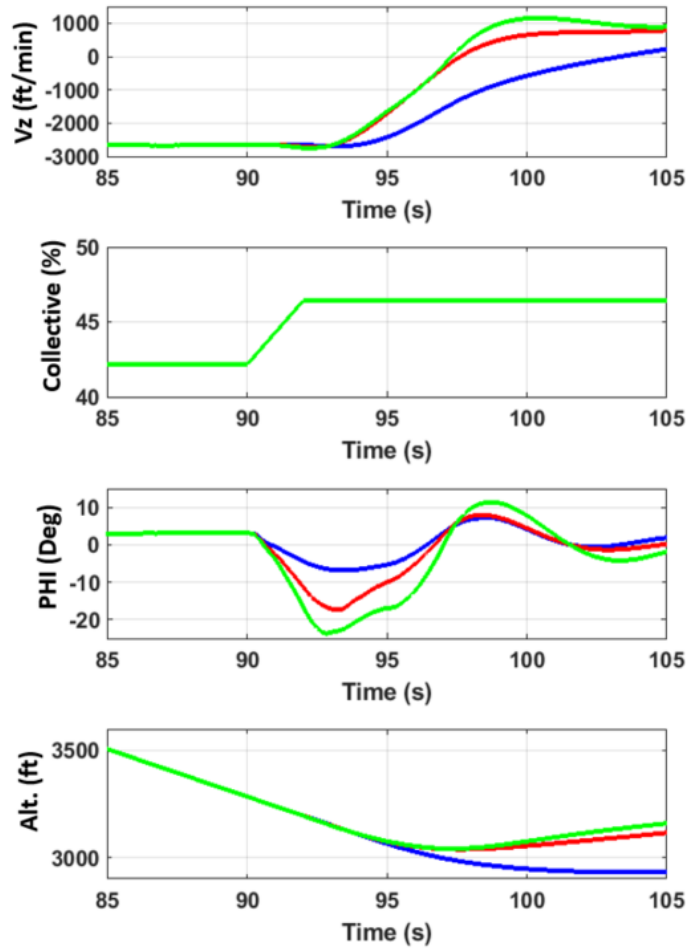
5.7.6 Roll attitude in Vuichard recovery

A comparable parametric study has been done for the Vuichard technique. The effect of the roll angle magnitude reached during the Vuichard recovery has been evaluated in vertical descent and fully VRS.

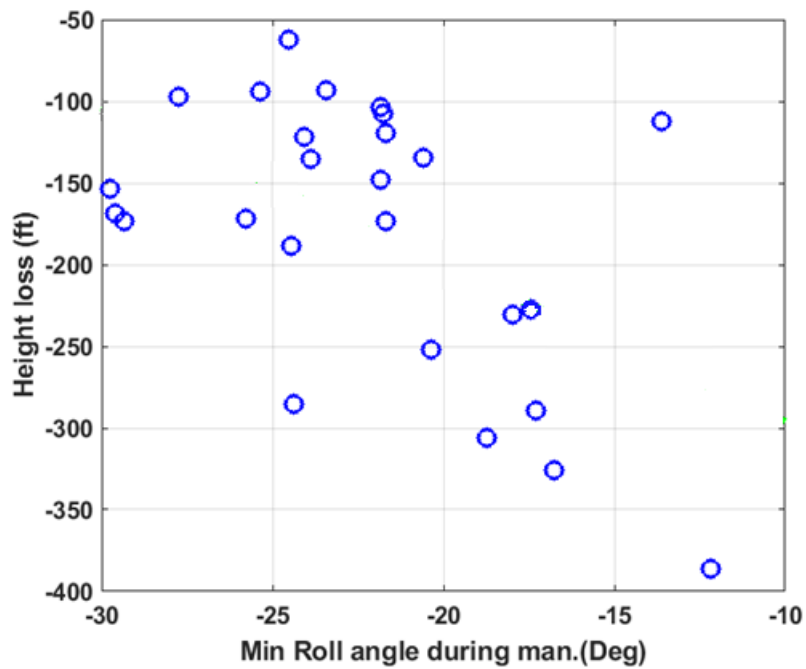
Figure 5-23 shows three simulations where the minimum roll angle reached during the manoeuvre (starting at 90s) were -6.8° , -17.3° and -23.6° . The respective loss of height being 351 ft, 245 ft and 242 ft, indicating that the loss of height is reduced as the roll angle is increased.

The effect of the roll angle on the height loss for Vuichard recoveries in fully VRS is shown in Figure 5-24, where the minimum roll angle reached during the Vuichard procedure in all corresponding Fennec runs are plotted. Contrary to the forward manoeuvre, and despite the important dispersion, there seems to be a decrease of the height loss with the roll angle as outlined by the fitting curve in green. This trend was already outlined in §4.2.4.

► Figure 5-23 Effect of the roll angle on the height loss



► Figure 5-24 Height loss depending on minimum roll angle in Vuichard recoveries in fully VRS



5.8 Simulator trials

Previous simulations demonstrate the ability of the off-line tool to simulate VRS entries and recoveries, in different flight conditions or with different “pilot” controls. We can therefore assume that, using a flight mechanics code validated against flight data, this simulation tool could be used to explore a greater number of flight cases with a good degree of confidence and, as already shown, could be adapted to the realisation of parametric studies. Nevertheless, real-time piloted simulations remain necessary to study such manoeuvres, by enabling a pilot to experience and evaluate the realism of the helicopter behaviour and the workload needed to proceed to recovery manoeuvres.

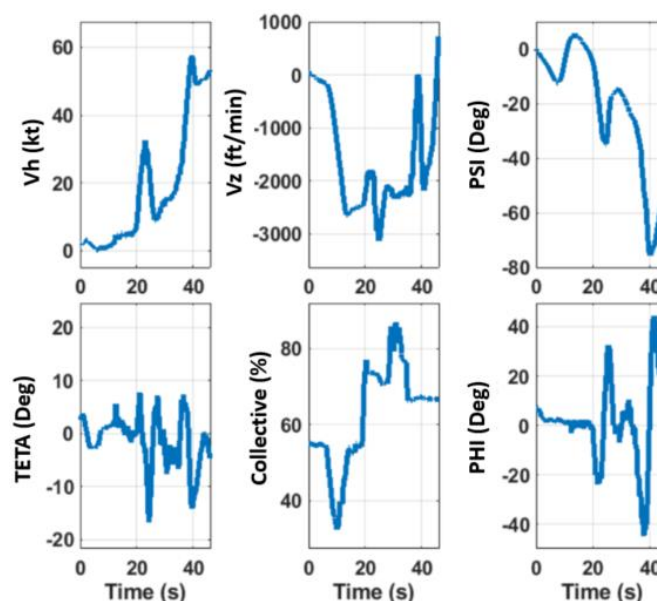
One of the pilot who participated to the flight test campaign performed simulator trials on the ONERA research simulator PycsHel. Both Fennec and Dauphin helicopter models were tested, as well as the two VRS models. These simulator trials were only focussed on vertical descent cases, in which Vuichard and forward recovery techniques were assessed. The number of test cases with respect to the type of recovery technique realised and VRS model used are summarised in Table 5-1:

Table 5-1 Number and types of recovery manoeuvres performed in the simulator

DAUPHIN		Recovery	
		Forward	Vuichard
VRS Model	ONERA	3	2
	ATR	6	
FENNEC		Recovery	
		Forward	Vuichard
VRS Model	ONERA	4	3
	ATR	6	4 (all invalid)

A major limit has to be raised: as for off-line simulations, the real-time simulator only features an ideal engine model offering an unlimited power and a constant rotor RPM. Thus, the pilot had no workload associated to the management of the torque/power.

► Figure 5-25 Impossibility to assess the Vuichard technique



As shown in Figure 5-4, the ATR VRS model generates periodic pitch and roll angle variations of relatively large amplitudes. As well as being considered unrealistic by the pilot, roll oscillations lead to PIO on the lateral axis, leading to the impossibility to properly perform the Vuichard recovery in the simulator as this can be seen in Figure 5-25.

Indeed, at 20s, the recovery manoeuvre was initiated through a simultaneous increase of the collective and a roll variation to the left. But the ATR VRS model inducing roll variations, the pilot always experienced difficulties to reach and hold a desired roll angle. Pitch attitude variations due to this VRS model increased the workload and cross-coupling effects. Four runs were done on the Fennec model, all considered unusable. Thus the Vuichard manoeuvre wasn't tested on the Dauphin model.

5.8.1 Simulator trial results

Table 5-2 provides, for both helicopters, the averaged loss of height and recovery duration depending on the recovery technique practiced, the VRS models and compared to the ones measured in flight. As indicated, simulator and flight test cases are corresponding to vertical descent and a recovery manoeuvre initiated in fully developed VRS.

In simulator, the averaged loss of heights are much greater than those observed in flight for both helicopters. This can be certainly explained by the fact that, as already outlined, the collective decrease lead to higher descent rate in simulation. Recovering from higher descent rate contributing to increase the loss of height. Height loss and recovery time are always higher with the ATR VRS model inducing much more workload and cross-couplings effects due to attitude variations.

On Fennec, recovery time is very comparable between flight tests and the OA model for both techniques, as well as on Dauphin for the forward manoeuvre. On Dauphin, recovery duration is much lower with the OA model for the Vuichard technique, which can be explained by the lack of representativeness of the flight mechanics model in terms of cross-couplings and associated attitude changes faced in flight, and the reduced workload in simulator, where power margins and helicopter limits exceedances had not to be managed. Nevertheless the averaged loss of height is comparable with the one in flight.

Table 5-2 Average loss of height and recovery duration in simulator compared to flights

Vertical descent - Fully developed VRS					
DAUPHIN	Simulator			Flight tests	
	Forward		Vuichard	Forward	Vuichard
	OA	ATR	OA		
Average loss of height (ft)	408,54	461,26	270,47	236,4	251,72
Average Recovery duration (s)	8,74	10,42	7,57	8,52	13,71
Vertical descent - Fully developed VRS					
FENNEC	Simulator			Flight tests	
	Forward		Vuichard	Forward	Vuichard
	OA	ATR	OA		
Average loss of height (ft)	342,94	435,84	286,69	217,77	185,5
Average Recovery duration (s)	8,71	11,54	9,22	9,85	9,85

Only considering flight test data, it has to be noted that in these conditions, the averaged loss of height is slightly lower during a forward rather than a Vuichard recovery on the Dauphin, while this is the opposite on

the Fennec. Recovery durations are the same on the Fennec, while it takes a longer time to recover on the Dauphin when performing the Vuichard technique. This will be detailed in the next sub-chapter.

In addition to the pilot feedback, a specific data processing has been carried out on pilot controls in order to estimate the pilot control activity during the recovery procedures. Thus, Table 5-3 provides the calculated standard deviations (noted std) of the pilot commands on the three axes in simulator compared to flights.

Table 5-3 Controls activity in simulator compared to flights (vertical descent, established VRS)

DAUPHIN	Simulator			Flight tests	
	Forward		Vuichard	Forward	Vuichard
	OA	ATR	OA		
std Lateral (%)	6,13	9,93	15,48	7,75	12,63
std Longitudinal (%)	9,25	18,42	9,25	5,99	8,68
std Pedals (%)	7,87	4,56	7,87	4,53	5,8

FENNEC	Simulator			Flight tests	
	Forward		Vuichard	Forward	Vuichard
	OA	ATR	OA		
std Lateral (%)	6,64	12,62	15,03	6,41	10,6
std Longitudinal (%)	14,79	20,33	7,07	7,54	8,75
std Pedals (%)	6,26	3,8	12,37	5,72	6,65

In flight, standard deviations are always higher during the Vuichard recovery. If this can be expected on the lateral axis, it can also be shown on the longitudinal and yaw axes, highlighting the strong cross-couplings involved in this manoeuvre. Interestingly, the standard deviation on the lateral cyclic is higher than on the longitudinal during the forward procedure on the Dauphin.

In simulator, the ATR VRS model implies higher greater control variations on all axes, which is due to the generated attitude variations.

On both helicopters, the OA VRS model gives consistent results where the maximum standard deviation is observed on the predominant axis of the manoeuvre. On the Fennec, the standard deviation on the yaw axis is much higher during the Vuichard technique. This can be potentially explained by the need of tuning the efficiency of the pedals in the simulator in the beginning of the trials. A better calibration could improve the results by lowering the need of pedal activity. It has to be noted that this controls activity is not directly comparable to the pilot workload, while contributing to it. This also provides objective criteria on the parasitic effects occurring during the manoeuvres as this will be detailed in the next chapter

5.8.2 Pilot feedback on simulator trials

On both helicopter models, a specific tuning of the pedals efficiency was requested at the beginning of the trails. In addition, the collective/yaw coupling was considered not representative.

When entering VRS, a reduction of effectiveness of the cyclic pitch controls may be experienced in flight, resulting in a decrease of the control power on both longitudinal and lateral axes. A reduction of effectiveness of the pedals can also be observed, leading to yaw motion. In order to represent these effects, the ATR VRS model offers the possibility to reduce the efficiency of the cyclic but this parameter has to be carefully set. At the beginning of the trials, the efficiency was too reduced to properly perform any recovery procedure.

In a general manner, pitch and roll oscillations generated by the ATR model were considered unrealistic, leading to PIO on both axes, more exacerbated on the lateral one. This was impossible to target a predefined attitude

angle (especially the roll angle). Thus, the Vuichard recovery manoeuvre was made particularly difficult to execute, even though numerous parasitic effects were not rendered.

Forward manoeuvres performed with the OA model were generally more realistic than the Vuichard manoeuvres, and more corresponding to what can be experienced in flight.

On Dauphin, and during Vuichard manoeuvre, the Fenestron/rear elements effects are neglected in simulation. In flight, much more actions on pedals are needed and parasitic effects are more important as this will be detailed hereafter.

5.9 Conclusions of the numerical investigation

As part of the objectives of the “VRS-Helicopter Vortex Ring State Experimental Research”, the goal of this specific study was to evaluate the correctness of flight mechanics code and two different VRS models and reproducibility of recovery techniques. Off-line simulations were compared against flight test data, and simulator trials were carried out in the ONERA research simulator in order to evaluate the representativeness of the VRS models thanks to piloted simulations. The objective was to highlight potential shortcomings of the VRS models and thus the reservations to be taken into account when the vortex phenomenon and recovery techniques are evaluated through simulations, whether in delayed or in real time on simulators. Not expected at the beginning of the study, discrepancies in helicopter responses between simulation and flight data were noticed, and outlined flight mechanics deficiencies.

It was thus demonstrated that:

- The off-line simulation tool developed at ONERA and dedicated control strategies give the possibility to reproduce many different VRS test cases.
- When following flight data or in the framework of parametric studies, some influencing parameters and tendencies are well captured, such as the effect on height loss of delayed collective increase or pitch and roll angle maximum values.
- The vertical speed response was generally not representative of the flights, especially when using the OA VRS model. That’s true in terms of maximum descent rates reached after a collective pitch decrease, but also after a collective pitch increase in fully developed VRS.
- When using the ATR VRS model, the collective pitch increases are much more representative in fully developed VRS. On the contrary, pitch and roll artificial oscillations are not realistic, being too strong and too periodic. This prevented to assess this model with the Vuichard technique in the ONERA simulator. The cyclic efficiency coefficient proposed by this model has to be carefully set, to properly represent the power control reduction that can be experienced in flight.

It has to be noted that these results are due to the lack of model adjustment and tuning when it was used at ONERA. An instability coefficient can be adapted to limit these oscillations and make them more realistic. Based on these observations and evaluations, a tuning of this model will be done at ONERA, as this is always done in FFS simulators.

- Simulator trials remain mandatory to correctly evaluate helicopter model behaviour and recovery techniques representativeness. In this study, these trials offered the possibility to evaluate both helicopter and VRS models with a pilot.
- It was thus confirmed that the cross-couplings and parasitic effects are neglected by the simulation, and more specifically on the Dauphin helicopter, equipped with a Fenestron and large rear aerodynamic elements.
- In addition, the absence of engine model and thus the lack of engine limits (Torque, NG) highly reduced the pilot workload during simulator trials compared to real flights. But this parameter has a great effect and it was demonstrated in flight that a higher workload tends to lower the recovery efficiency.

Although there was almost no doubt at the beginning of this study that the VRS models could be improved, the lacks of the flight mechanics model were not expected or at least, were under-estimated. Indeed, particularly

present on the Dauphin helicopter, severe cross-couplings were experienced in flight when performing a lateral recovery. Neglected cross-coupling and parasitic effects tend to highly reduce the required workload during simulator tests, contributing to distort the results. Exacerbated on the Dauphin, different models may be the cause of these discrepancies. A study of the Fenestron model should be carried out, as well as the aerodynamic models of the rear elements such as the vertical fin or the horizontal empennage which is equipped with relatively large vertical fins on this machine. Investigations should be carried out to verify the aerodynamic polar curves and the generated forces and moment at very high angles of attacks as well as to ensure that empennage vertical fins are properly taken into account.

Following this study, some general recommendations have been drawn in reference [4] on the use of simulation models to study the vortex phenomenon and, more specifically, to evaluate the recovery techniques. In addition, dedicated improvements as well as suggestions for future researches have been proposed.

6. General conclusions

This document presents the analysis of the eight flight tests that were performed in the framework of the Helicopter Vortex-Ring-State Experimental Research project (EASA.2022.C11).

The purpose was:

- the determination of the VRS flight envelope for the used helicopter types;
- the comparison of the results with available predictions obtained with analytical and simulation methods available; and
- the evaluation of the effectiveness of the Vuichard VRS recovery manoeuvre and comparison with the forward manoeuvre for the used helicopter types.

Despite not foreseen in the initial research tender specification, a comparison between the Vuichard recovery technique and the recovery technique defined by the helicopter manufacturer was performed in order to provide a baseline for future similar evaluations on other aircraft/rotor designs.

It was highlighted that the VRS domains of both helicopters determined during this flight test campaign are very comparable to those obtained in previous experimental investigations and a good consistency is observed between the ONERA predicted VRS domains and the actual test points. Depending on the criteria used to define the VRS entries and exits, these domains can differ, as this was already observed.

Many influencing parameters were studied and their effect on recovery performance analysed. Among them, the vertical speed at which the recovery is initiated, the torque (i.e. power) applied and the effect of a delay in its application, or the maximum roll or pitch angles.

While, on average, a slight increase of the performance could be seen with the Vuichard recovery manoeuvre on the Fennec, this was not the case on the Dauphin, mainly due to the large increase of the workload on this machine during this manoeuvre. In any case, we didn't notice a large difference between the two recovery methods except during recoveries performed at the early stages of VRS and where the Vuichard manoeuvre shows better performance than the forward one in terms of both time of recovery/height loss.

Surprisingly, the inversed Vuichard recovery gave very interesting results and should be further investigated as the total number of runs performed was too limited to draw conclusions.

What was not expected at the beginning of the study is the effect of the workload on recovery performance. Highly dependent on the helicopter, this criteria has to be always considered in the evaluations.

Therefore, this parameter is a major lack of the off-line simulations when used to evaluate this type of manoeuvres.

A specific study of VRS models has been done to evaluate their capability to reproduce VRS entries and recovery manoeuvres. If some lacks were outlined, the major result is that, up to now, simulator trials remain necessary to correctly evaluate the recovery techniques. Nevertheless, this requires tuned induced velocity/VRS models and flight mechanics codes to well represent VRS symptoms and effects. In addition, cross-couplings having a large effect on pilot workload, it is mandatory to verify the representativeness of these parasitic effects in the simulation.

Flight tests remain essential to better understand all the mechanisms involved in VRS generation and the evaluation of recovery techniques, but VRS flight tests are (and will continue to be) very demanding in terms of instrumentation, competences and costs. Necessary to validate numerical approaches, necessary from an operational perspective, results of VRS flights remain, however, highly dependent on the tested helicopter.

Unfortunately, the scope of the work cannot be infinite in the framework of a project, as well as the number of flights and helicopter types. EASA, ONERA and DGA-EV were fully aware that the current research project would not answer all the questions about VRS, but it is hoped that the flight tests performed and their analysis contributed to provide further information about the characterisation of the VRS as well as recovery techniques.

Bibliography

1. D-1.1 VRS Knowledge Report – <https://www.easa.europa.eu/en/research-projects/vrs-helicopter-vortex-ring-state-experimental-research>
2. For Helicopter Flight Instructors – Training Guide, together4safety - EASA, 2022.
3. Airbus Helicopters Safety Information Notice N° 3123-S-00 - 2022-04-12
4. Binet, L., Cornefert, T., “Evaluation of the representativeness of flight mechanics models during Vortex-Ring-State entries and recovery manoeuvres”, 50th European Rotorcraft Forum, Marseille, France, 2024.
5. Taghizad, A., Jimenez, J., Binet, L., Heuzé, D., “Experimental and theoretical investigations to develop a model of rotor aerodynamics adapted to steep descents”, 58th Annual Forum of the American Helicopter Society, 2002.
6. Jimenez, J., Taghizad, A., Arnaud, A., “Helicopter flight tests in steep descent: Vortex-Ring-State analysis and induced velocity models improvement”, CEAS Aerospace Aerodynamics Research Conference, 2002.

Appendix

List of recorded parameters on both helicopters

Parameter	Denomination	Dauphin	Fennec
Temps	Time	√	√
DDM0	Cyclic Longitudinal position	√	√
DDM1	Cyclic Longitudinal position after AP actuator	√	√
DDL0	Cyclic Lateral position	√	√
DDL1	Cyclic Lateral position after AP actuator	√	√
DDLTLH	Left roll servo-actuator position	√	
DDLTRH	Right roll servo-actuator position	√	
DDMT	Pitch servo-actuator position		√
DDNO	Pedal position	√	√
DN	Tail rotor servo-actuator position	√	√
DDT0	Collective grip position	√	√
PSE	Static pressure	√	√
DPE	Differential pressure	√	√
JX	Longitudinal acceleration	√	√
JY	Lateral acceleration	√	√
JZ	Normal acceleration	√	√
P	Roll rate	√	√
Q	Pitch rate	√	√
R	Yaw rate	√	√
BETAS	Sideslip angle	√	√
PSI	Heading	√	√
PHI	Roll angle	√	√
TETA	Pitch angle	√	√
TTE	External Total Temperature	√	√
RA	Radar height	√	√
NR	Rotor rotational speed	√	√
NGLH	Left engine - Gas generator speed	√	
NGRH	Right engine - Gas generator speed	√	
NG	Gas generator speed		√
NFLH	Left engine - free turbine speed	√	
NFRH	Right engine - free turbine speed	√	
PALH	Left "anticipator" position	√	
PARH	Right "anticipator" position	√	
PTQMOTLH	Left engine torque pressure	√	
PTQMOTRH	Right engine torque pressure	√	
P2LH	Left engine compressor pressure	√	
P2RH	Right engine compressor pressure	√	
FFVLH	Left engine fuel flow	√	
FFVRH	Right engine fuel flow	√	
FUVLH	Left engine fuel totalizer	√	
FUVRH	Right engine fuel totalizer	√	

PLALH	Left fuel flow control lever position	√	
PLARH	Right fuel flow control lever position	√	
T4LH	Left engine T4 temperature	√	
T4RH	Right engine T4 temperature	√	
T4	T4 temperature		√
VIMIX	Longitudinal VIMI speed	√	√
VIMIY	Lateral VIMI speed	√	√
PMOT	Power calculated from Torque	√	√
ALT_CAL	GPS Altitude	√	√
FOB	Fuel On Board	√	
MASS	Mass	√	√
MRED	Reduced Mass ($M/\sigma \cdot (N_r/N_{r0})^2$)	√	√
MSSIGMA	MASS/Sigma (σ)	√	√
LAT_CAL	GPS Latitude	√	√
LONG_CAL	GPS Longitude	√	√
TQMOT	Total Torque	√	√
TQMOTLH	Left Engine Torque	√	
TQMOTRH	Right Engine Torque	√	
TQTR	Tail rotor torque	√	
VCE	Calibrated Air Speed	√	√
ZPE	Pressure Altitude	√	√
VX	Speed X axis - VIMI GPS	√	√
VY	Speed Y axis - VIMI GPS	√	√
VUP	Vertical Speed GPS	√	√
VZP	Barometric Vertical Speed	√	√
VZ	Vertical Speed (Temperature effect correction)	√	√
TISA	ISA Temperature	√	√



European Union Aviation Safety Agency

Konrad-Adenauer-Ufer 3
50668 Cologne
Germany

Mail EASA.research@easa.europa.eu
Web www.easa.europa.eu

An Agency of the European Union

